AFTAC Project No. VT/1705

PRELIMINARY EVALUATION OF THE NORWEGIAN LONG PERIOD ARRAY

SPECIAL REPORT NO. 5
EXTENDED ARRAY EVALUATION PROGRAM

Prepared by
John S. Eyres, Philip R. Laun, and William H. Swindell

T. W. Harley, Program Manager
Area Code 703, 836-3882 Ext. 300

TEXAS INSTRUMENTS INCORPORATED
Services Group
P. O. Box 5621
Dallas, Texas 75222

Contract No. F33657-71-C-0843
Amount of Contract: $511,580
Beginning 1 April 1971
Ending 31 March 1972

Prepared for

AIR FORCE TECHNICAL APPLICATIONS CENTER
Alexandria, VA 22313

Sponsored by

ADVANCED RESEARCH PROJECTS AGENCY
Nuclear Monitoring Research Office
ARPA Order No. 1714
ARPA Program Code No. 1F10

30 April 1972

Acknowledgement: This research was supported by the Advanced Research Projects Agency, Nuclear Monitoring Research Office, under Project VELA-UNIFORM, and accomplished under the technical direction of the Air Force Technical Applications Center under Contract No. F33657-71-C-0843.

UNCLASSIFIED

Security Classification

DOCUMENT CONTROL DATA – R & D

(Security classification of title, body of abstract and indexing annotation must be entered when the overall report is classified)

1. ORIGINATING ACTIVITY *(Corporate author)*
Texas Instruments Incorporated
Services Group
P.O. Box 5621, Dallas, Texas 75222

2a. REPORT SECURITY CLASSIFICATION
UNCLASSIFIED

2b. GROUP

3. REPORT TITLE
Preliminary Evaluation of the Norwegian Long Period Array, Special Report No. 5, Extended Array Evaluation Program

4. DESCRIPTIVE NOTES *(Type of report and inclusive dates)*
Special

5. AUTHOR(S) *(First name, middle initial, last name)*
John S. Eyres, Philip R. Laun, and William H. Swindell

6. REPORT DATE	7a. TOTAL NO. OF PAGES	7b. NO. OF REFS
30 April 1972	164	6

8a. CONTRACT OR GRANT NO.
Contract No. F33657-71-C-0843

b. PROJECT NO.
AFTAC Project No. VT/1705

c.

d.

9a. ORIGINATOR'S REPORT NUMBER(S)

9b. OTHER REPORT NO(S) *(Any other numbers that may be assigned this report)*

10. DISTRIBUTION STATEMENT
APPROVED FOR PUBLIC RELEASE; DISTRIBUTION UNLIMITED

11. SUPPLEMENTARY NOTES

12. SPONSORING MILITARY ACTIVITY
Advanced Research Projects Agency
Nuclear Monitoring Research Office
Arlington, Virginia 22209

13. ABSTRACT

This ~~special~~ report presents results from the preliminary evaluation of the long-period Norwegian Seismic Array. Signal and noise characteristics, array processing performance, matched and chirp filtering performance, detection threshold estimation, and discriminant behavior are discussed.

DD FORM 1 NOV 65 1473

1a

UNCLASSIFIED

Security Classification

14. KEY WORDS	LINK A		LINK B		LINK C	
	ROLE	WT	ROLE	WT	ROLE	WT
Extended Array Evaluation Program						
Special Report, 1 April 1971 to 31 March 1972						
NORSAR (Long Period) Evaluation						
- Signal and noise characteristics						
- Array processing improvements						
- Matched filtering improvements						
- Detection threshold estimation						
- Discriminants behavior						

AFTAC Project No. VT/1705

PRELIMINARY EVALUATION OF THE NORWEGIAN LONG PERIOD ARRAY

SPECIAL REPORT NO. 5
EXTENDED ARRAY EVALUATION PROGRAM

Prepared by
John S. Eyres, Philip R. Laun, and William H. Swindell

T. W. Harley, Program Manager
Area Code 703, 836-3882 Ext. 300

TEXAS INSTRUMENTS INCORPORATED
Services Group
P.O. Box 5621
Dallas, Texas 75222

Contract No. F33657-71-C-0843
Amount of Contract: $511,580
Beginning 1 April 1971
Ending 31 March 1972

Prepared for

AIR FORCE TECHNICAL APPLICATIONS CENTER
Alexandria, VA 22313

Sponsored by

ADVANCED RESEARCH PROJECTS AGENCY
Nuclear Monitoring Research Office
ARPA Order No. 1714
ARPA Program Code No. 1F10

30 April 1972

Acknowledgement: This research was supported by the Advanced Research Projects Agency, Nuclear Monitoring Research Office, under Project VELA-UNIFORM, and accomplished under the technical direction of the Air Force Technical Applications Center under Contract No. F33657-71-C-0843.

AFTAC Project No. VT/1705

PRELIMINARY EVALUATION OF THE NORWEGIAN LONG PERIOD ARRAY

SPECIAL REPORT NO. 5
EXTENDED ARRAY EVALUATION PROGRAM

Prepared by
John S. Eyres, Philip R. Laun, and William H. Swindell

T. W. Harley, Program Manager
Area Code 703, 836-3882 Ext. 300

TEXAS INSTRUMENTS INCORPORATED
Services Group
P.O. Box 5621
Dallas, Texas 75222

Contract No. F33657-71-C-0843
Amount of Contract: $511,580
Beginning 1 April 1971
Ending 31 March 1972

Prepared for

AIR FORCE TECHNICAL APPLICATIONS CENTER
Alexandria, VA 22313

Sponsored by

ADVANCED RESEARCH PROJECTS AGENCY
Nuclear Monitoring Research Office
ARPA Order No. 1714
ARPA Program Code No. 1F10

30 April 1972

Acknowledgement: This research was supported by the Advanced Research Projects Agency, Nuclear Monitoring Research Office, under Project VELA-UNIFORM, and accomplished under the technical direction of the Air Force Technical Applications Center under Contract No. F33657-71-C-0843.

ABSTRACT

This special report describes work performed under the Extended Array Evaluation Program conducted by Texas Instruments, Incorporated at the Seismic Array Analysis Center over the period 1 April 1971 to 31 March 1972.

A preliminary evaluation of the long-period NORSAR has been completed using data from the period 1 May 1971 to 9 January 1972. Approximately 112 events, primarily from the Sino-Soviet bloc, and 26 long noise samples, have been processed to obtain signal and noise characteristics, multichannel filter and beamsteer processor performance, matched and chirp filter performance, and a preliminary estimate of the NORSAR detection capability.

TABLE OF CONTENTS

TABLE OF CONTENTS
(continued)

LIST OF FIGURES

LIST OF FIGURES
(continued)

LIST OF FIGURES
(continued)

LIST OF FIGURES
(continued)

LIST OF TABLES

LIST OF TABLES
(continued)

SECTION I
INTRODUCTION

This report presents the results of a preliminary evaluation of the long-period Norwegian Seismic Array (NORSAR) using seismic data recorded during the time period 1 May 1971 through 9 January 1972. The evaluation of NORSAR has three overall objectives:

- Determine a good method of enhancing the signal-to-noise ratio of Eurasian events.
- Determine the array detection capability for Eurasian events.
- Evaluate the performance of various discriminants at NORSAR for Eurasian events.

These objectives were accomplished by using analysis procedures similar to those used to evaluate ALPA (Texas Instruments, 1971). Six separate studies were undertaken:

- Noise analysis.
- Signal analysis.
- Array processing effectiveness.
- Matched filtering performance.
- Detection threshold estimation.
- Behavior of standard discriminants.

Results for each study are presented in subsequent sections of this report.

The long-period NORSAR is an array of 22 seismometer sites spread over an area approximately 100 km in diameter and located north of Oslo, Norway. Each site contains three seismometers (25- second period) aligned in vertical, north-south, and east-west directions. A diagram of the array is shown in Figure I-1.

Amplitude and phase calibrations of the NORSAR sites were not available; all of the results in this report are based on data which are uncorrected for instrument response. The nominal value of 2.47 millimicrons per computer count at 25 seconds was used to convert number to ground motion. The nominal NORSAR system response is shown in Figure I-2.

The results presented in the following sections are based on the analysis of events located in or near the Sino-Soviet area. The only exception was a United States underground nuclear explosion (CANNIKIN). Consideration only of these areas essentially restricted the data to events lying east of NORSAR. The performance of NORSAR for westerly events may be somewhat different; however, an estimate of that performance may be inferred from results presented in the noise analysis section of this report.

Transmission of NORSAR long-period data is accomplished by a communications system called the Trans-Atlantic Link (TAL). Received NORSAR data are multiplexed with LASA and ALPA data and recorded on magnetic tape. Data became available at SAAC during the first quarter of 1971, however, because of various difficulties with both the transmission hardware and software, data quality prior to 30 April was not satisfactory for analysis. Thus, results presented are based on data recorded after April 30, 1971.

Events for analysis were selected on the basis of location, magnitude, and depth. Source information was primarily from the NOAA-ERL "PDE" lists and the SAAC (LASA) bulletins. During the last quarter, the NDPC (NORSAR) bulletin became available and was also used. The criteria for selecting events for analysis were:

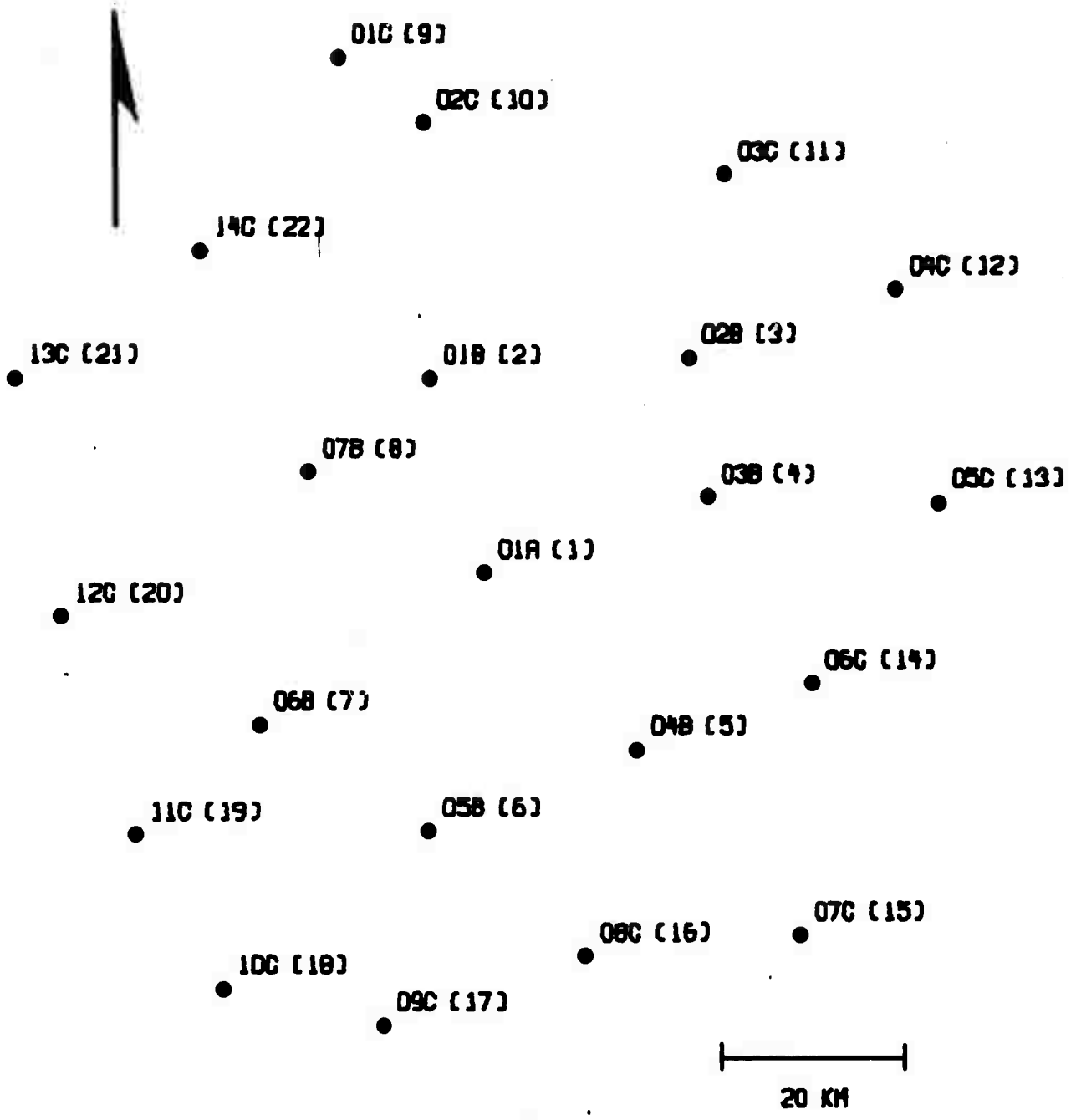

FIGURE I-1

SITE DIAGRAM OF LONG PERIOD NORSAR

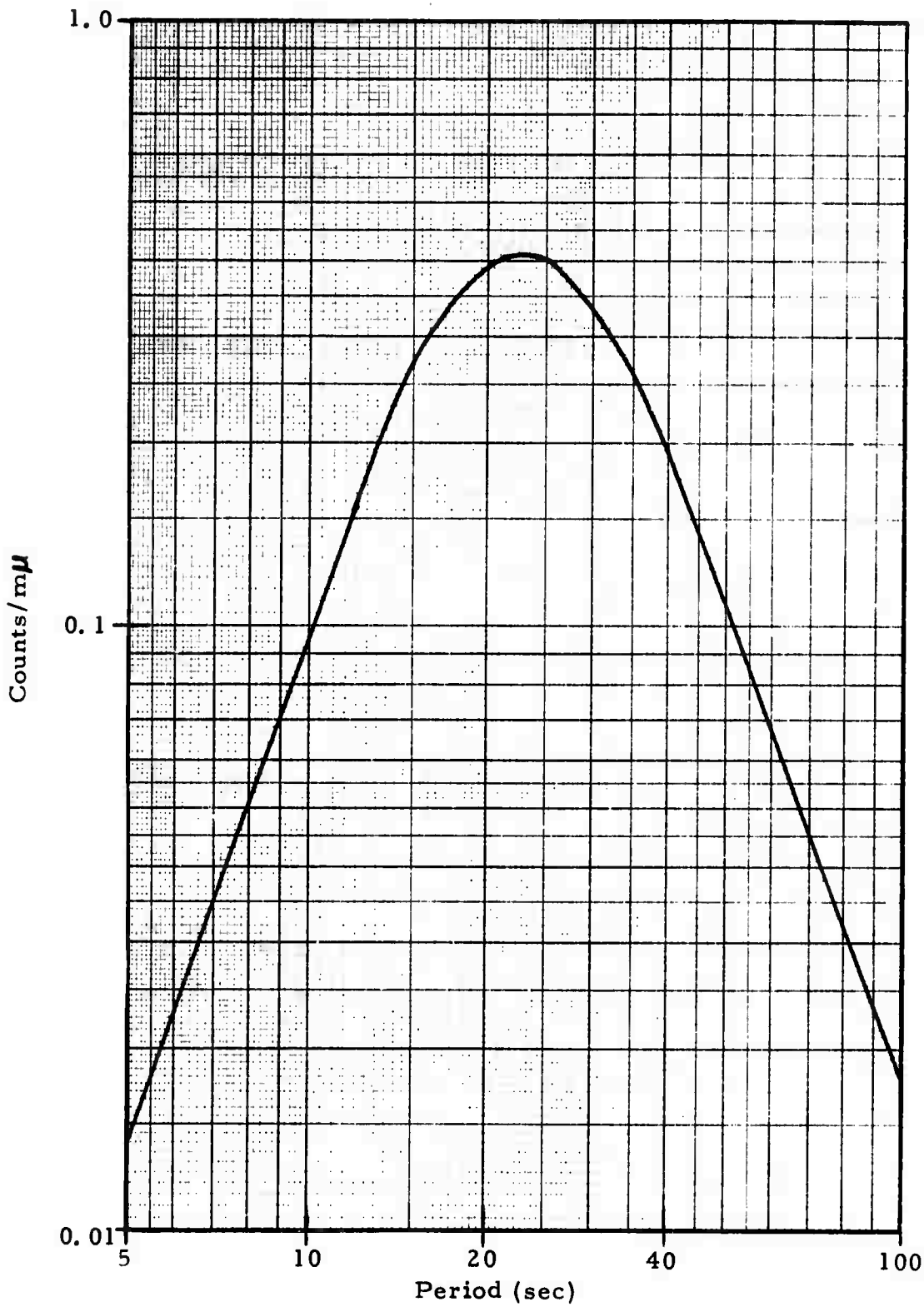

FIGURE I-2

NOMINAL AMPLITUDE RESPONSE OF LP SEISMOMETER

- Epicenter in or near the Sino-Soviet area.
- Magnitude (m_b) between 4.0 and 6.0.
- Depths less than 70 km.
- No interfering events.

During the eight month period beginning 1 May 1971, 251 events were considered for analysis. Edit attempts were made on 152 of these; Table I-1 lists the reasons for rejecting 99 events.

The 152 edited events are listed in Table I-2; of these, 112 were suitable for processing. The events selected but not edited are eliminated primarily because of excessive data dropouts during events. This was a fairly serious problem during the summer of 1971 but by fall had reduced in severity to a minor one. The dropouts were caused either by NORSAR being down or, as was usually the cause, by transmission failure. The duration of data loss was from one second to ten seconds and occasionally went for several minutes. There was one eight-day period (about days 180-188) when no data was received due to a TAL problem. Since this fall, NORSAR has become fully operational and the data loss rate from dropouts is small. Other causes for eliminating edited events included:

- Unreported interfering event.
- Unremovable spikes or transients in the data.
- Mislocation (as determined from particle motion and/or misrotation effects)

In addition to signals, noise data was specially edited for separate analysis. The procedure was to obtain as long an interval as possible without known events occurring. Noise edits were obtained at approximately 10 day intervals. The date and length of the noise edits are listed in the noise analysis section.

TABLE I-1

TABULATION OF NORSAR LP EVENTS
SELECTED BUT NOT EDITED

NORSAR down	47
SAAC down	1
TAL down	1
Time gaps on tape	36
Mislocated events	6
Interfering events	6
Other	2
Total	99

TABLE I-2

LIST OF EDITED NORSAR LP EVENTS
(PAGE 1 OF 7)

Designation	Date	Origin Time	Lat.	Long.	m_b	Depth	Source Bulletin	Comment
TIB/121/18NL	05/01/71	18.35.56	35.4N	84.3E	4.5	N	S	M, U
SIN/121/20NL	05/01/71	20.40.12	36.5N	80.4E	4.3	N	S	T, U
TIB/123/00NL	05/03/71	00.33.23	30.8N	84.5E	5.4	16	P	
CAU/123/15NL	05/03/71	15.47.30	44.0N	46.1E	4.5	N	S	
TUR/126/04NL	05/06/71	04.24.34	39.0N	29.7E	4.6	N	P	
CAU/126/02NL	05/06/71	12.23.07	43.6N	46.2E	4.5	N	S	
ICE/127/06NL	05/07/71	06.56.15	63.4N	29.2E	4.0	N	S	
NRS/129/19NL	05/09/71	19.06.31	66.0N	61.1E	3.6	N	S	
CAS/135/04NL	05/15/71	04.53.05	38.1N	49.1E	4.6	N	P	
KUR/135/21NL	05/15/71	21.03.46	43.4N	147.3E	4.7	48	P	
SIN/136/17NL	05/16/71	17.20.57	36.1N	77.9E	4.6	84	P	D
CHI/141/02NL	05/21/71	02.58.37	26.7N	101.8E	4.9	45	P	
KUR/142/07NL	05/22/71	07.32.17	43.3N	146.4E	4.3	42	P	
TUR/142/16NL	05/22/71	16.43.59	38.8N	40.5E	6.3	N	P	B, U
TUR/143/01NL	05/23/71	01.02.55	37.6N	30.1E	4.4	N	P	
EKZ/145/04NL	05/25/71	04.02.58	49.8N	78.2E	5.2	O	P	
KUR/146/01NL	05/26/71	01.46.11	43.5N	146.7E	4.7	59	N	
TDZ/147/00NL	05/27/71	00.30.28	38.3N	69.0E	4.8	36	P	
KUR/147/16NL	05/27/71	16.50.31	43.8N	146.4E	5.2	36	P	
KOM/148/10NL	05/28/71	10.21.43	55.8N	166.6E	4.5	N	P	
KUR/150/00NL	05/30/71	00.21.43	45.9N	150.9E	4.4	70	P	IE, U
KUR/152/21NL	06/01/71	21.20.27	43.6N	150.2E	4.6	N	P	

TABLE I-2

LIST OF EDITED NORSAR LP EVENTS
(PAGE 2 OF 7)

Designation	Date	Origin Time	Lat.	Long.	m_b	Depth	Source Bulletin	Comment
TIB/155/20NL	06/04/71	20.49.58	32.2N	92.1E	5.0	N	P	
CHI/156/10NL	06/05/71	10.21.28	37.3N	113.7E	4.7	N	P	
EKZ/157/04NL	06/06/71	04.02.57	50.0N	77.8E	5.5	0	P	
TUR/161/09NL	06/10/71	09.31.55	39.1N	29.6E	4.9	N	P	
AFG/161/09NL	06/10/71	09.42.51	36.5N	71.7E	4.5	383	P	IE, U
JAP/161/19NL	06/10/71	19.59.53	41.1N	138.4E	5.7	226	P	D
ERS/165/13NL	06/14/71	13.48.56	56.2N	123.6E	5.6	N	P	
ERS/165/14NL	06/14/71	14.25.57	56.2N	123.5E	4.6	N	P	
KAM/166/14NL	06/15/71	14.04.09	52.8N	160.8E	5.1	55	P	
SIN/166/22NL	06/15/71	22.04.13	41.5N	79.3E	5.6	N	P	
SIN/166/23NL	06/15/71	23.17.34	41.6N	79.2E	4.9	N	P	
SIN/167/13NL	06/16/71	13.46.50	41.3N	79.3E	5.1	N	P	B, U
KUR/168/09N3	06/17/71	09.32.05	44.4N	148.9E	4.9	N	P	B, U
EKZ/170/04NL	06/19/71	04.03.58	50.0N	77.7E	5.5	0	P	
CHI/170/08NL	06/19/71	08.10.21	39.1N	73.7E	4.2	N	S	M, U
SIN/170/17NL	06/19/71	17.23.03	41.5N	79.3E	5.2	N	P	
CHI/173/10NL	06/22/71	10.25.33	41.3N	79.3E	4.8	47	P	B, U
TIB/184/05NL	07/03/71	05.03.24	35.1N	80.3E	5.5	N	S	M, U
TIB/184/07NL	07/03/71	08.02.08	35.2N	80.9E	5.0	N	S	B, U
TIB/186/00NL	07/05/71	00.26.36	35.6N	80.2E	5.0	N	S	B, U
KUR/186/00NL	07/05/71	00.58.01	44.9N	152.4E	3.7	N	S	
KUR/189/06NL	07/08/71	06.48.30	49.7N	156.4E	4.1	N	S	
ERS/190/09NL	07/09/71	09.37.42	50.5N	132.6E	3.4	N	S	V, U
KUR/190/16NL	07/09/71	16.44.16	43.5N	147.7E	4.9	46	P	

TABLE I-2

LIST OF EDITED NORSAR LP EVENTS
(PAGE 3 OF 7)

Designation	Date	Origin Time	Lat.	Long.	m_b	Depth	Source Bulletin	Comment
KUR/191/02NL	07/10/71	02.04.27	50.6N	153.2E	3.6	31	S	
KUR/191/03NL	07/10/71	03.05.01	43.6N	147.7E	4.8	36	P	
KUR/191/09NL	07/10/71	09.01.35	45.0N	150.5E	4.6	N	P	
WRS/191/17N1	07/10/71	16.59.59	64.2N	55.2E	5.3	0	P	C, U
EKZ/192/05NL	07/11/71	05.10.37	52.0N	75.9E	3.7	N	S	M, U
KAM/193/02NL	07/12/71	02.12.30	53.1N	160.0E	4.9	N	P	
KUR/193/06NL	07/12/71	06.08.15	44.7N	149.0E	4.6	N	S	
CHI/194/02NL	07/13/71	02.56.58	39.0N	75.1E	4.3	62	P	
ERS/197/23NL	07/16/71	23.15.27	55.4N	123.7E	4.0	N	S	IE, U
WKZ/198/21NL	07/17/71	21.45.45	46.6N	54.8E	4.3	N	S	B, U
SIB/199/14NL	07/18/71	14.43.40	64.0N	97.7E	4.3	N	S	IE, U
SRS/200/20NL	07/19/71	20.41.20	49.1N	38.6E	3.8	N	S	
SRS/205/11NL	07/24/71	11.11.42	48.0N	28.2R	3.5	N	S	
TDZ/205/11NL	07/24/71	11.43.39	39.5N	73.2E	5.6	N	P	
KUR/205/12NL	07/24/71	12.37.31	48.3N	152.3E	3.6	N	S	
AFG/206/01NL	07/25/71	01.15.34	36.4N	70.7E	4.9	213	P	D
KAM/206/01NL	07/25/71	01.23.19	55.1N	162.6E	4.0	N	S	
KUR/206/08NL	07/25/71	08.35.19	44.2N	147.0E	4.0	N	S	IE, U
KUR/206/09NL	07/25/71	09.48.16	44.9N	152.4E	3.2	N	S	
CHI/206/12NL	07/25/71	12.52.45	29.0N	121.3E	4.2	N	S	M, U
SIN/207/01NL	07/26/71	01.48.34	39.9N	77.2E	6.0	N	P	IE, U
CHI/208/09NL	07/27/71	08.53.04	38.5N	78.2E	4.4	N	S	M, U
CHI/208/13NL	07/27/71	12.48.32	38.9N	78.1E	5.3	N	S	
KUR/209/12NL	07/28/71	02.40.03	45.9N	155.2E	4.1	25	S	IE, U

TABLE I-2

LIST OF EDITED NORSAR LP EVENTS
(PAGE 4 OF 7)

Designation	Date	Origin Time	Lat.	Long.	m_b	Depth	Source Bulletin	Comment
KUR/209/11NL	07/28/71	11.14.29	48.9N	154.7E	3.4	50	S	
BSA/210/19N1	07/29/71	19.40.15	42.5N	33.2E	4.5	N	S	
KUR/211/10NL	07/30/71	10.33.53	49.4N	155.7E	5.0	50	S	M, U
OKH/212/00NL	07/31/71	00.41.12	55.4N	149.1E	3.8	N	S	
SIB/212/01NL	07/31/71	01.11.30	61.5N	163.2E	3.5	N	S	
KUR/213/02NL	08/01/71	02.06.07	50.4N	156.8E	5.6	20	P	
WRS/213/11NL	08/01/71	10.53.53	57.6N	49.0E	4.3	N	S	
KUR/213/18NL	08/01/71	18.55.11	44.4N	148.9E	4.5	N	P	
KAM/213/21NL	08/01/71	21.42.35	55.5N	160.8E	3.9	40	S	M, U
HIN/216/00NL	08/04/71	00.24.37	36.3N	70.7E	5.6	206	P	B, IE, U
HIN/216/01NL	08/04/71	01.59.03	36.4N	70.8E	5.0	206	P	D
KAM/216/20NL	08/04/71	20.58.53	55.4N	161.9E	5.1	90	P	IE, U
KUR/217/10NL	08/05/71	10.55.51	45.0N	151.7E	4.5	60	P	
SIN/219/15NL	08/07/71	15.21.53	36.1N	77.7E	4.8	N	P	
TUR/219/17NL	08/07/71	17.07.24	38.9N	29.9E	4.5	20	P	
SIN/221/01NL	08/09/71	01.03.17	42.1N	83.4E	4.2	N	P	
IRA/221/02NL	08/09/71	02.54.37	36.3N	52.7E	5.2	27	P	
TUR/221/04NL	08/09/71	04.40.47	37.6N	29.8E	4.8	11	P	
TUR/221/11NL	08/09/71	11.32.31	37.6N	30.0E	4.4	28	P	B, U
KUR/224/20NL	08/12/71	20.57.58	49.7N	156.0E	4.5	45	P	
CHI/228/04NL	08/16/71	04.58.00	28.9N	103.7E	5.5	N	P	
CHI/228/13NL	08/16/71	13.29.25	28.8N	103.7E	4.8	N	P	B, U
CHI/228/18NL	08/16/71	18.53.55	28.9N	103.7E	5.3	N	P	B, U
TUR/229/04NL	08/17/71	04.29.33	37.1N	36.8E	5.0	N	P	

TABLE I-2

LIST OF EDITED NORSAR LP EVENTS
(PAGE 5 OF 7)

Designation	Date	Origin Time	Lat.	Long.	m_b	Depth	Source Bulletin	Comment
CHI/229/09NL	08/17/71	09.36.16	28.9N	103.7E	4.9	N	P	
CHI/229/17NL	08/17/71	17.07.40	28.9N	103.7E	4.9	N	P	
KUR/230/19NL	08/18/71	19.58.21	43.7N	147.5E	4.7	60	P	
KUR/231/22NL	08/19/71	22.15.38	49.3N	155.4E	6.0	N	P	B, U
NRS/233/19NL	08/21/71	19.34.23	81.9N	118.9E	4.6	N	P	
IRA/234/17NL	08/22/71	17.54.15	30.1N	50.7E	5.1	N	P	
CHI/235/05NL	08/23/71	05.36.11	28.8N	103.7E	5.2	N	P	U, double event
KUR/235/21NL	08/23/71	21.55.18	45.6N	151.0E	5.7	N	P	
KUR/236/09NL	08/24/71	09.52.52	45.3N	151.3E	4.7	N	P	
CRS/236/16NL	08/24/71	16.33.23	52.2N	91.4E	5.2	N	P	
IRA/237/00NL	08/25/71	00.38.35	28.2N	52.3E	4.1	N	P	
IRA/238/06NL	08/26/71	06.55.09	30.0N	50.7E	4.8	45	P	
IRA/239/05NL	08/27/71	05.20.15	30.2N	50.7E	5.0	54	P	
IRA/239/07NL	08/27/71	07.59.11	30.1N	50.7E	4.4	63	P	
SRS/240/16NL	08/28/71	16.34.44	37.6N	55.8E	4.8	N	P	
SIN/241/15NL	08/29/71	15.16.57	36.5N	78.5E	5.0	N	P	
HIN/243/01NL	08/31/71	01.52.17	36.5N	70.8E	4.3	87	P	D
CHI/249/21NL	09/06/71	21.46.46	43.8N	123.6E	3.8	N	P	
URL/250/15NL	09/07/71	15.35.28	68 N	66 E	3.6	N	N	
SWR/251/12N3	09/08/71	12.56.33	45 N	44 E	4.2	N	N	IE, M, U
TRS/251/22NL	09/08/71	22.35.16	41.1N	43.8E	4.8	N	P	
CHI/252/14N1	09/09/71	14.25.35	43.8N	123.6E	3.9	N	S	IE, U

TABLE I-2

LIST OF EDITED NORSAR LP EVENTS
(PAGE 6 OF 7)

Designation	Date	Origin Time	Lat.	Long.	m_b	Depth	Source Bulletin	Comment
ERS/256/14NL	09/13/71	14.26.01	52.3N	133.8E	3.7	N	S	
CHI/258/07NL	09/15/71	07.10.47	33 N	101 E	4.2	N	N	
CHI/258/11NL	09/15/71	11.22.43	34 N	101 E	4.2	N	N	
TDZ/259/10NL	09/16/71	10.59.27	40 N	68 E	4.2	N	N	
CAU/262/06NL	09/19/71	06.44.49	43.0N	47.1E	4.4	N	S	
WRS/262/11NL	09/20/71	11.00.07	57.8N	41.1E	4.5	N	P	
BLS/263/06NL	09/20/71	06.16.58	44.0N	33.0E	4.0	N	S	
BLS/263/08NL	09/20/71	08.02.51	43.2N	32.9E	4.2	N	S	
BLS/263/10NL	09/20/71	10.57.49	43.3N	32.3E	4.2	N	S	
ERS/266/21N1	09/23/71	21.08.03	53.4N	120.3E	4.2	15	S	
AFG/268/08NL	09/25/71	08.53.71	37.8N	69.7E	4.5	56	P	
KSH/269/16N1	09/26/71	16.30.27	35.8N	74.9E	4.4	N	N	M, U
TDZ/269/17N2	09/26/71	17.00.02	37.4N	72.5E	4.4	N	N	M, U
HIN/269/23NL	09/26/71	23.48.06	37 N	71 E	4.6	N	N	M, U
NRS/270/05N3	09/27/71	05.59.55	73.4N	55.1E	6.4	0	P	C
SIN/273/10N2	09/30/71	10.48.51	44.6N	81.4E	4.0	N	S	
SIN/273/12NL	09/30/71	12.43.45	50 N	88 E	4.5	N	N	
TDZ/274/16NL	10/01/71	16.27.48	38.6N	69.8E	4.9	36	P	
WRS/277/10NL	10/04/71	10.00.02	61.6N	47.1E	5.1	13	P	IE
AFG/277/20NL	10/04/71	20.59.52	36.3N	71.9E	4.3	N	N	B, U
SIN/281/09NL	10/08/71	09.20.13	40.9N	79.4E	4.4	N	S	
EKZ/282/06NL	10/09/71	06.02.57	50.0N	77.7E	5.4	0	P	
CHI/283/05NL	10/10/71	05.53.57	33.9N	95.0E	4.4	N	N	
CAU/283/09NL	10/10/71	09.06.06	43.1N	43.8E	4.0	15	S	

TABLE I-2

LIST OF EDITED NORSAR LP EVENTS
(PAGE 7 OF 7)

Designation	Date	Origin Time	Lat.	Long.	m_b	Depth	Source Bulletin	Comment
IND/283/19N3	10/10/71	19.02.45	26.2N	94.2E	4.7	N	N	
IRA/288/14N1	10/15/71	14.19.32	37.3N	54.6E	4.7	39	P	
CAU/288/17NL	10/15/71	17.08.06	41.4N	48.6E	4.9	N	P	
EKZ/294/06NL	10/21/71	06.02.57	50.0N	77.6E	5.6	0	P	
CKZ/301/13NL	10/28/71	13.44.49	43.1N	67.1E	4.3	N	N	M, U
KRG/301/13N2	10/28/71	13.30.57	41.9N	72.4E	5.5	N	P	
UZB/301/16N3	10/28/71	16.14.16	39 N	65 E	4.0	N	N	M, U
TIB/302/17NL	10/28/71	17.16.52	34 N	86 E	5.0	N	N	
ALN/310/22N1	11/06/71	22.00.00	51.1N	179.1E	6.8	2	P	
EKZ/349/07NL	12/15/71	07.52.59	50.0N	77.9E	4.9	0	P	
WKZ/356/06NL	12/22/71	06.59.56	47.9N	48.2E	6.0	0	P	
EKZ/364/06NL	12/30/71	06.20.58	49.7N	78.1E	5.8	0	P	

Abbreviations:

T = timing word errors

IE = interfering event

C = interfering calibration

B = bad spikes, glitches, clips, etc.

M = erroneous source parameters

U = unuseable data

V = vertical components look alike

P = PDE Bulletin

S = SAAC/LASA Bulletin

N = NORSAR Bulletin

D = Too Deep

The processing of the large volume of data produced a large amount of information in the form of time domain plots, spectra and so on. For conciseness, we have condensed the results wherever possible to the form of graphs and tables or representative samples.

SECTION II

NOISE ANALYSIS

A. INTRODUCTION

The objective of the noise analysis was to characterize the NORSAR noise field. The following information has been compiled:

- Spectral Content
- Spatial Variability
- Time Variability
- Noise Directionality
- Coherence

B. DATA

The data samples used in this study are given by day, hour, length and number of available sites in Table II-1. The samples were taken at approximately ten day intervals when, with few exceptions, at least one hour of noise was available.

The data were sampled at two second intervals and segmented into 256 second segments. These data were then examined for bad or dead sites and bad components and the bad sites were omitted from further processing. The segments containing spikes, glitches, and signals were also eliminated. A crosspower matrix (CPS) was generated for each noise sample at 64 frequencies from 0.00 to 0.250 Hz ($\Delta f = 0.00391$Hz) by:

- Discrete Fourier transforming individual segments for each component and site.

TABLE II-1

NORSAR NOISE SAMPLES

Day	Start Time	Length	No. of Sites Available
121	18:00	00.39.24	16
135	10:00	01.33.52	8
141	05:00	01.16.48	14
150	13:21	00.57.28	14
164	10:00	04.37.20	14
171	12:15	01.16.48	14
191	23:00	00.51.12	11
201	02:00	00.59.44	18
211	16:37	01.12.32	15
220	20:20	04.24.32	19
231	19:50	02.04.44	17
241	17:00	02.42.08	15
250	20:37	01.55.12	16
256	18:00	06.02.40	14
261	05:20	03.03.28	16
272	17:00	01.50.58	17
281	05:20	01.21.04	16
291	08:50	00.59.44	16
301	00:06	01.38.08	16
310	04:00	02.20.48	14
321	20:15	04.09.28	20
332	06:00	04.03.12	19
340	07:45	02.16.32	18
348	04:00	02.16.32	15
361	20:00	02.29.10	17
009	16:30	06.19.44	18

- Hanning the transforms
- Cross multiplying to obtain crosspower terms
- Stacking the crosspowers

The components were not rotated and were processed separately as Vertical, North-South and East-West.

After generating the CPS matrices, the single channel power spectra were examined to eliminate anomalous data and components from further processing. Further processing consisted of beam-forming, frequency-wave-number power spectra (conventional and high resolution) and multichannel coherencies.

Amplitude and phase calibrations for NORSAR sites were not available so none of the spectra are corrected for instrument response. The nominal value of 2.47 millimicrons per computer count at 25 seconds (0.04 Hz) was used to normalize the power density spectra.

The number of sites available (Table II-1) is further amplified in Figure II-1, to give the percentage of times a particular site was omitted from the processing. The reasons for eliminating the worst offenders are:

- Site 2 E-W was parallel to the N-S component from day 152 to day 229.
- Site 6 N-S has had a high noise level and glitches.
- Site 9 horizontal components were switched from about day 291 through day 009/72.
- Site 10 E-W had spikes and a high noise level 60% of the time from day 121 to 261, but has been usable continuously after these dates.

FIGURE II-1
PERCENTAGE OF TIMES
SITE REJECTED
(26 NOISE SAMPLES)

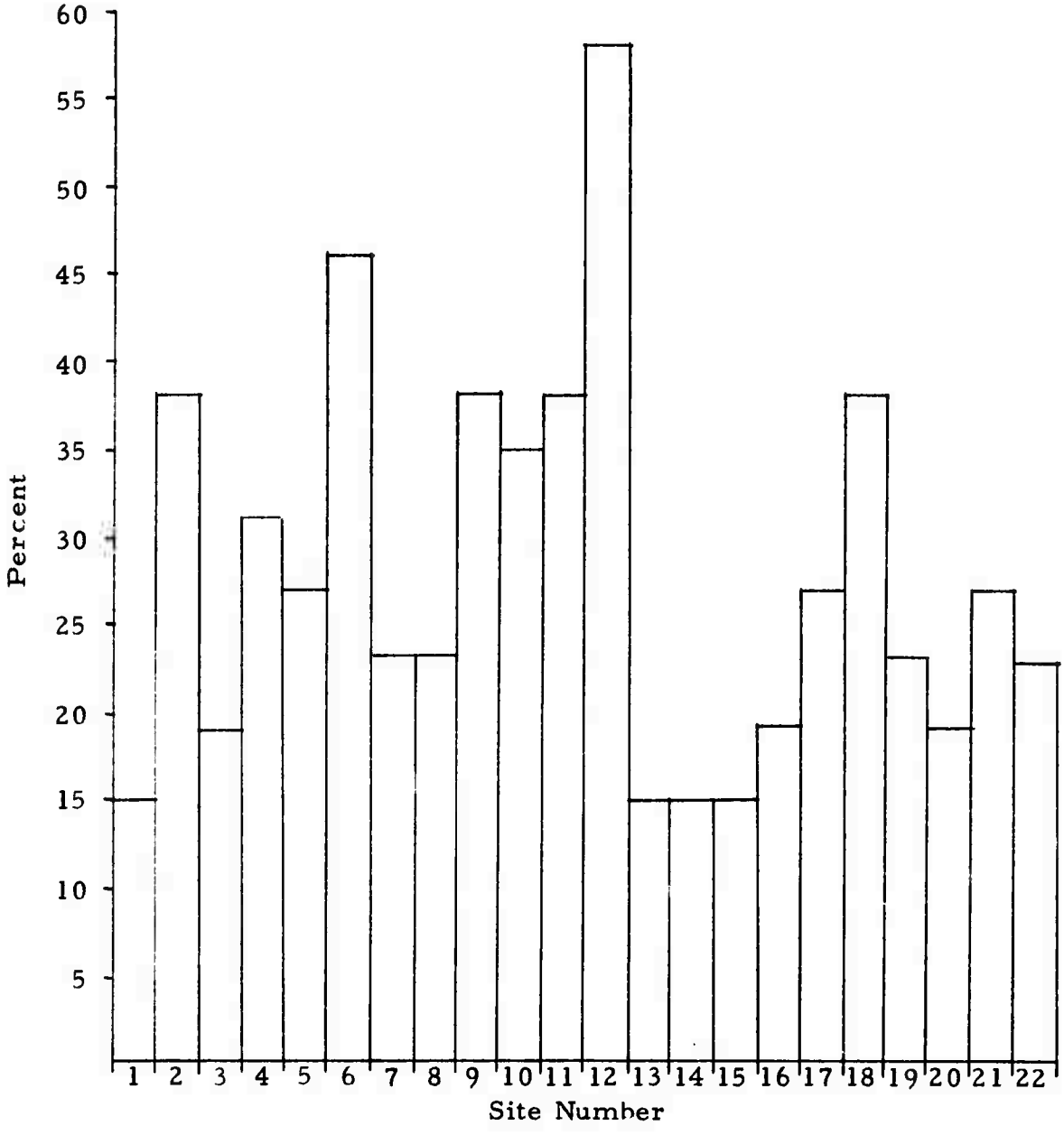

- Site 11 horizontal components have had a high incidence of spikes and glitches.
- Site 12 vertical was troubled by intermittent high frequency chatter up to day 220. The horizontals also have had high noise levels.
- Site 18 (all three components) has been dead intermittently.

The average number of sites available for the noise analysis was 15. For the noise analysis the bandwidth 20 to 40 seconds (0.025 to 0.050 Hz) was used for the majority of processing because it is the expected signal bandwidth and because the results could be compared directly to other long period data.

C. SPECTRAL CONTENT

Single site power density spectra were generated on all noise samples to determine the general shape of the spectra and its variation day-to-day and site-to-site. Figures II-2 through II-7 show examples of single site power density spectra selected from the noise samples. Note that none have been corrected for instrument response, which perhaps explains the higher level of the verticals (relative to the horizontals) at frequencies above 0.10 Hz on most of these spectra.

Between days 121 to 231 the power spectra for day 220 (Figure II-4) is the most typical, with a fairly broad peak at 16-18 seconds and a slight secondary peak at 8-9 seconds. The noise spectrum of day 164 (Figure II-3) is similar to that of day 220 with the exception of the plateau around 50 seconds on the horizontals. The power of this long period energy varies considerably site to site (if it appears at all), indicating a near-site effect rather than propagating energy. This is confirmed by the multichannel coherence data (presented later) which shows this long period horizontal energy to be essentially incoherent.

The spectrum on day 191 (Figure II-2) has a different character than the other samples from this interval. The spectrum shows a narrow

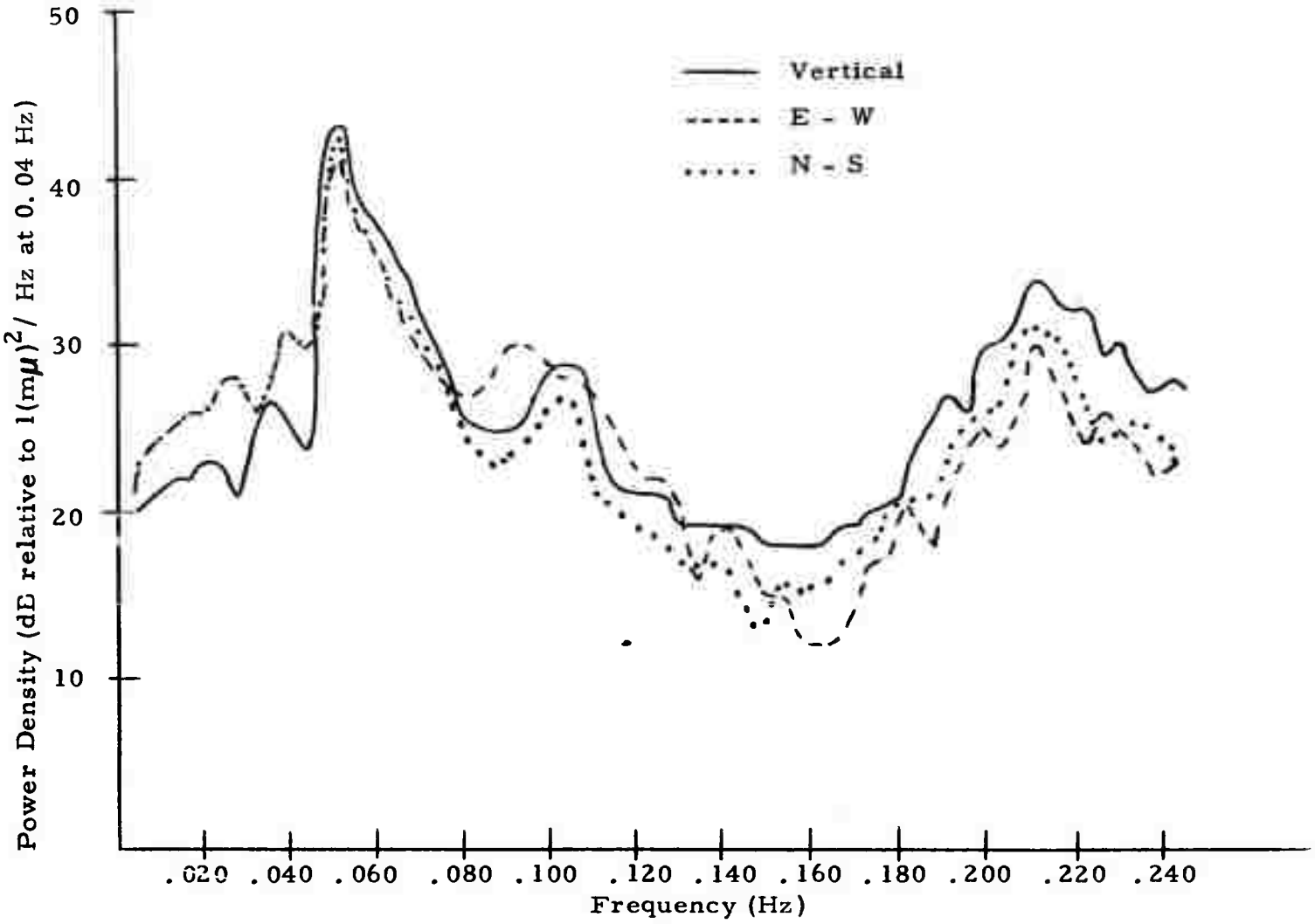

FIGURE II-2

NOISE SPECTRUM ON DAY 191 (SITE 1)

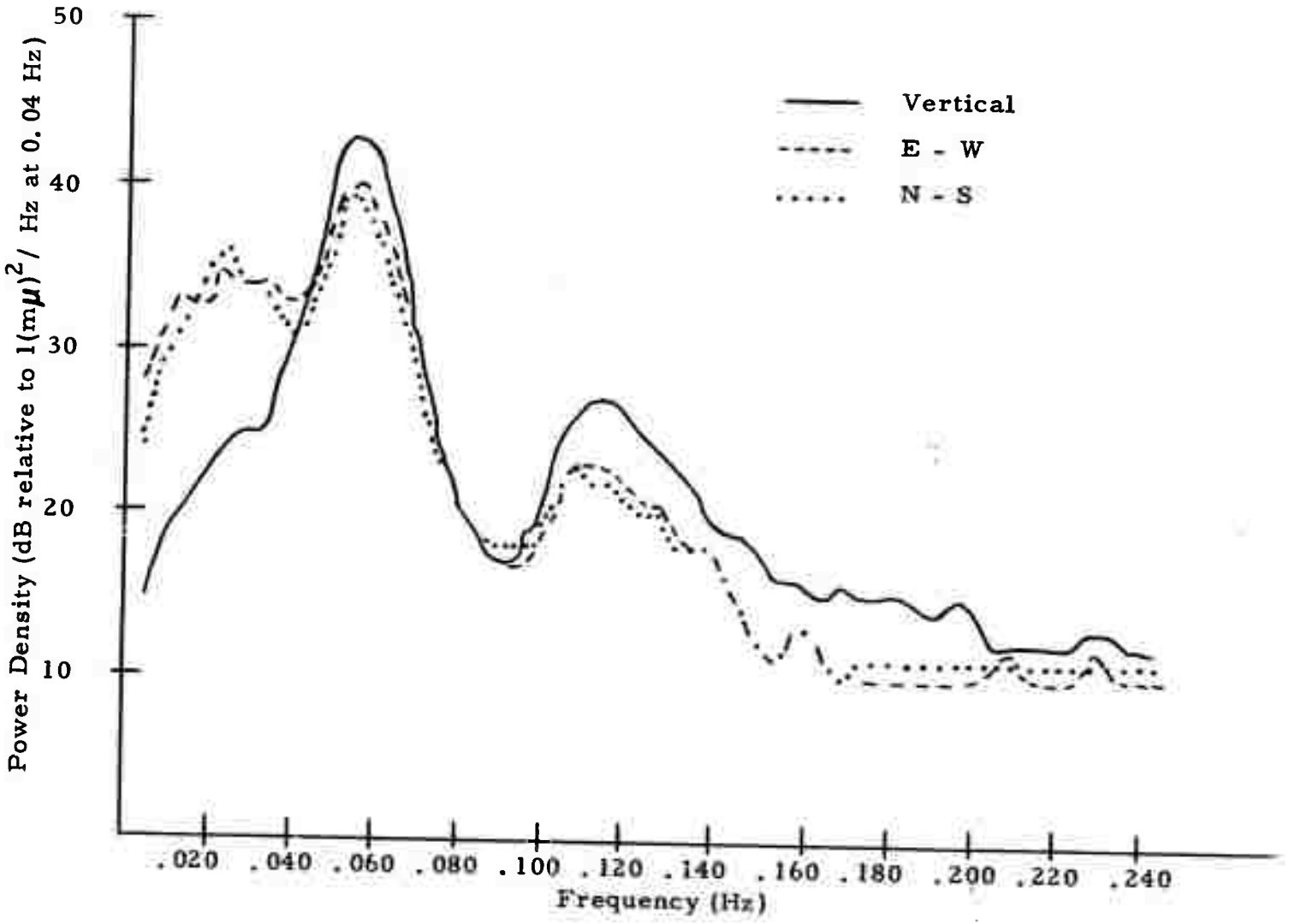

FIGURE II-3

NOISE SPECTRUM ON DAY 164 (SITE 4)

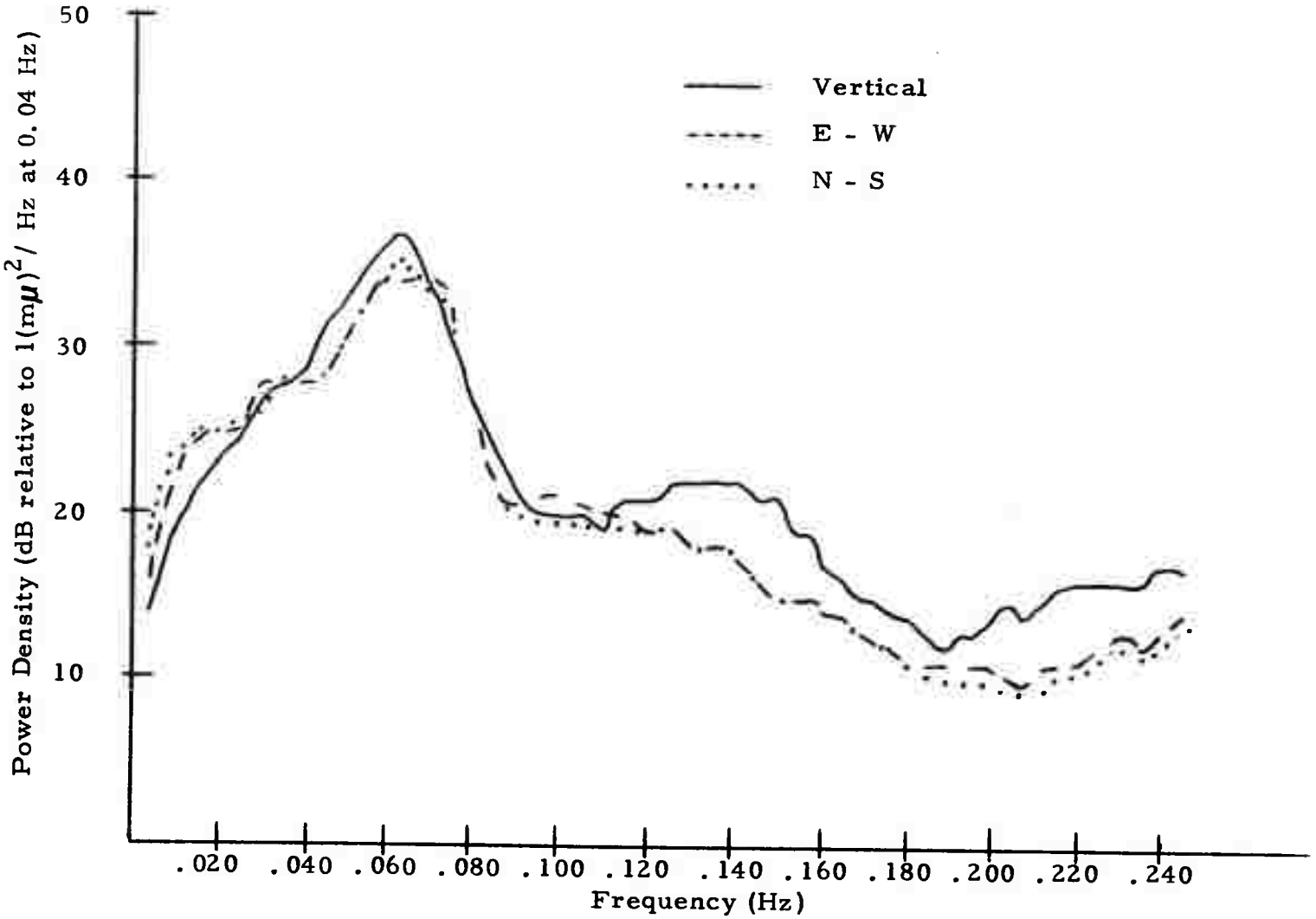

FIGURE II-4

NOISE SPECTRUM OF DAY 220 (SITE 22)

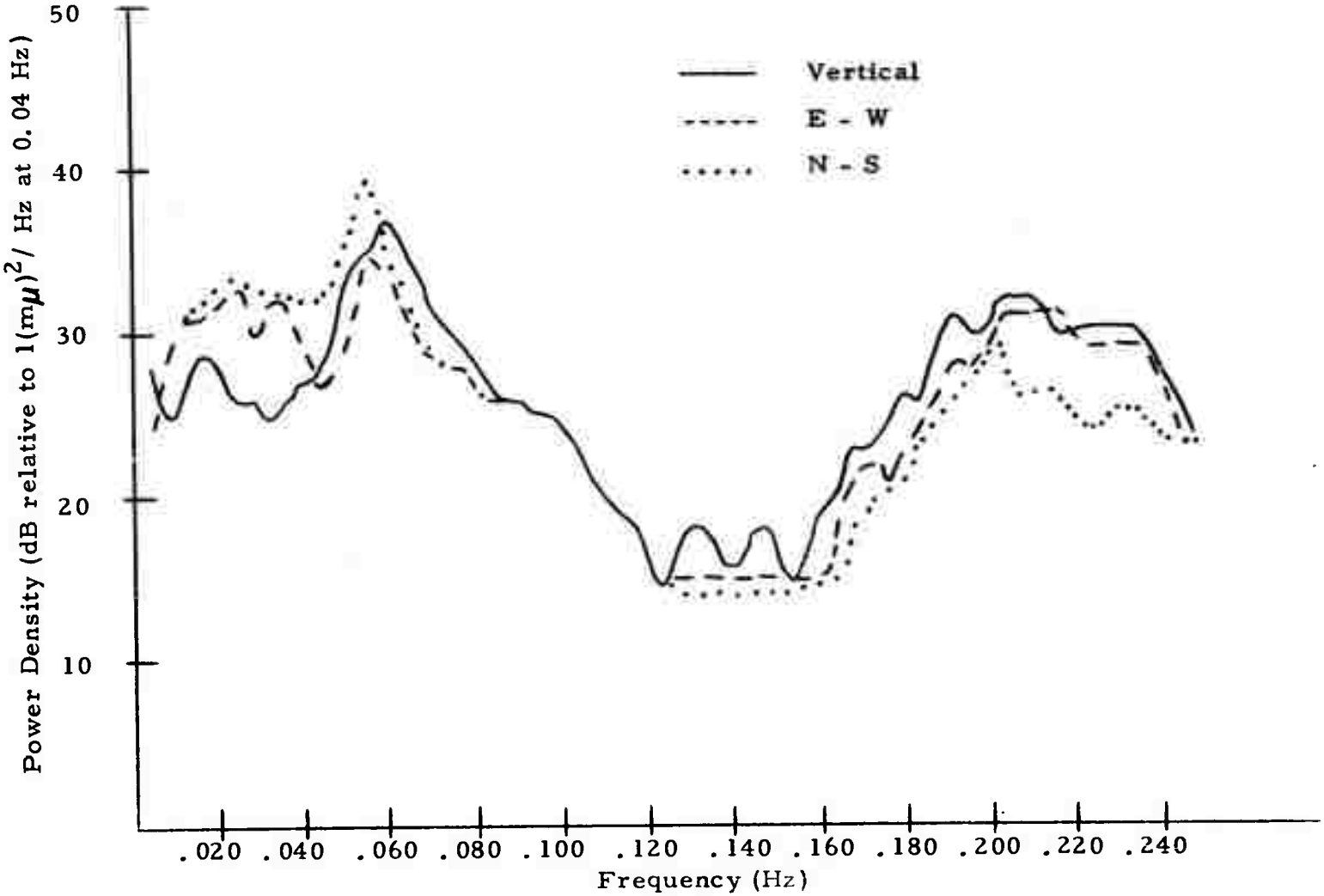

FIGURE II-5

NOISE SPECTRUM ON DAY 272 (SITE 1)

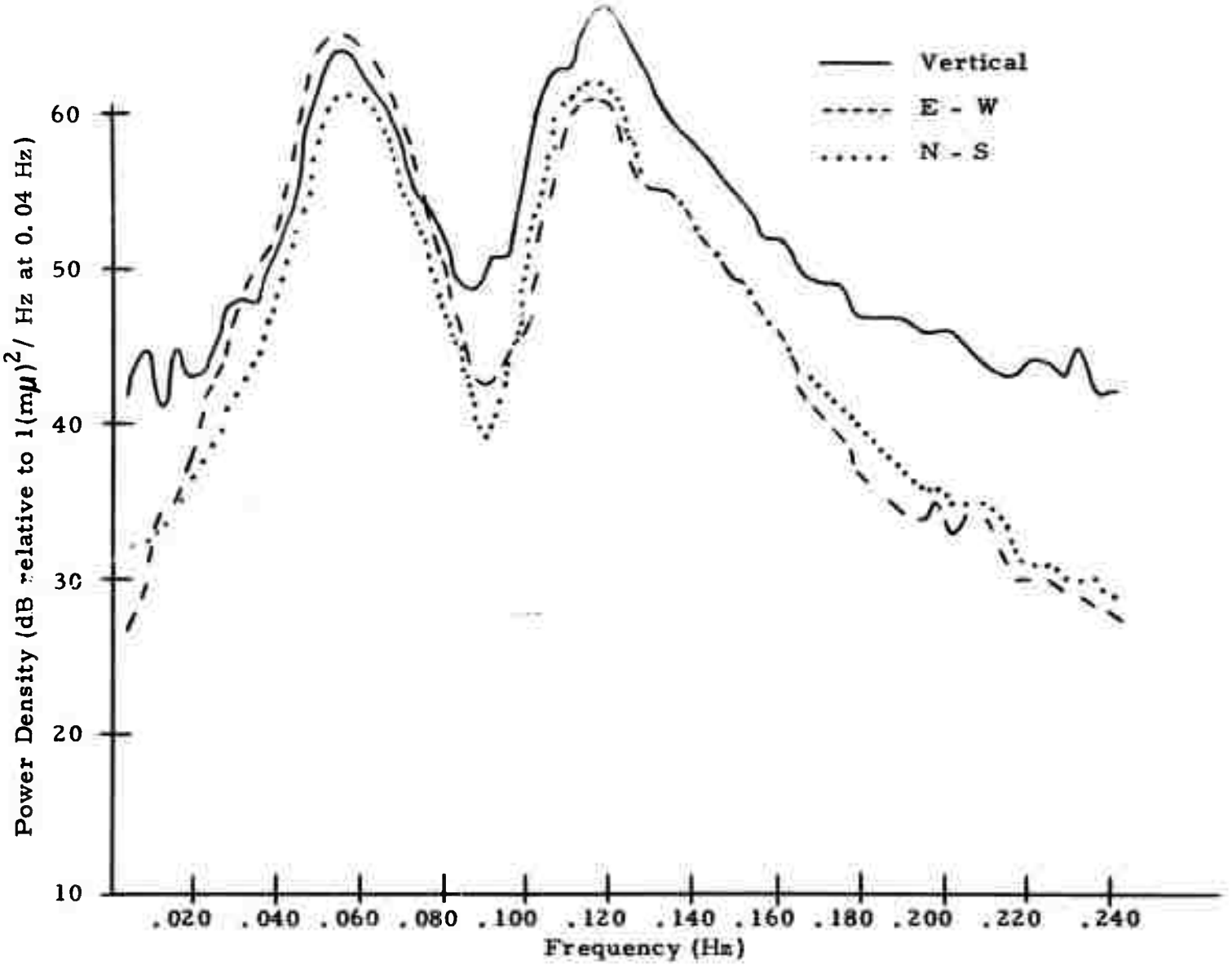

FIGURE II-6

NOISE SPECTRUM ON DAY 348 (SITE 22)

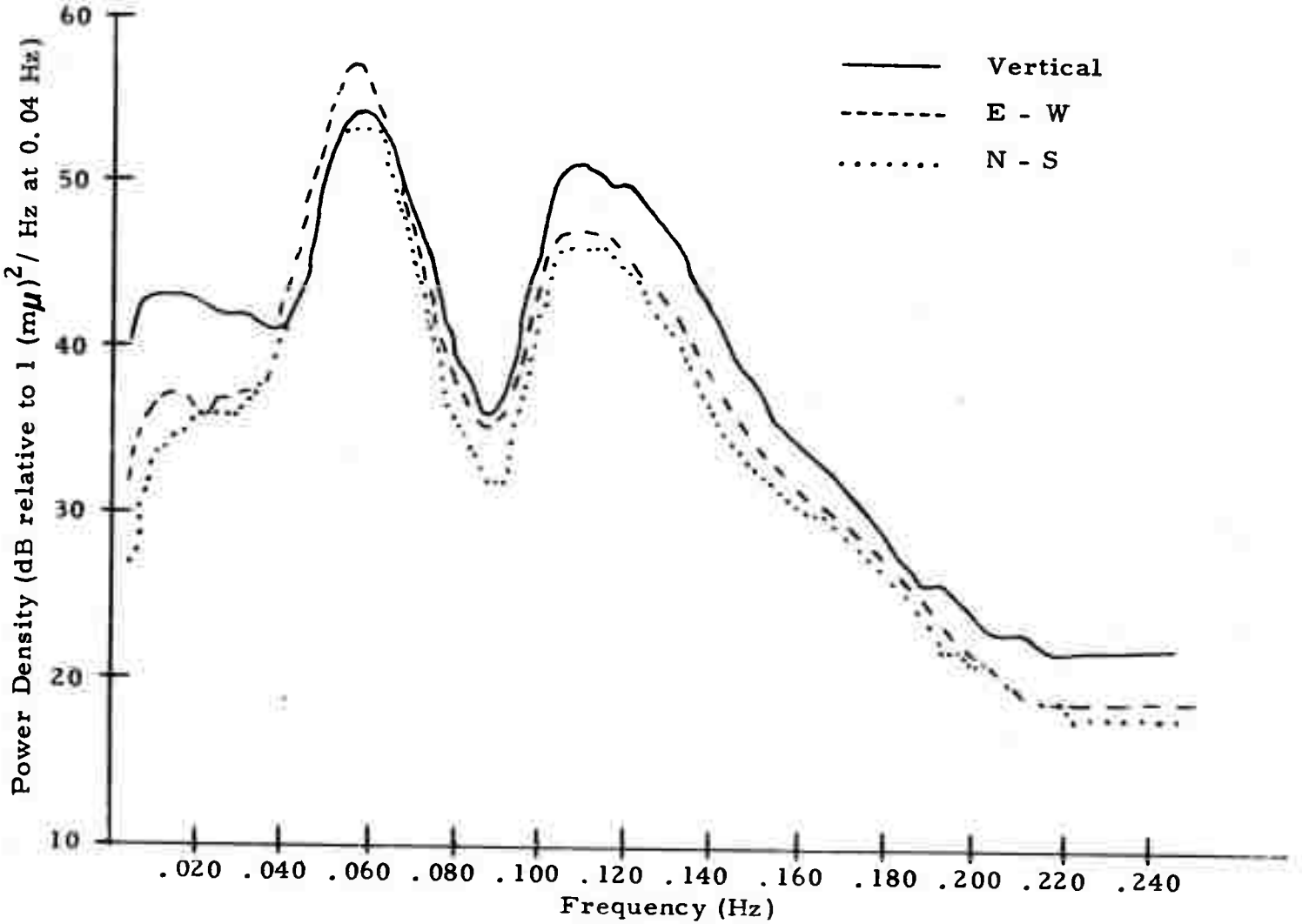

FIGURE II-7

NOISE SPECTRUM ON DAY 009/72 (AVERAGE SINGLE SITE)

microseismic peak at 16 seconds and a larger peak at 4-6 seconds. This spectrum is similar to that of day 272 (Figure II-5) and to others between days 231 and 321 (described below).

On days 231 to day 321 a strong broad peak from 4-6 seconds and slight evidence of the 8-10 second peak appears as characteristic features of the spectra. The 16 to 18 second peak also is present. Figure II-5 shows the day 272 spectrum, which is a typical example. The possibility of aliasing of the 4-6 second microseisms was investigated by sampling the data at one second intervals and regenerating the power spectra. The spectra of the re-sampled data were consistent with the original spectra and no significant aliasing effects were found.

From day 321 through day 009/72, 16 to 18 second and 8 to 10 second microseisms dominate the spectra. In addition, there is a significant increase in power density levels over the entire spectra. Figures II-6 and II-7 show typical spectra from this time period.

D. SPATIAL VARIABILITY

The purpose of the analysis described in this subsection was to check for particularly noisy sites or gain inequalities between sites in the 20 to 40 second band.

Because an unusually noisy site or gain inequalities might be expected to be time independent, the RMS value in millimicrons (mμ) of the 20 to 40 second band was averaged by site and component from day 121 to 301. Days 135 and 191 were omitted due to the large variability of the long period energy on these days. Also, the RMS values of the two horizontals were averaged.

Figures II-8 shows the vertical and average horizontal RMS values for each site. The average RMS value for the verticals is 6.6 mμ and

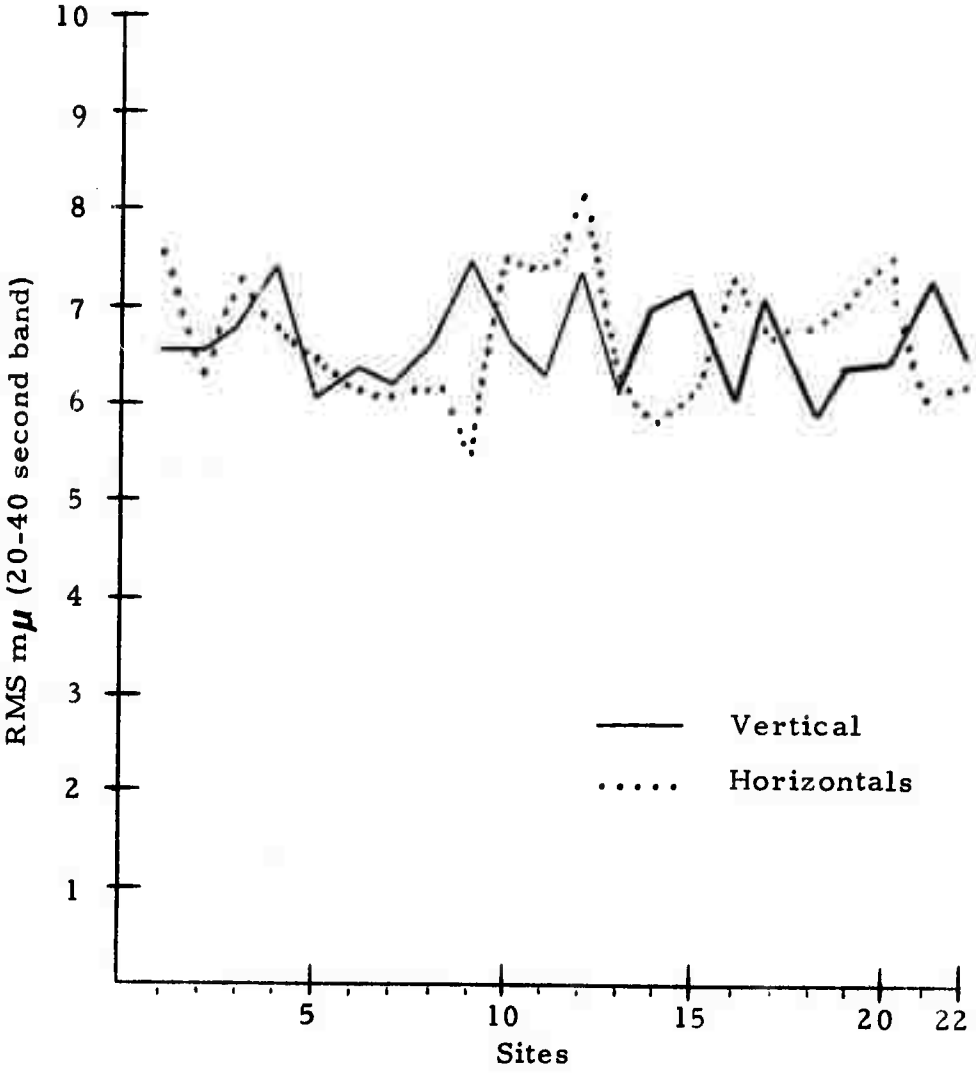

FIGURE II-8

SQUARE ROOT OF AVERAGE POWER
(20 TO 40 SECOND PERIOD BAND) VS SITE

for the horizontals is 6.4 mμ. The maximum variation is 2 dB, which compares with the results for ALPA (Texas Instruments, 1971). These results show that the NORSAR noise field does not vary significantly across the array and also implies that the seismometers are well equalized site-to-site.

E. TIME VARIABILITY

The RMS level of the noise samples in the 20-40 second band was plotted versus time to determine whether noise levels were seasonally dependent. Each RMS level was computed over the entire sample. Figure II-9 shows the variation of the average (across sites) noise in mμ versus day for the vertical and the horizontals (which again were averaged). There is a definite seasonal dependence of the noise levels. From day 121 to day 300 the noise level was reasonably flat; after day 320 the level increased by about a factor of three (excluding the very high level on day 348). This implies a decrease of about 0.5 M_s units in the array's detection threshold during winter noise. However, the increase in multichannel filter performance and change in noise azimuth (both discussed later) may partially offset this loss due to increased noise level.

More noise samples will be needed after day 009/72 to determine when the levels drop back to summer values.

F. NOISE DIRECTIONALITY

In order to investigate possible noise sources at NORSAR and to further investigate the seasonal dependence of the noise power level, the direction of the noise spectral peak was obtained from wavenumber spectral analysis.

Table II-2 gives the day, frequency, dominant noise azimuth and velocity for each of the twenty-six samples. The frequencies used were those corresponding to maximum values in the power density spectra on each day (Figure II-10). The azimuths and velocities are from high-resolution

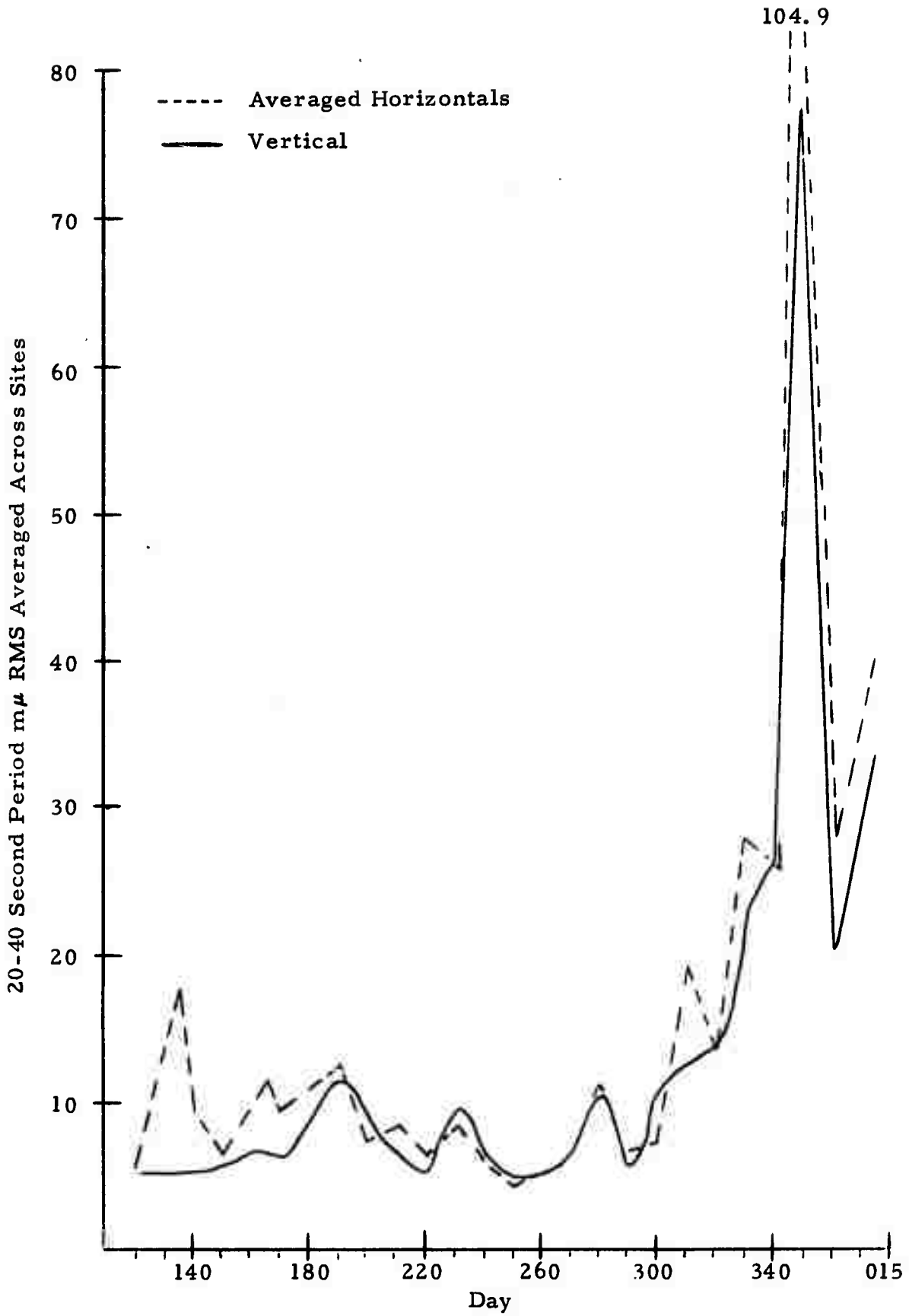

FIGURE II-9

AVERAGE SITE AMPLITUDE - mμ RMS
(20-40 SECOND PERIOD) VS DAY OF YEAR

TABLE II-2

VERTICAL PEAK POWER AZIMUTH AND VELOCITY

Day	Frequency	Azimuth	Velocity km/sec
121	.059	197°	3.6
135	.059	92°	3.8
141	.055	108°	3.8
150	.066	5°	3.6
164	.059	240°	3.8
171	.051	195°	3.7
191	.051	90°	3.7
201	.059	60°	3.8
211	.059	100°	3.6
220	.059	303°	3.7
231	.078	0°	3.3
241	.059	92°	3.6
250	.059	95°	3.8
256	.055	65°	3.6
261	.055	290°	3.7
272	.055	85°	3.7
281	.074	40°	3.6
291	.082	285°	3.5
301	.078	5°	3.5
310	.082	252°	3.6
321	.066	282°	3.6
332	.062	255°	3.6
340	.055	277°	3.7
348	.059	0°	3.7
361	.062	290°	3.7
009/72	.055	0°	3.8

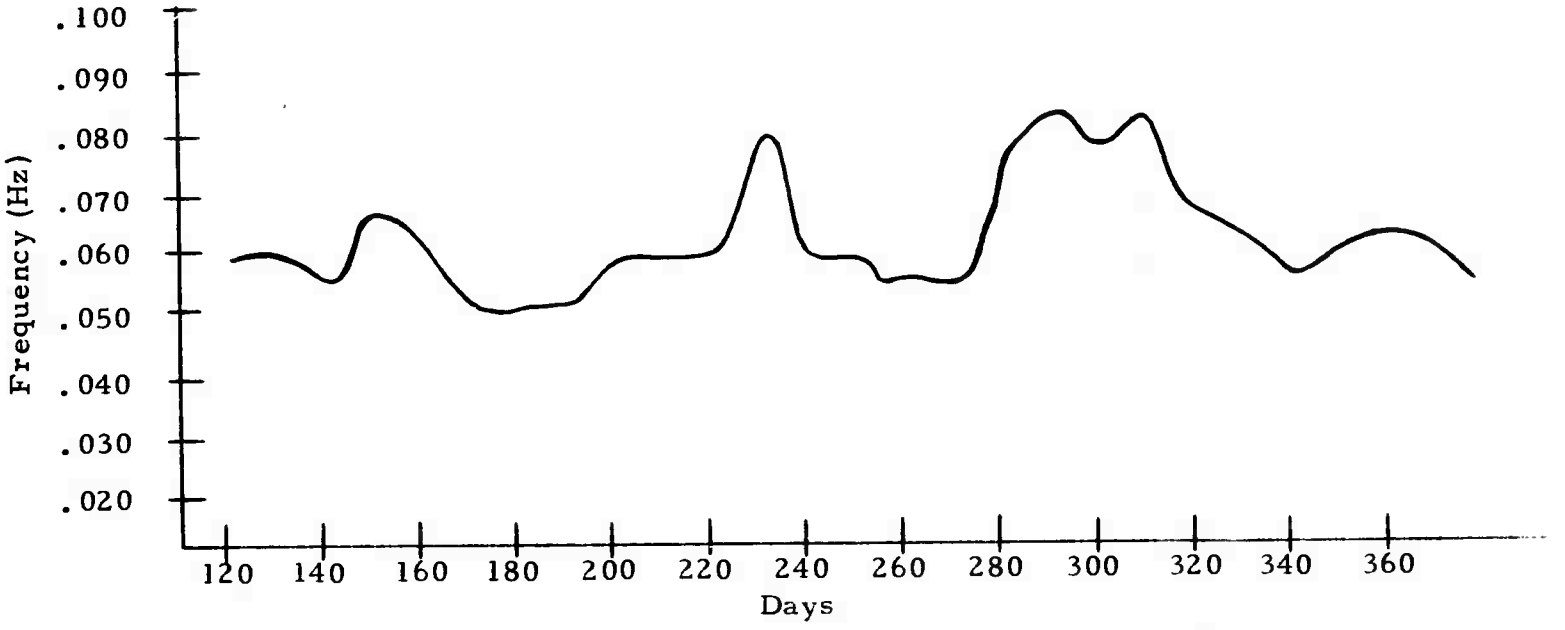

FIGURE II-10

FREQUENCY OF MICROSEISMIC PEAK VS DAY

frequency-wavenumber spectra. Because the horizontals contained both Love and Rayleigh energy (Table II-2), velocities are confined to the verticals. The peak of the power spectrum was used because it is generally highly coherent. As can be seen in Figure II-10, the frequency of the microseismic peak is always above the 20 to 40 second band, however, the peak often is broad and can contribute significant power to the 20 to 40 second band.

As in the case of the noise levels, the noise azimuths also appear to be seasonally dependent. From days 121 to 291, 10 of the 17 samples have peak noise azimuths from the East (40° to 108°), but from day 291 through 009/72 (coincident with an increase in noise level) the peak azimuths are all from 252° to 5°.

A consideration of only the peak power azimuth is slightly misleading in that all of the wavenumber spectra for these noise samples have secondary peaks only 3 to 6 db down from the peak. Later figures show typical wavenumber spectra that were obtained.

Figure II-11 shows the 20 to 40 second RMS beamsteer noise level as a function of azimuth. The plot was obtained by forming beams at 30° increments for each of 15 summertime noise samples and averaging over all noise samples. Noise levels are slightly (2 db) lower between about 150° and 270°; since the noise generally propagates from the East during this time period, better rejection would be expected for "back azimuth" beam directions.

Of particular interest is the beam noise level for data beamsteered to 90° (the azimuth to Central Asia). Figure II-12 shows the 20 to 40 second RMS value on the 90° beam versus day. The general shape of this curve is similar to that of Figure II-9. Up to day 300 the beam noise is about 2 mμ except that day 191 has a 6 mμ level. The peak on day 191 is due to the propagating noise being highly peaked at exactly the beam direction; the array

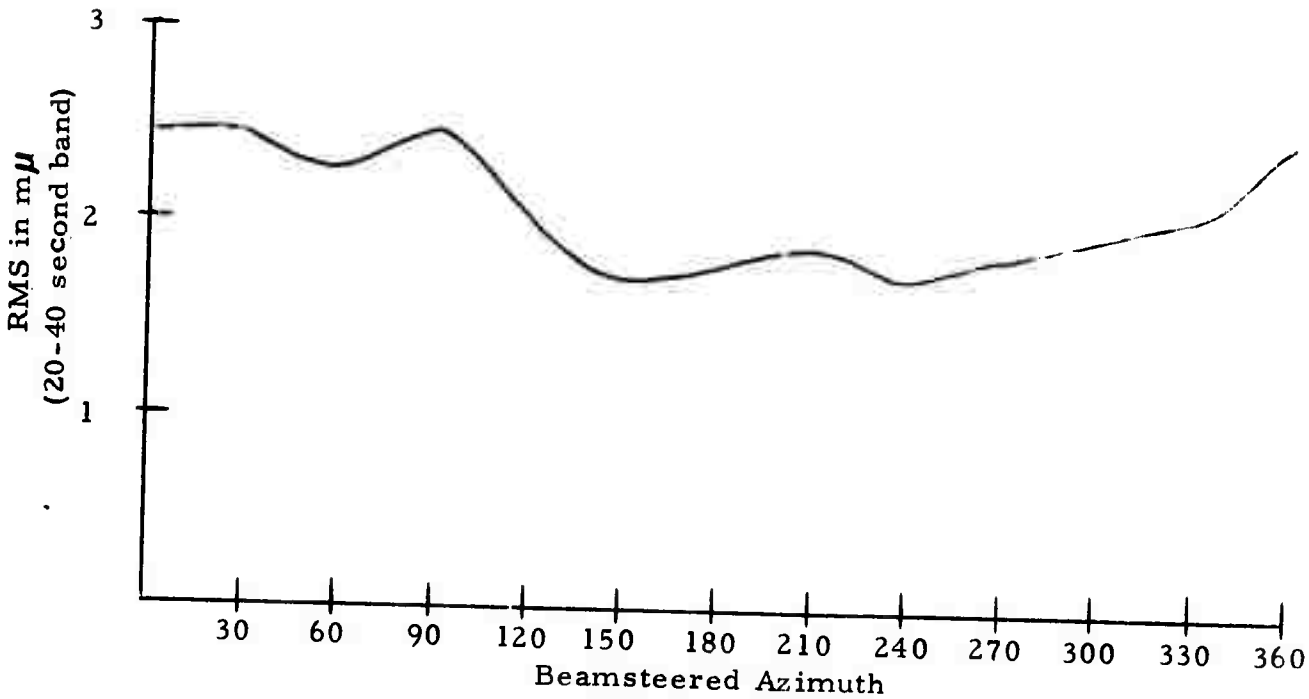

FIGURE II-11

AVERAGE (ACROSS DAYS) BEAMSTEERED AMPLITUDE
(mμ RMS 20-40 SECOND BAND) VS BEAM DIRECTION

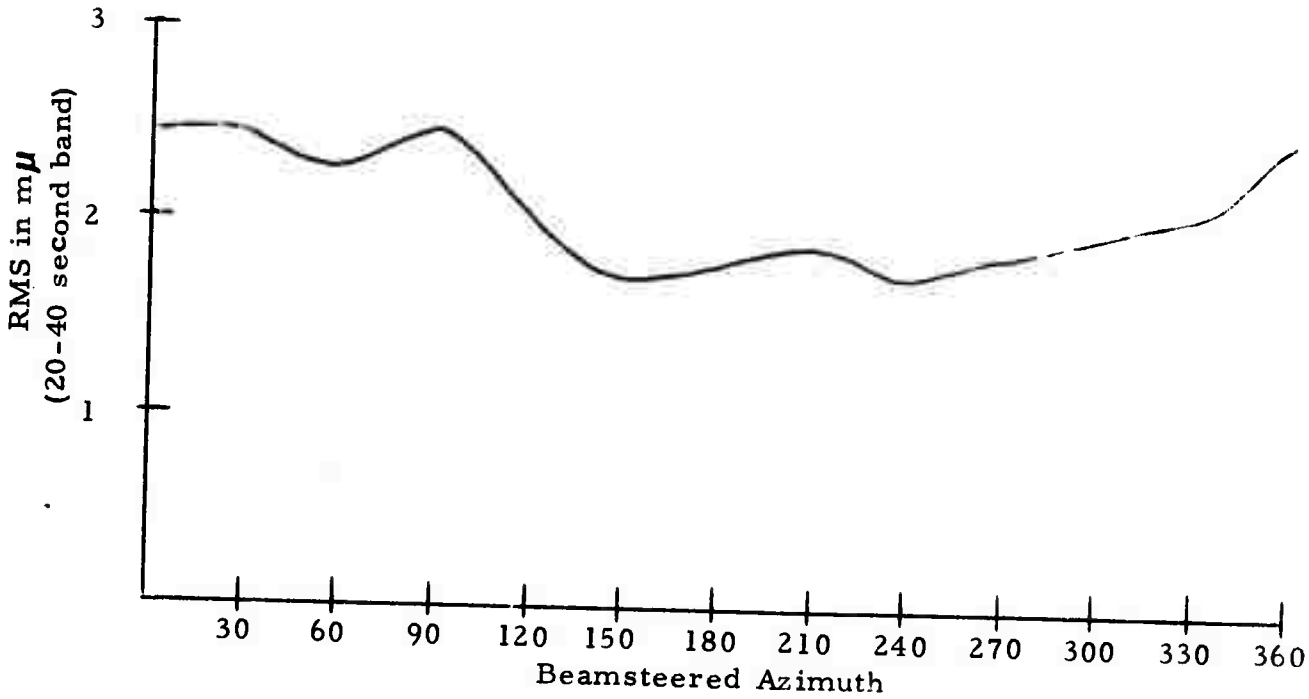

FIGURE II-11

AVERAGE (ACROSS DAYS) BEAMSTEERED AMPLITUDE
(mμ RMS 20-40 SECOND BAND) VS BEAM DIRECTION

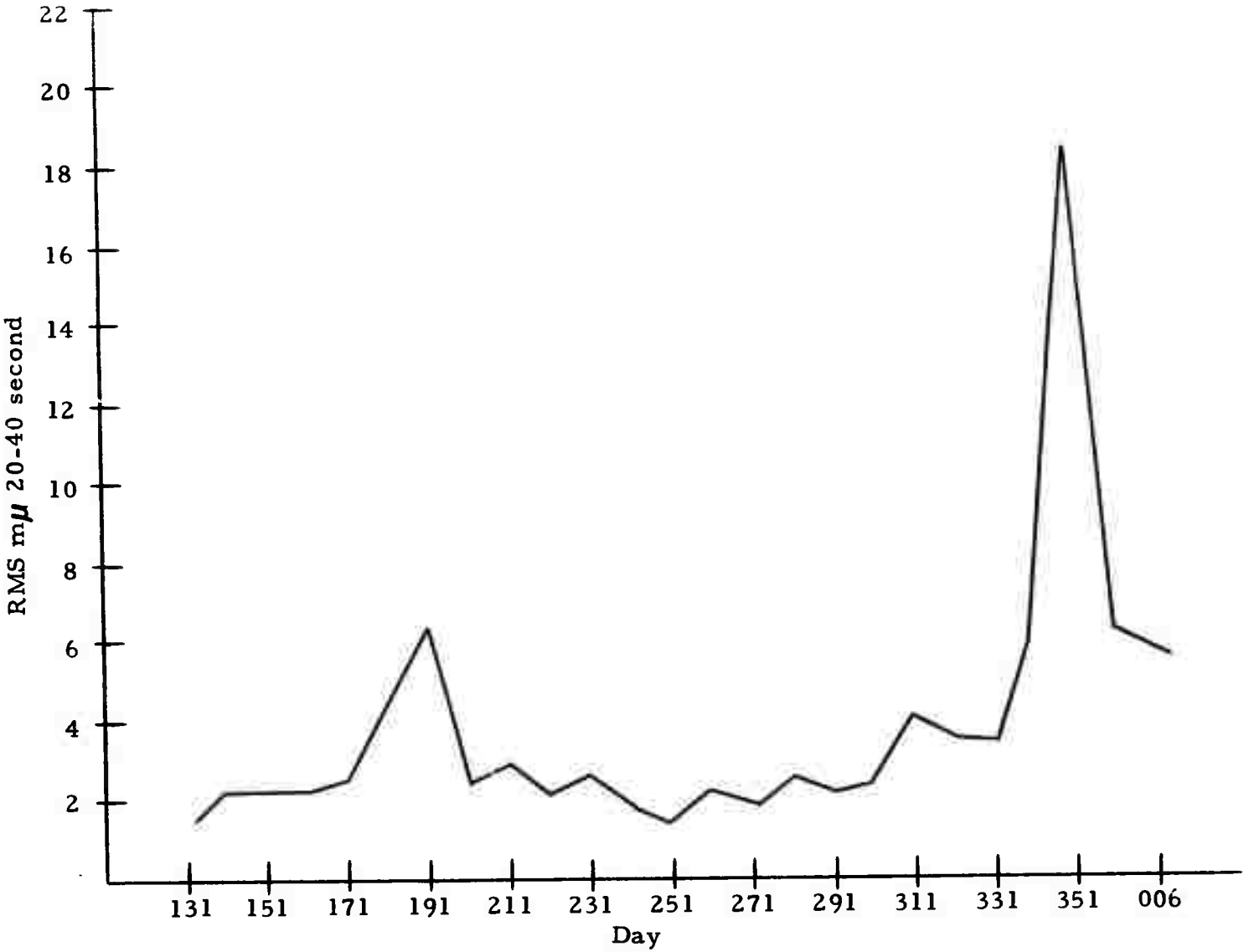

FIGURE II-12

AMPLITUDE IN mμ RMS (20-40 SECOND PERIOD BAND)
OF DATA BEAMSTEERED TO 90° AZIMUTH VS DAY

gave less than 6 db noise rejection for this sample. Other noise samples having a peak at about 90° were more diffuse in wavenumber space. After day 300 the beam noise appears to be 4 to 8 mμ. The high value at day 348 is due to the large increase in noise level on that day.

It is interesting to note that for noise samples up to day 291, the array averaged 10 db noise rejection. For samples after day 291 (when the noise generally propagated from the Northwest) the array averaged 13 db noise rejection. Thus the increase in winter noise levels is partially offset by increased array capability (for signals from the East). However the 90° beam noise levels are still at least a factor of two higher, implying a 0.3 M_s unit decrease in detection capability.

Figures II-13 to II-21 display the preliminary results of an attempt to correlate noise sources with ocean wave action. The nine figures are for noise samples on days 191, 348 and 361. The choices were made for the following reasons:

- Day 191: Summer noise sample with a high, narrow-band peak in the power density spectrum and a strong wavenumber spectral peak at 90° azimuth.
- Day 348: A winter sample with an extremely high noise level peaked at 0° in the wavenumber spectrum and spread over a wide range of azimuths from 268° to 7°.
- Day 361: A winter sample with a peak on the wavenumber spectrum at 290° and spread over a wide azimuth range from 266° to 40° but with a beam noise level and wave height chart similar to day 191.

The wave height charts (Figures II-13, II-16 and II-19) are reproduced from the National Weather Service charts updated and published every twelve hours and

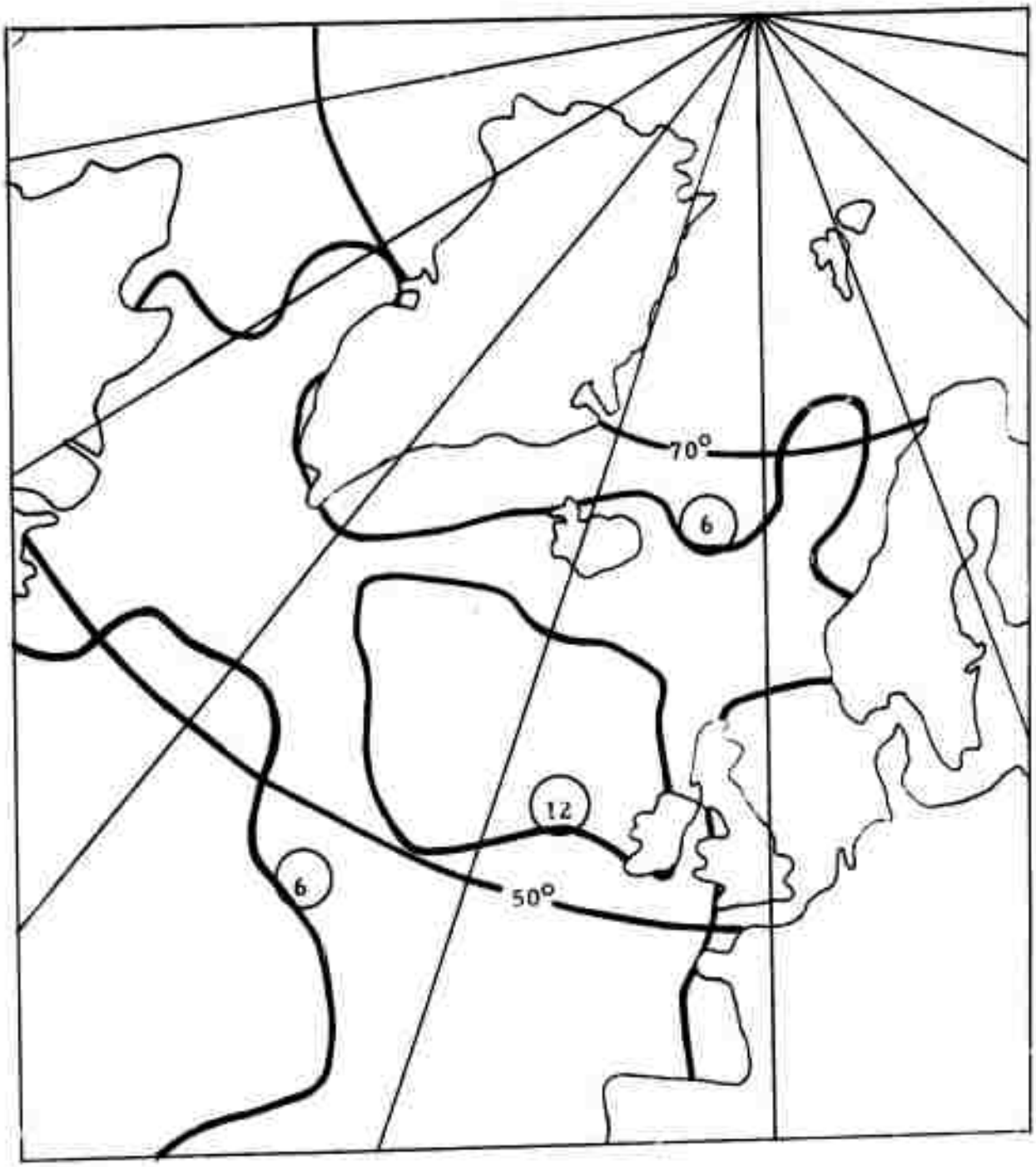

FIGURE II-13

COMBINED SEA & SWELL PROGNOSIS CHART
0000Z DAY 191 VALID FOR 24 HR. FROM 0000Z 10 JULY 1971

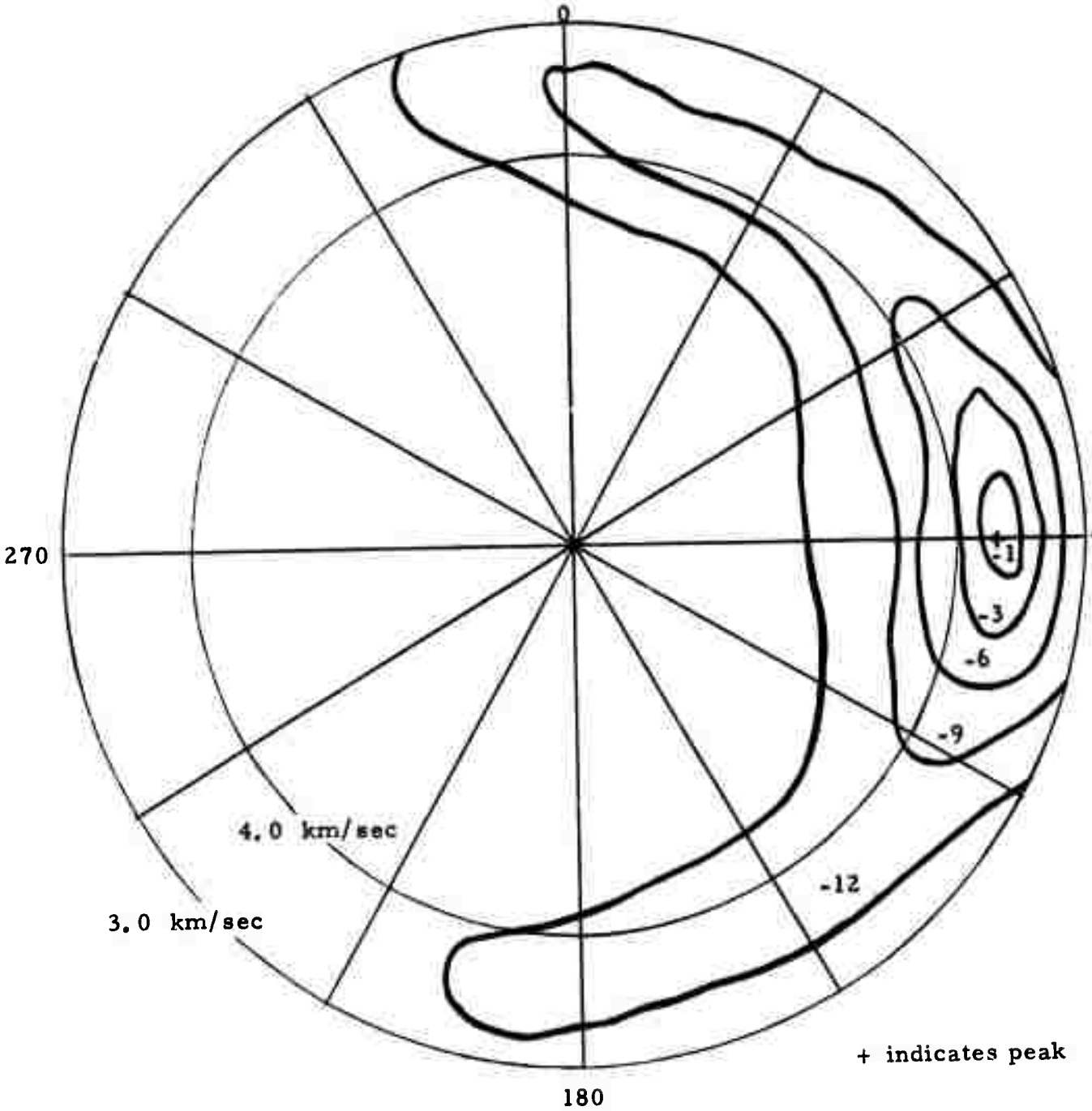

FIGURE II-14

VERTICAL HIGH RESOLUTION WAVENUMBER SPECTRA
AT 0.051 Hz ON DAY 191

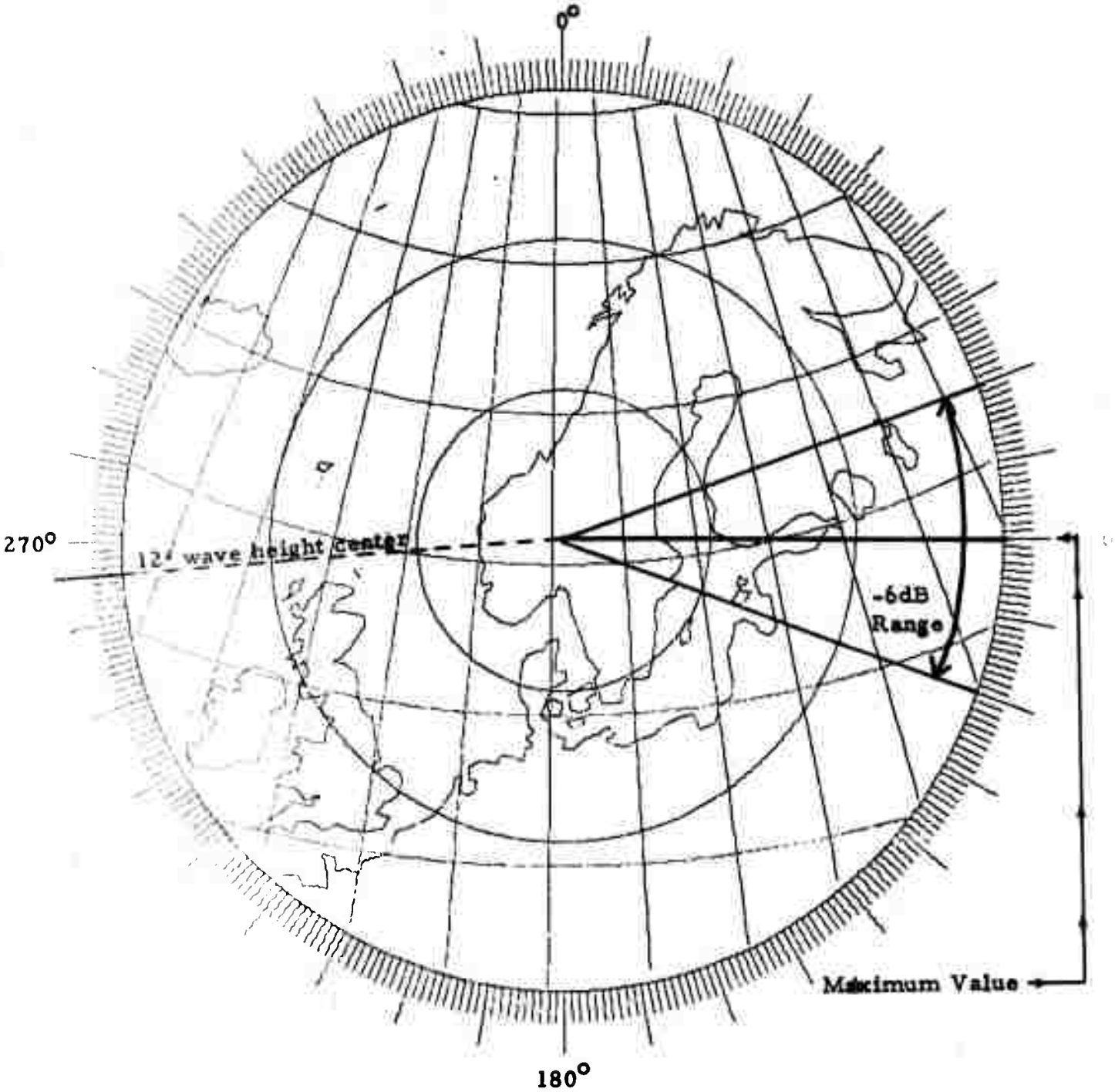

FIGURE II-15

NEAR NORSAR AREA SHOWING AZIMUTH OF PEAK AND -6 dB WAVENUMBER SPECTRAL VALUES AND AZIMUTH TO WAVE HEIGHT PEAKS ON DAY 191

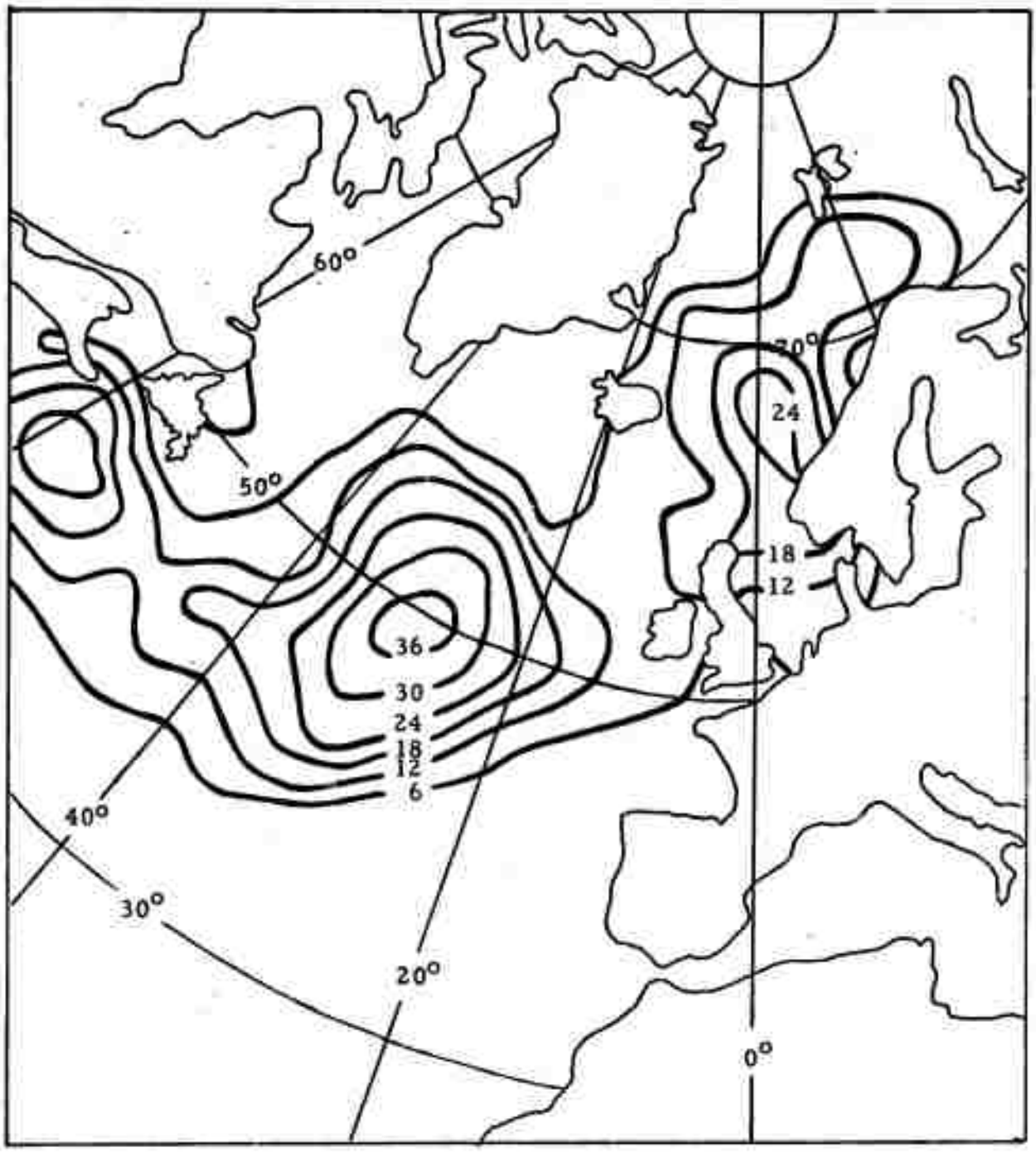

FIGURE II-16

COMBINED SEA & SWELL PROGNOSIS CHART
1200Z DAY 347 VALID FOR 24 HOURS FROM 1200Z 13 DEC 1971

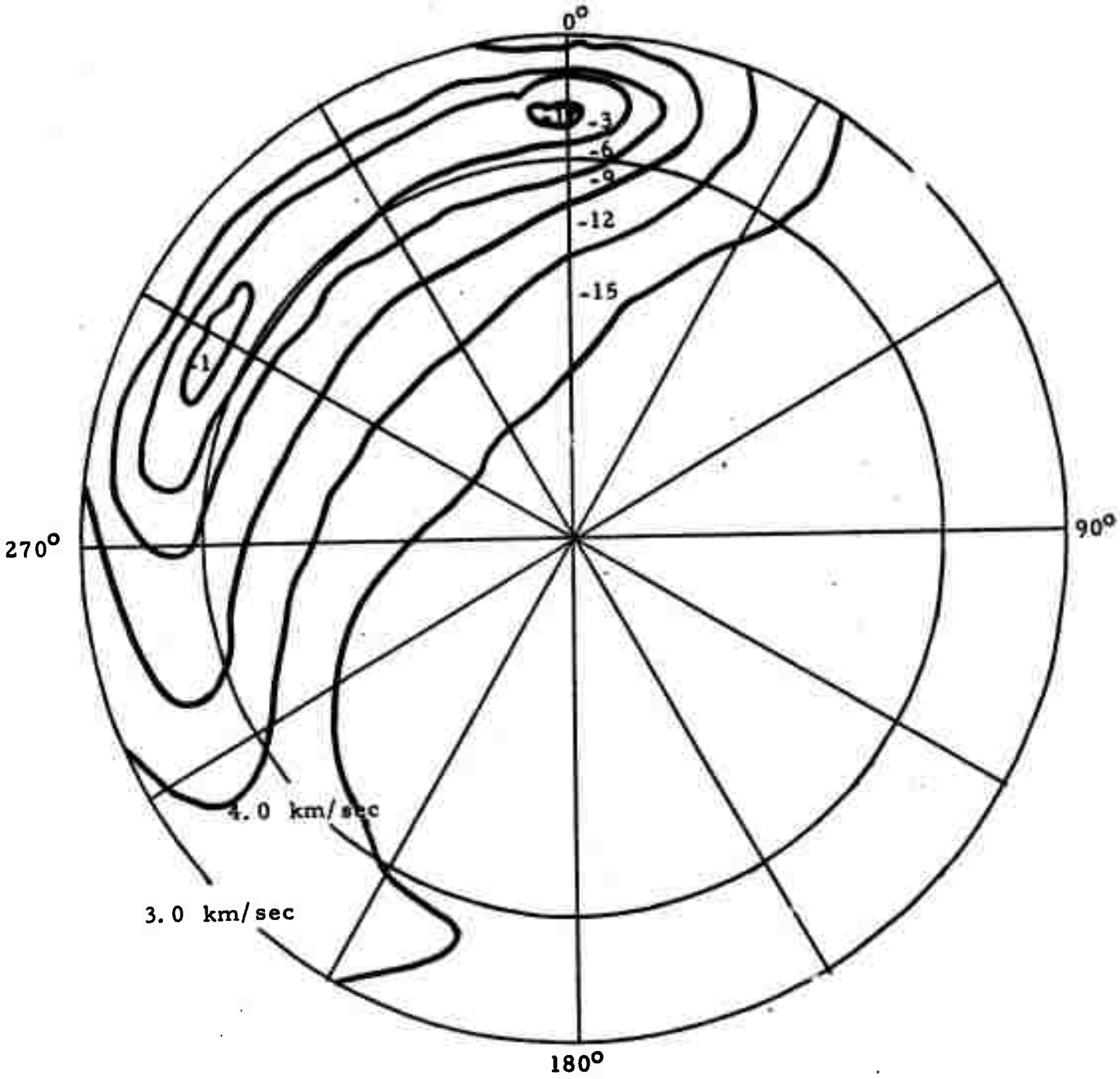

FIGURE II-17

VERTICAL HIGH RESOLUTION WAVENUMBER SPECTRA
AT 0.059 Hz ON DAY 348

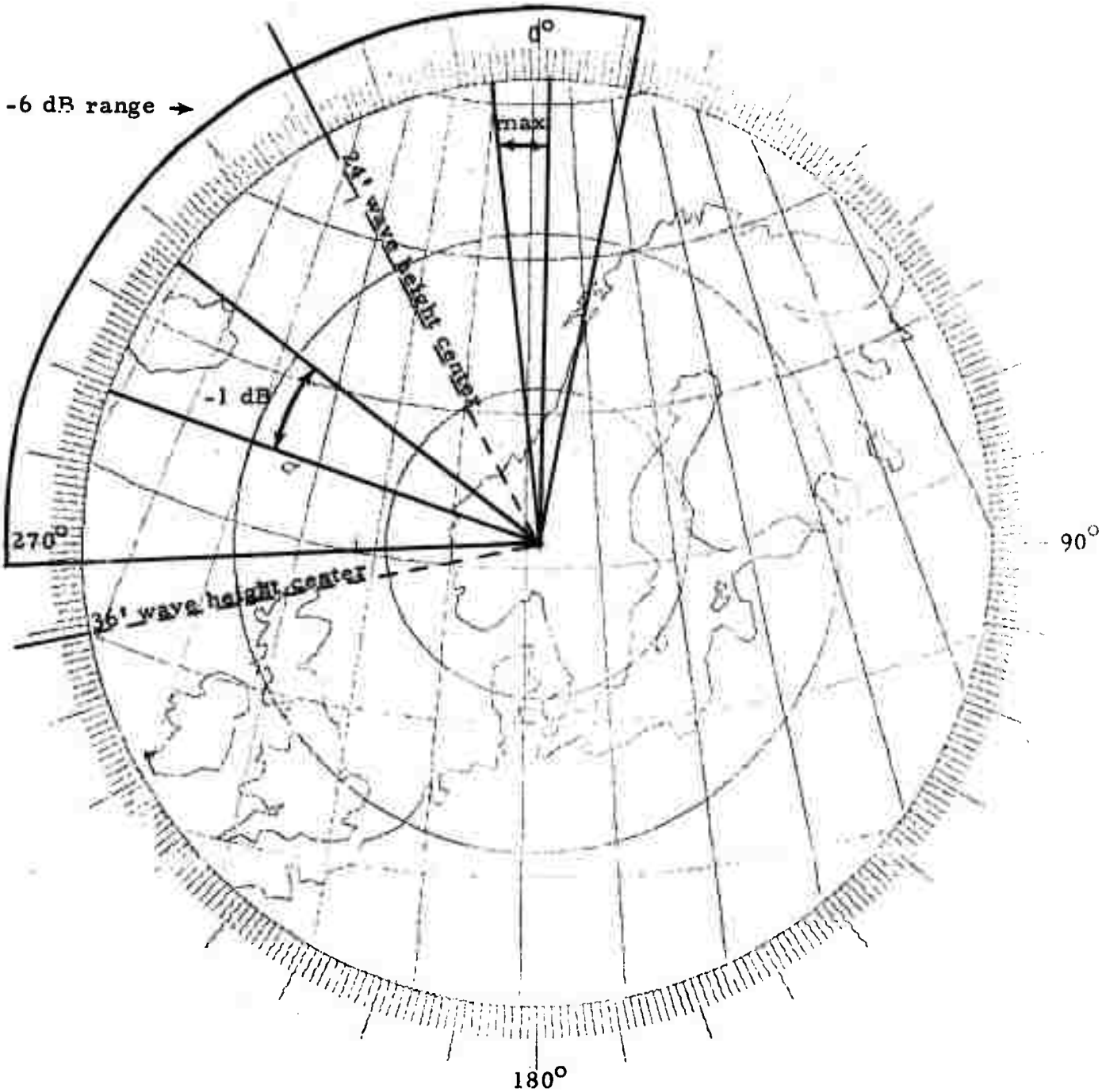

FIGURE II-18

NEAR NORSAR AREA SHOWING AZIMUTH OF PEAK AND -6 dB WAVENUMBER SPECTRAL VALUES AND AZIMUTH TO WAVE HEIGHT PEAKS ON DAY 348

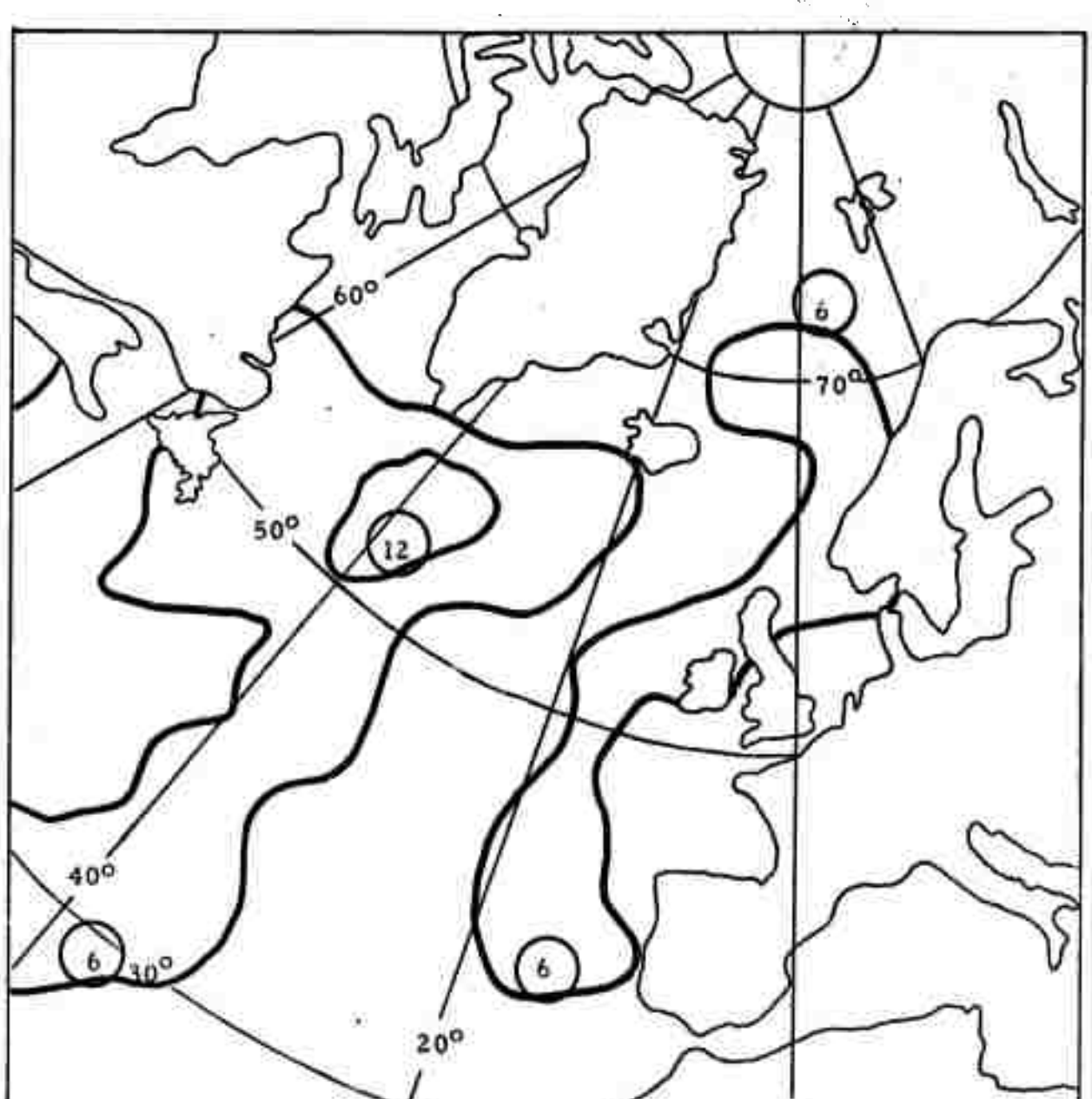

FIGURE II-19

COMBINED SEA & SWELL PROGNOSIS CHART
1200Z DAY 361 VALID FOR 24 HOURS FROM 1200Z 27 DEC 1971

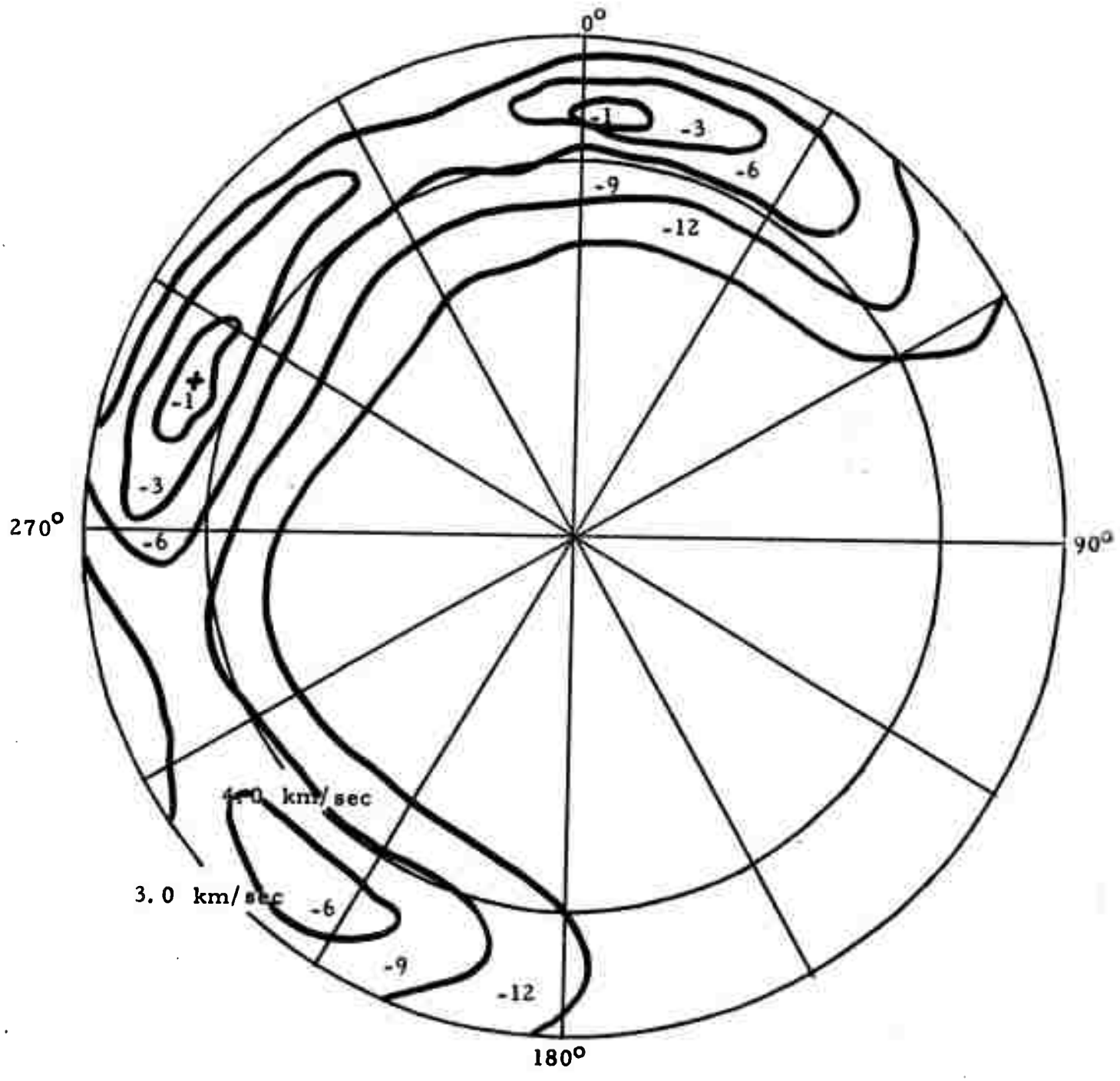

FIGURE II-20

VERTICAL HIGH RESOLUTION WAVENUMBER SPECTRA
AT 0.063 Hz ON DAY 361

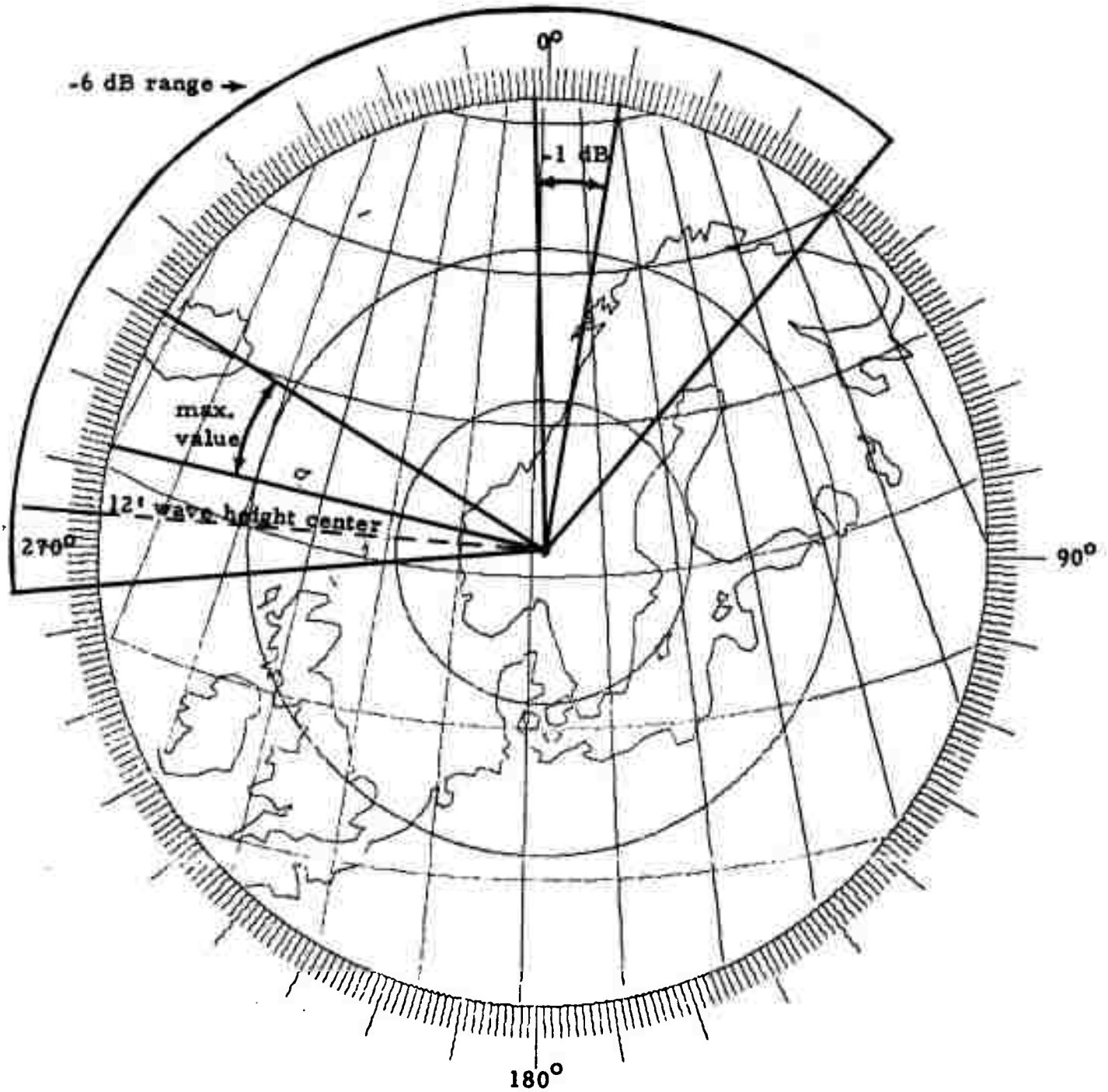

FIGURE II-21

NEAR NORSAR AREA SHOWING VERTICAL PEAK AND -6 dB WAVENUMBER SPECTRAL VALUES AND AZIMUTH TO WAVE HEIGHT PEAKS ON DAY 361

valid for twenty-four hours thereafter. The wave height contours represent the significant wave heights defined as the average of the highest one-third of the waves. Figures II-14, II-17 and II-20 are the high-resolution wavenumber spectra computed at the microseismic peak and contoured in 3 db increments from the peak. The outside circle corresponds to a velocity of 3.0 km/sec. Figures II-15, II-18 and II-21 are maps of the Scandinavian area centered at NORSAR with concentric circles every 5^{o} of distance and with the peaks and -6 db level azimuths of the wavenumber spectra and the azimuth to the maximum wave height areas superimposed.

Days 348 and 361 have similar wavenumber spectra except for absolute level, (Figures II-17 and II-20) but the wave height charts for these two days (Figures II-16 and II-19) are decidedly different. On day 348, the high seas off the Norwegian coast appear to be the cause of the microseismic energy. On day 361, the correlation between waveheight charts and wavenumber spectrum is not convincing. The similarity of the wave height charts of days 191 and 361 is surprising because the wavenumber spectra on these two days are completely different.

Wave height charts for all the noise samples are not presently available; of the nine wave height charts available only day 348 showed a strong correlation between the wave height and wavenumber spectrum. These data suggest that wave height is only directly correlated with the propagating microseismic noise when the waves are very large; apparently the microseism generating mechanism is too complex to be related directly to wave height.

G. COHERENCE

Multiple coherence plots were made for the three long noise samples on days 164, 220 and 009/72 to determine the potential ability of

multichannel filters (MCF's) to reduce the microseismic noise. Figures II-22 to II-24 are the multiple coherence plots for three days. The dots at the top of the plots show the location of the peaks in the power density spectra.

Of interest for signal processing in the 20 to 40 second band (0.025 to 0.050 Hz) is the fairly high coherence around the microseismic peak at 0.040 to 0.050 Hz. The MCF's should work best in this region, although coherences are not high enough to expect dramatic improvements over a beamsteer processor. At the lower frequencies coherence is very low, indicating that this noise is non-propagating energy. Since the noise field is random at low frequencies, MCF and beamsteer noise rejection should be similar. The NORSAR coherences are very similar to those observed at ALPA in the frequency band of interest.

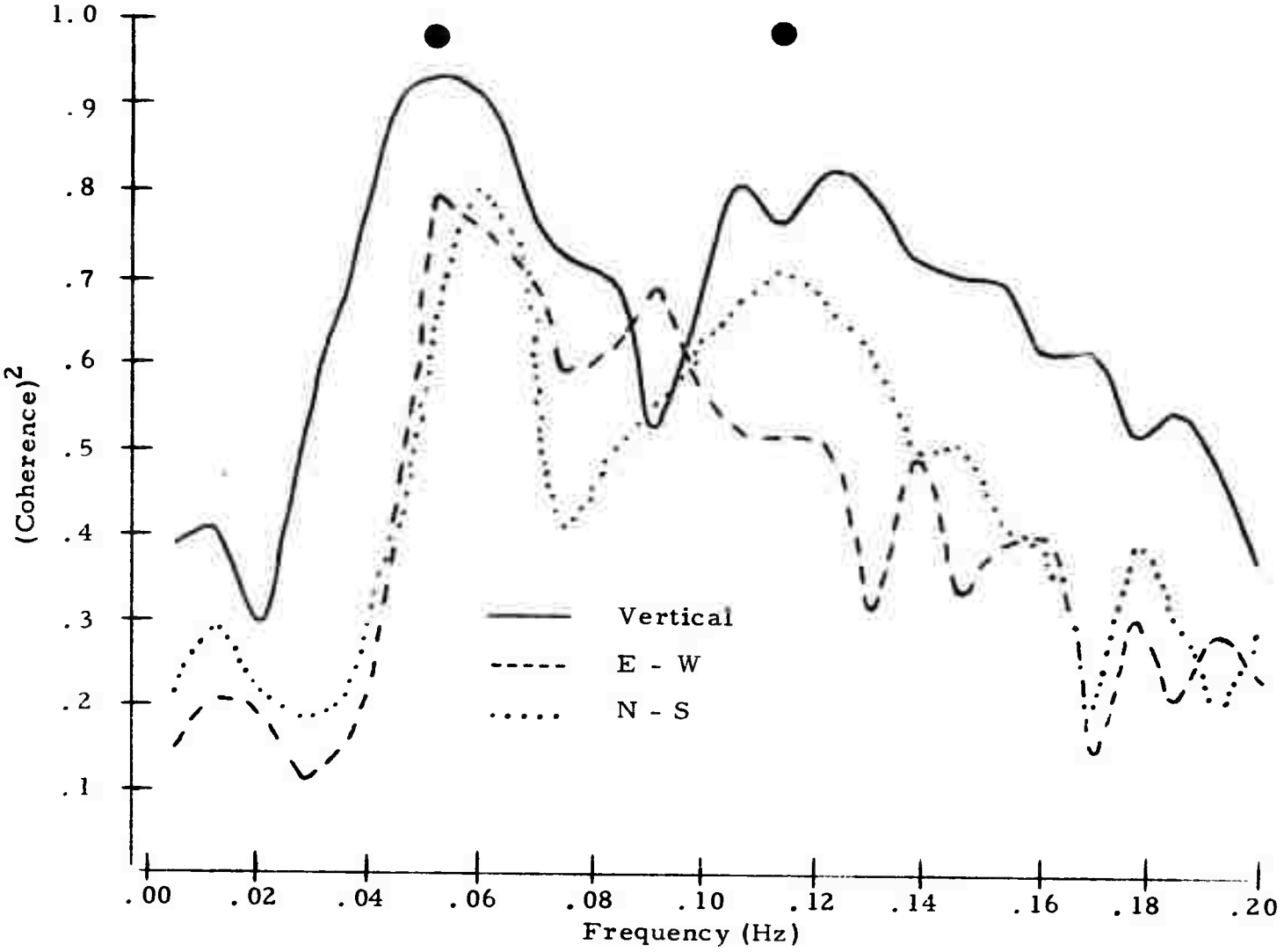

FIGURE II-22

MULTIPLE COHERENCE DAY 164.SITE 1 PREDICTED FROM SITES
2, 3, 4, 7, 8, 9, 11, 13, 14, 15, 16,
17, 18, 19, 22

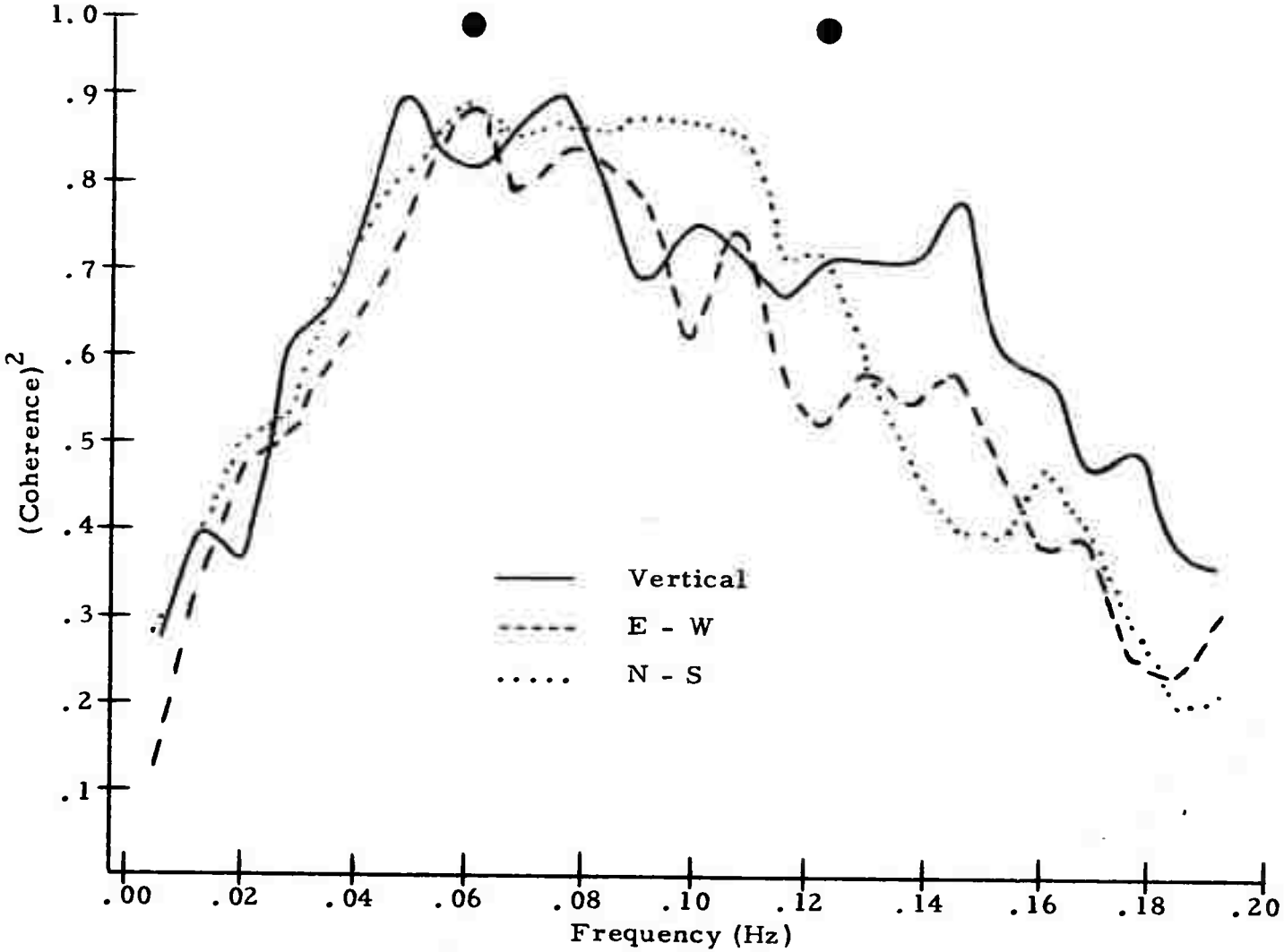

FIGURE II-23

MULTIPLE COHERENCE DAY 220. SITE 1 PREDICTED FROM SITES
3, 4, 5, 6, 7, 8, 9, 10, 13, 14, 15,
16, 17, 18, 20, 22

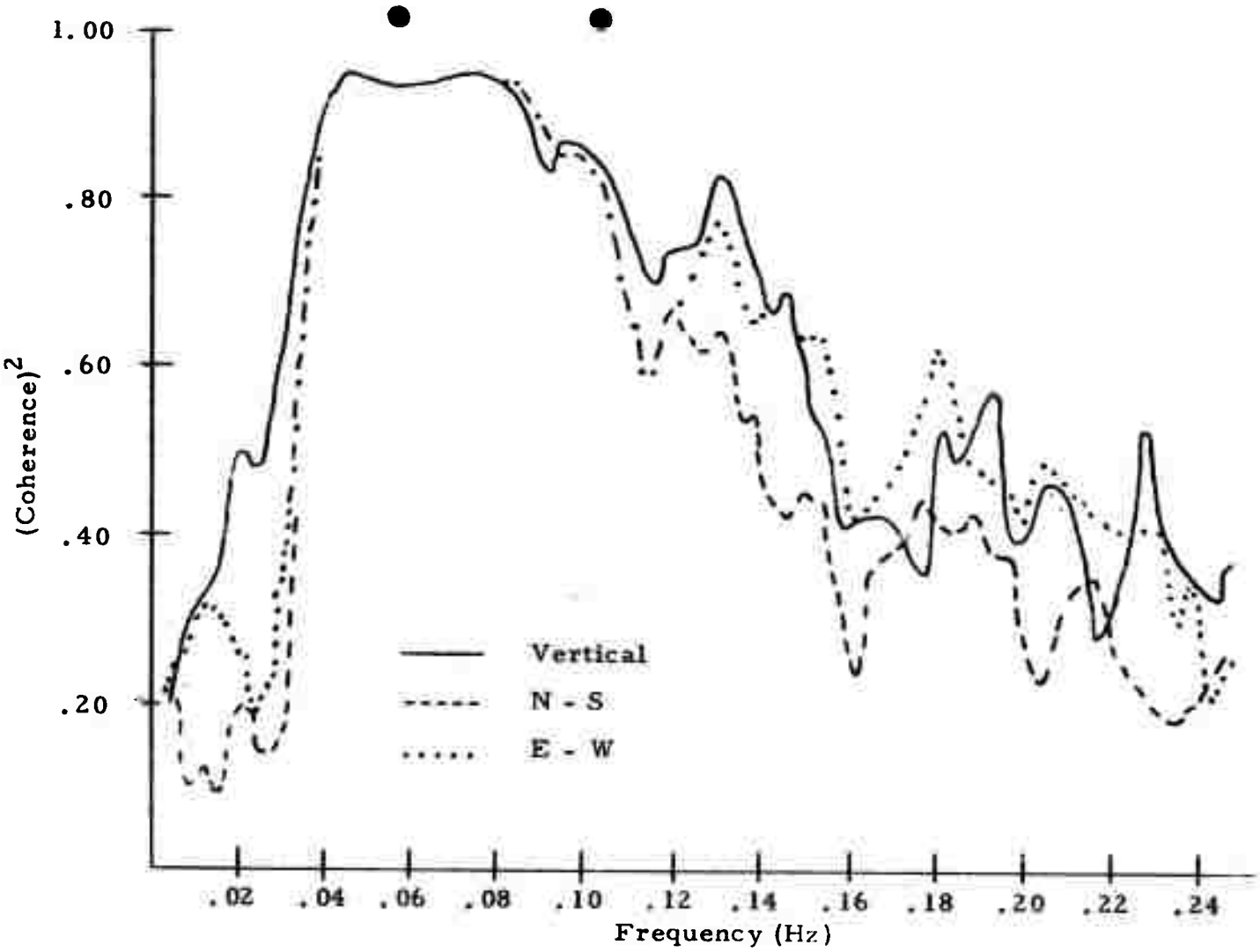

FIGURE II-24

MULTIPLE COHERENCE DAY 009/72. SITE 1 PREDICTED FROM SITES 3, 4, 5, 6, 7, 8, 9, 10, 13, 14, 15, 16, 17, 18, 20, 22

SECTION III
SIGNAL ANALYSIS

A. INTRODUCTION

The purpose of this study was to characterize signals recorded at NORSAR in terms of:

- Site-to-site signal similarities
- Moveout anomalies (deviations from plane wave propagation)
- Azimuthal variations (deviations from the great circle path)
- Spectral content
- Estimated group velocities

This information is useful to:

- Explain array processing signal losses
- Determine optimum bandpass filter bandwidths

Eighteen signals were selected for analysis on the basis of large signal to noise ratios, depth less than 50 km, and no interfering events. Pertinent information about these events is listed in Table III-1.

B. SIGNAL SIMILARITY

The signal similarity coefficent (ρ) between two sites i and j was described by Harley (1967) as

$$\rho = \frac{\Phi_{ij}(T)}{\Phi_{ii}(0)\ \Phi_{jj}(0)}$$

where: Φ_{ij} is the crosscorrelation of site i with site j

T is the lag corresponding to the crosscorrelation maximum

$\Phi_{ii}(0)$; $\Phi_{jj}(0)$ are the zero lags of the autocorrelation of sites i and j

TABLE III-1

EVENTS USED FOR SIGNAL ANALYSIS

Area Event	Delta	Azimuth	m_b	Source Time	Date
TURKEY					
TUR/126/04NL	24.7	143.0	4.4	04.24.34	05/06/71
TUR/143/01NL	24.6	143.5	4.4	01.02.55	05/23/71
TUR/161/09N1	24.7	142.8	4.6	09.31.54	06/10/71
TUR/229/04NL	28.8	133.7	5.0	04.29.33	08/17/71
TRS/251/22NL	28.1	119.6	4.8	22.35.16	09/08/71
KURILES/KAMCHATKA					
KUR/190/16NL	69.9	31.9	4.9	16.44.16	07/09/71
KUR/213/02NL	65.1	22.1	5.3	02.06.06	08/01/71
KAM/166/14NL	66.8	19.7	4.7	14.04.08	06/15/71
KOM/148/10NL	61.8	15.2	4.0	10.21.43	05/28/71
KUR/235/21NL	68.8	28.8	5.7	21.55.18	08/23/71
CHINA/TIBET					
TIB/123/00NL	55.6	87.4	5.2	00.33.22	05/03/71
CHI/156/10NL	63.7	59.9	4.9	10.21.28	06/05/71
CHI/228/04NL	66.4	72.7	5.5	04.58.00	08/16/71
IRAN					
IRA/221/02NL	35.9	113.7	5.2	02.54.37	08/09/71
IRA/234/17NL	40.4	121.7	5.1	17.54.15	08/22/71
IRA/239/05NL	40.3	121.2	5.0	05.20.15	08/27/71
CENTRAL RUSSIA					
CRS/236/16NL	44.0	63.8	5.2	16.33.23	08/24/71
ALEUTIANS					
ALT/310/22NL (Cannikan)	66.7	8.9	6.8	22.00.00	11/06/71

Thus ρ is simply the correlation coefficient between two time series, and its values lie between zero and one. Values of ρ greater than 0.85 indicates good signal similarity.

The signal similarity was measured over the Rayleigh wave on the vertical and radial components and the Love wave on the transverse component. The time windows used varied from 340 seconds to 800 seconds.

The results of this study are presented in Figures III-1 to III-13 in the form of a layout of the NORSAR array, with the values of ρ for each site superimposed. Contour lines of equal similarity have been made at ρ values of 0.95, 0.90, 0.80, 0.70, etc. Contour line values are circled.

Immediately evident on these figures is the elongation of the contours along the azimuth to the epicenter. This indicates that the signal similarity is better between sensors along the great circle route than between sensors normal to it. The phenomenon has been discussed by Mack (1971), and is attributed to the fact that the signal is not a point in wavenumber space but rather a distribution. The azimuth distribution affects the signal similarities perpendicular to the signal azimuth (which is apparently more severe) and the velocity distribution affects the signal similarity along the signal azimuth.

In Figures III-1 to III-3, where sites at the array center were used as a reference, the similarity values for ALT/310/22NL show a marked elongation for all three components. Since the elongation is observed on all three components with approximately the same severity for the other signals, the remainder of the figures show the vertical only.

Figures III-4 and III-5, for ALT/310/22NL, show results using sites 12 and 20 respectively as references. These sites are on opposite sides of NORSAR. In both cases the similarities drop off uniformly as the sensor separation normal to the event azimuth increases. Again, the elongation in the direction of the signal azimuth is obvious.

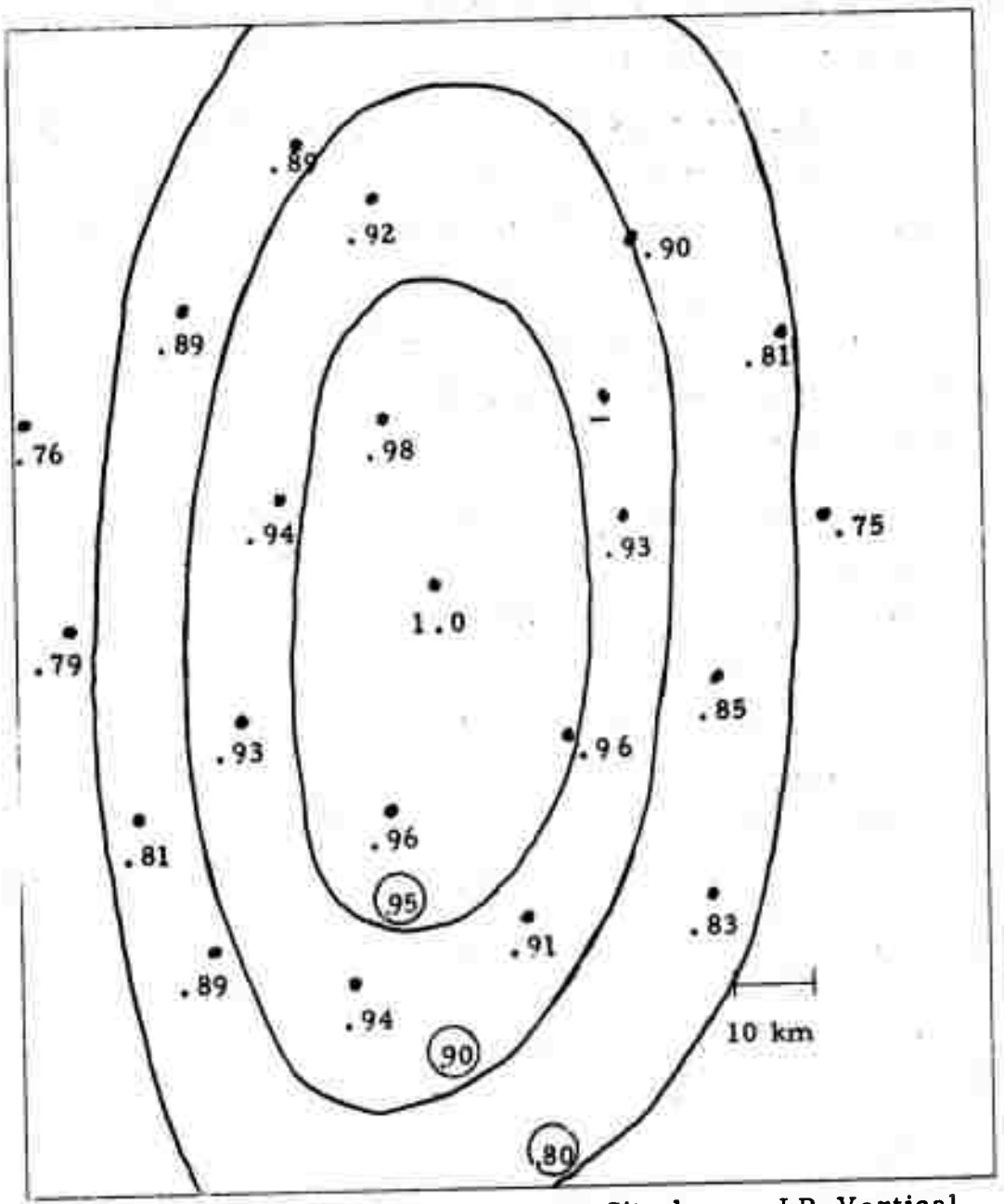

ALT/310/22NL Reference Site 1 LR-Vertical
Azimuth = 8.6°

FIGURE III-1

NORSAR SIGNAL SIMILARITY

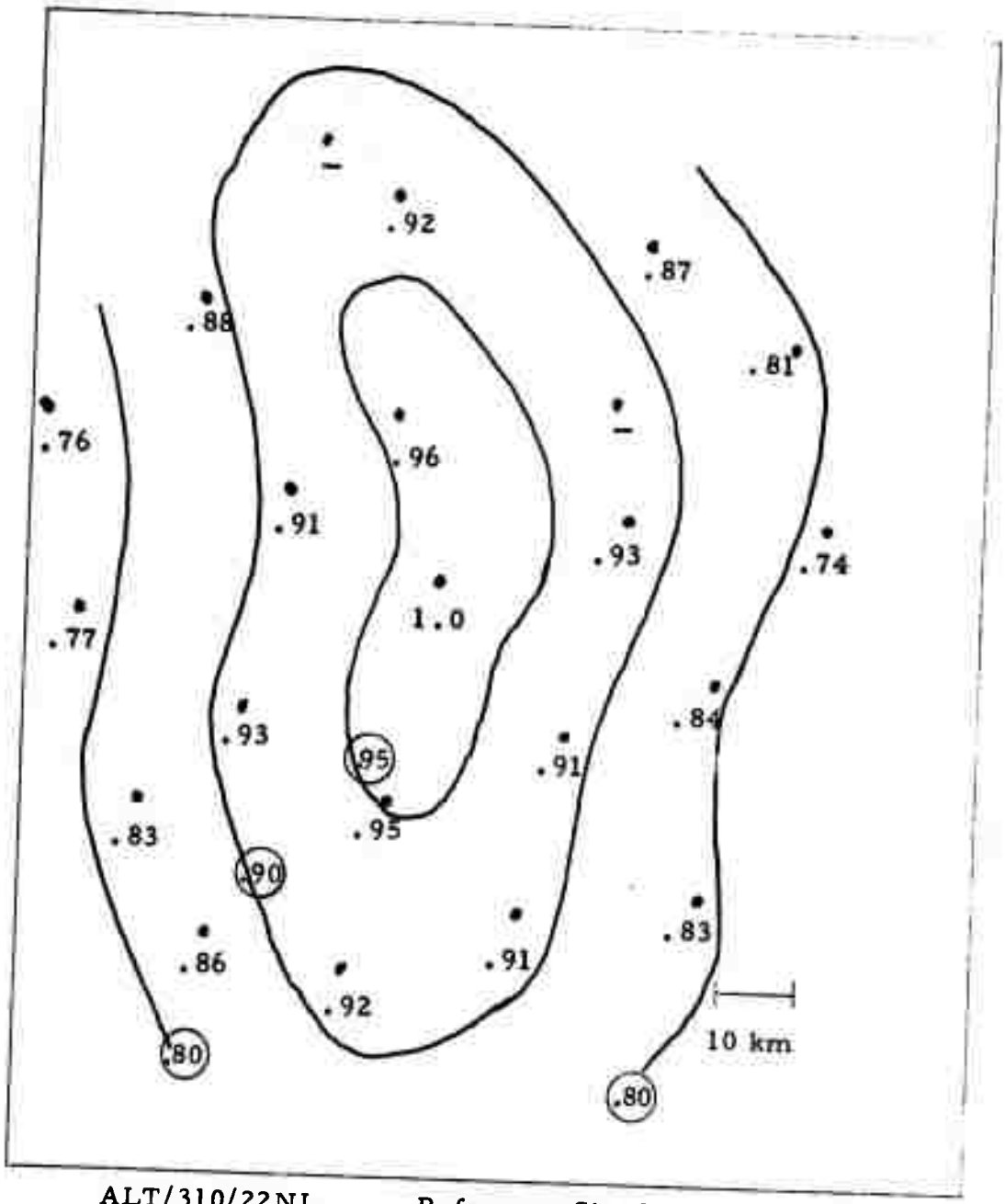

ALT/310/22NL Reference Site 1 LR-Radial
Azimuth = 8.6°

FIGURE III-2

NORSAR SIGNAL SIMILARITY

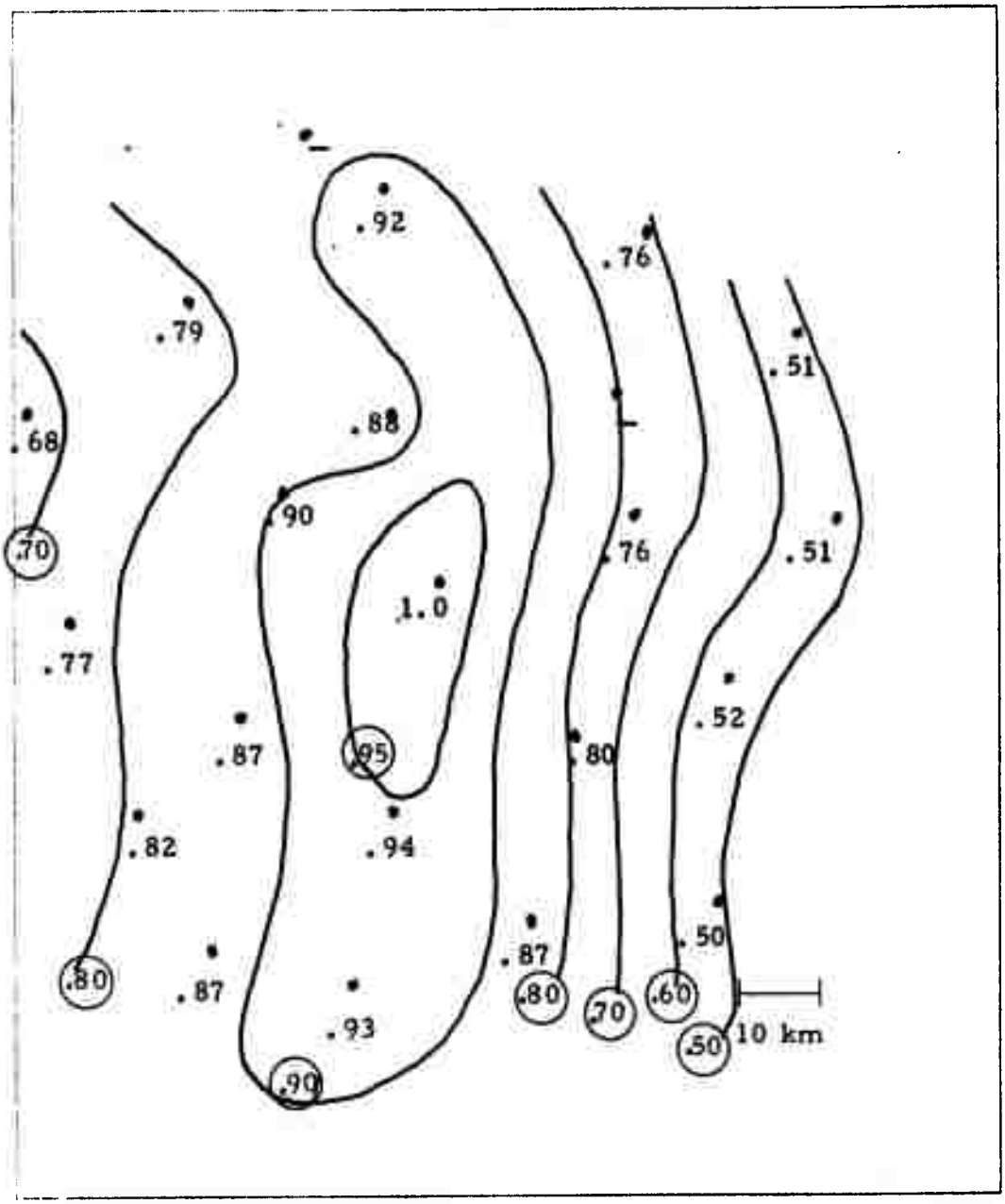

ALT/310/22NL Reference Site 1 LQ-Transverse
Azimuth = 8.6°

FIGURE III-3

NORSAR SIGNAL SIMILARITY

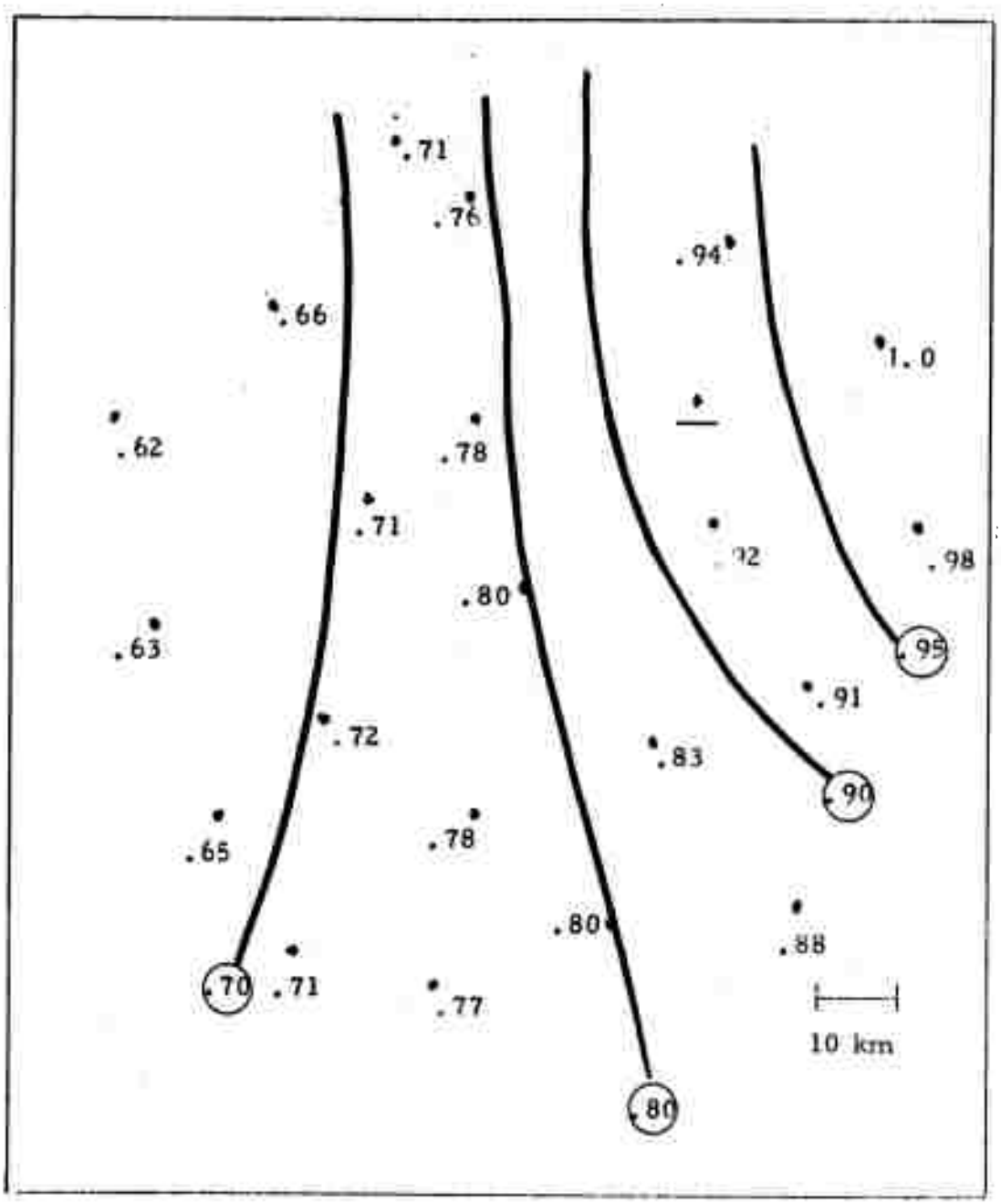

ALT/310/22NL Reference Site 12 LR-Vertical
Azimuth = 8.6°

FIGURE III-4

NORSAR SIGNAL SIMILARITY

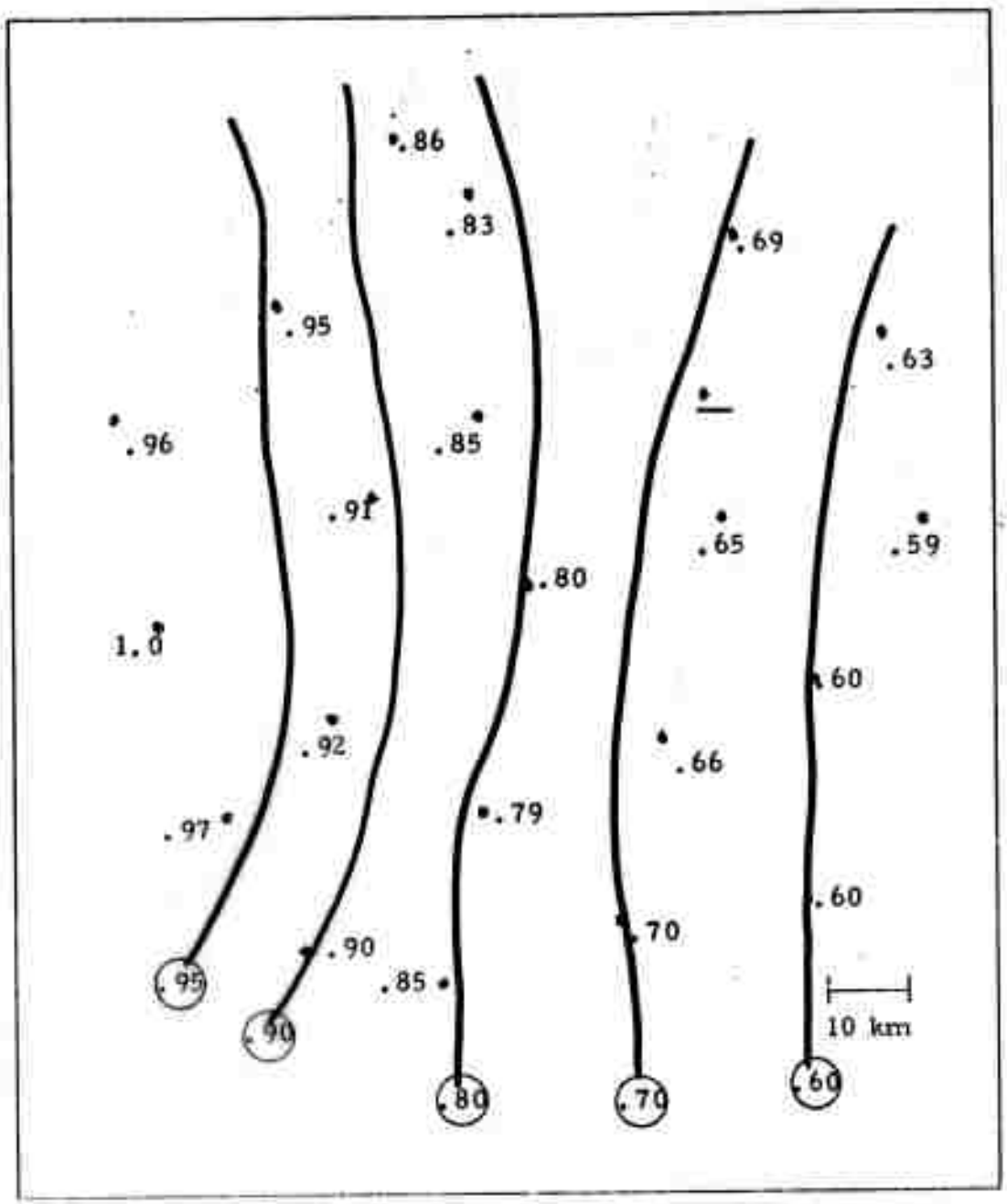

ALT/310/22NL Reference Site 20 LR-Vertical
Azimuth = 8.6°

FIGURE III-5

NORSAR SIGNAL SIMILARITY

Figures III-6 to III-13 show the signal similarity coefficient results for other signals at various azimuths. In all cases, the lines of equal similarity elongate in the direction of azimuth to the epicenter.

One way to get an azimuthal distribution in the surface wave arrival is to have discrete multipaths. A simple model (Figure III-14) was generated to determine the effect of multipaths on signal similarity. Two identical chirp waveforms, one arriving at all three sensors of a three-element linear array simultaneously, the other delayed with respect to the first and arriving at various angles, were used to simulate a discrete multipathed arrival. The results were as expected; the signal similarity decreased as the two outside sensors were moved farther apart and the two outside sensors were more dissimilar to one another than to the center sensor. These results show that discrete multipathing can produce the elongation observed.

There do not appear to be any sites whose similarity values differ from those observed elliptical patterns in Figures III-1 to III-13. The gradient (between center and outside seismometers) changes from event to event, and probably is related to the degree of multipathing for an event. The difference in similarity, $\delta\rho$, between the reference similarity (always 1.0) and the lowest value is a measure of the severity of dissimilarity across the array. Table III-2 shows that $\delta\rho$ typically is 0.3 although the CHI/156/10NL event has a $\delta\rho$ of 0.7. In every case the sensor having the lowest similarity value was at the largest distance normal to the signal azimuth. There does not appear to be any correlation between $\delta\rho$ and either azimuth or delta. Table III-2 also shows the number of similarity values below 0.75 for each event. KAM/166/14NL and CHI/156/10NL have three or more sites with low similarity values, suggesting that signal attenuation may be larger for these two events.

C. TRAVEL-TIME ANOMALIES

The lags associated with the maximum crosscorrelation value (discussed previously) were used to investigate intra-array moveout anomalies. The

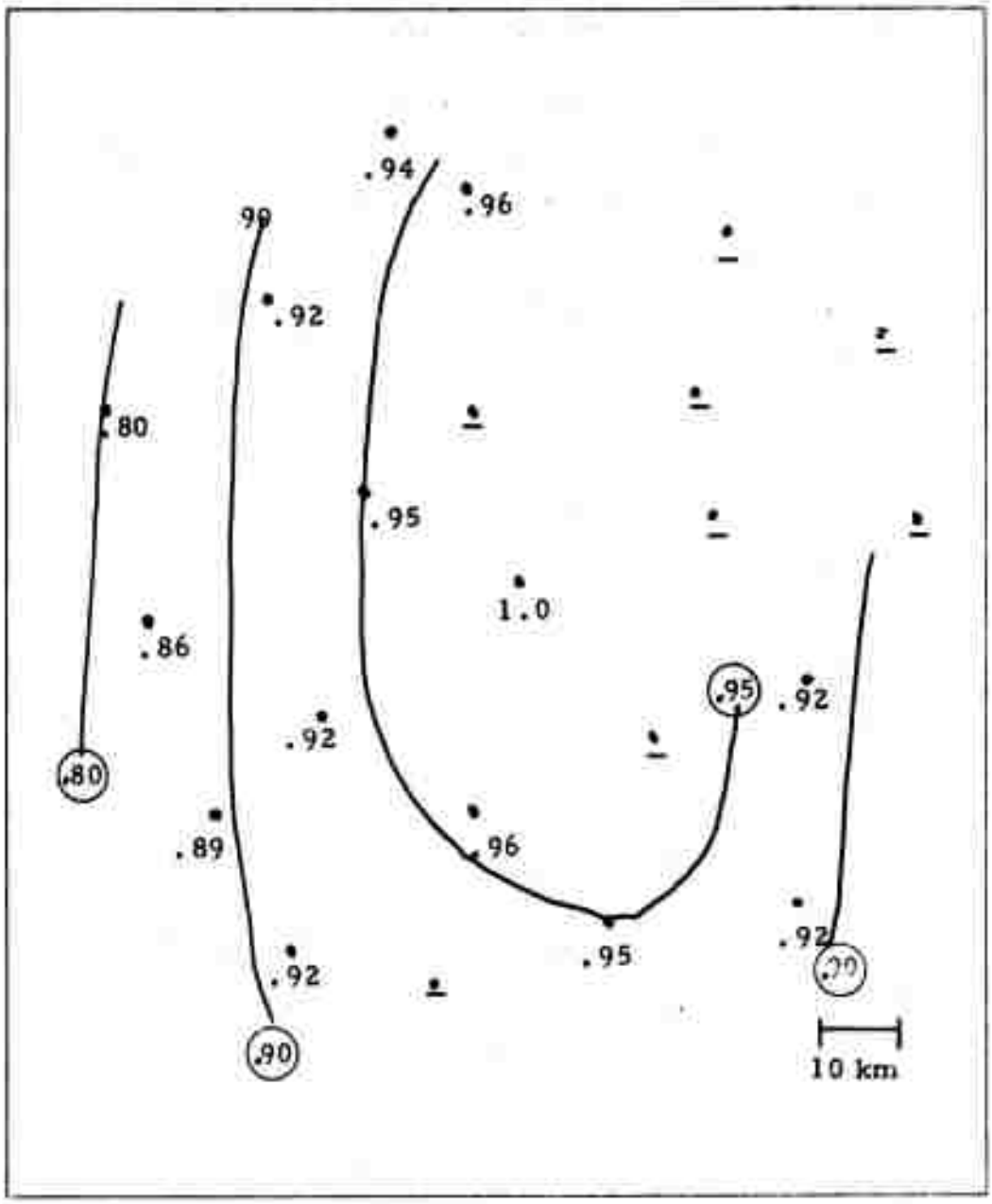

KOM/148/10NL Reference Site 1 LR-Vertical
Azimuth = 15°

FIGURE III-6

NORSAR SIGNAL SIMILARITY

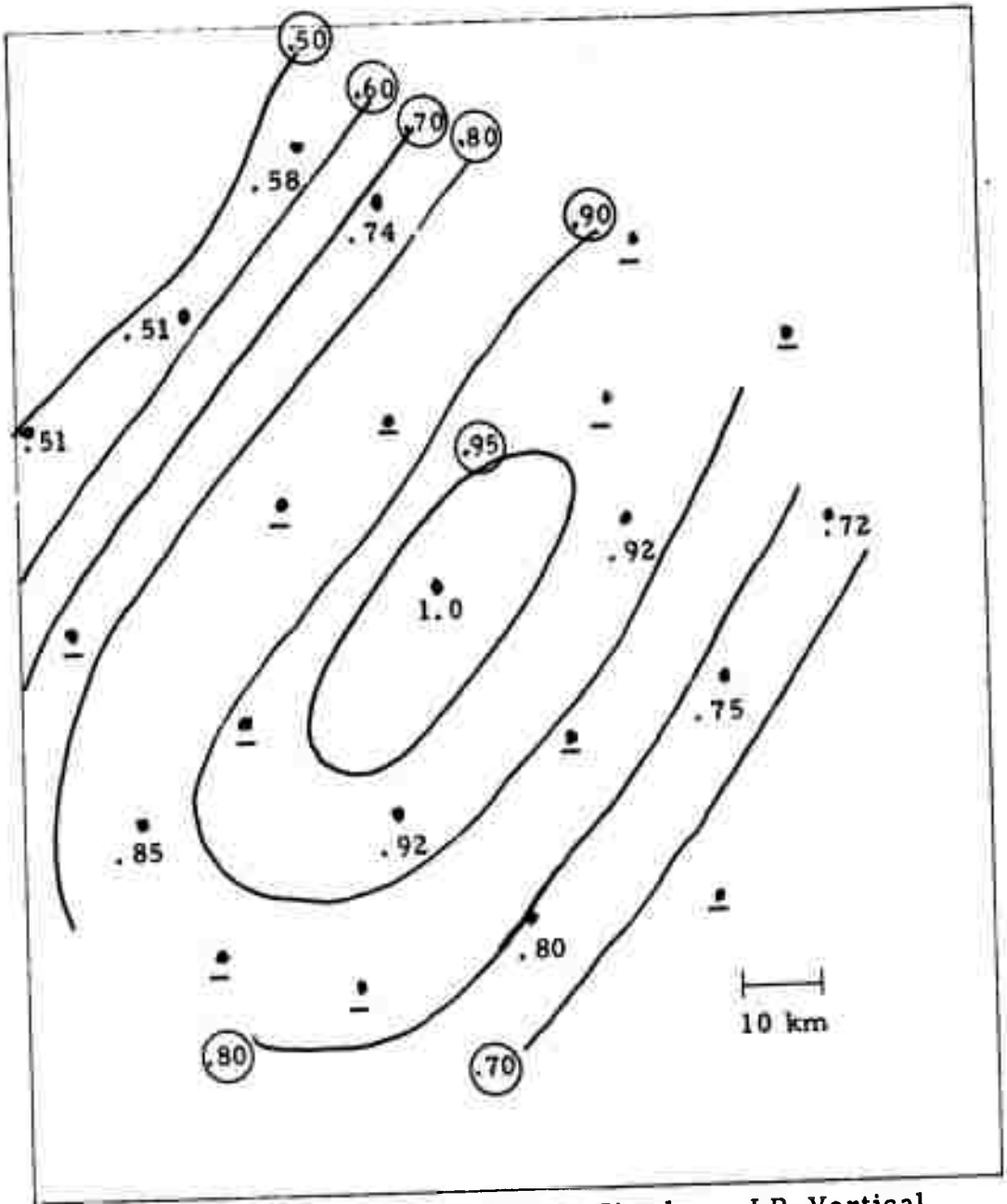

KAM/166/14NL Reference Site 1 LR-Vertical
Azimuth = 20°

FIGURE III-7

NORSAR SIGNAL SIMILARITY

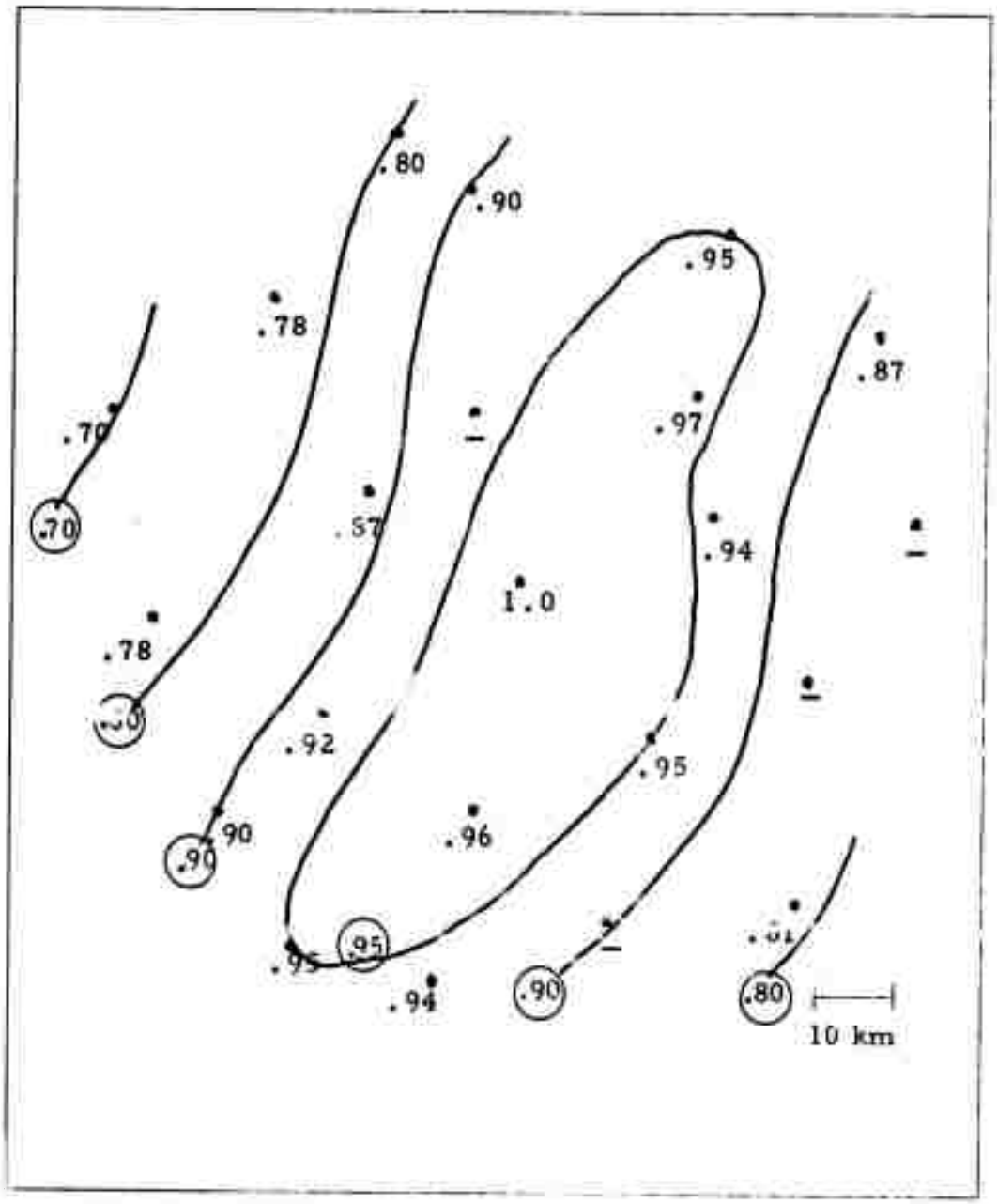

KUR/213/02NL Reference Site 1 LR-Vertical
Azimuth = 22°

FIGURE III-8

NORSAR SIGNAL SIMILARITY

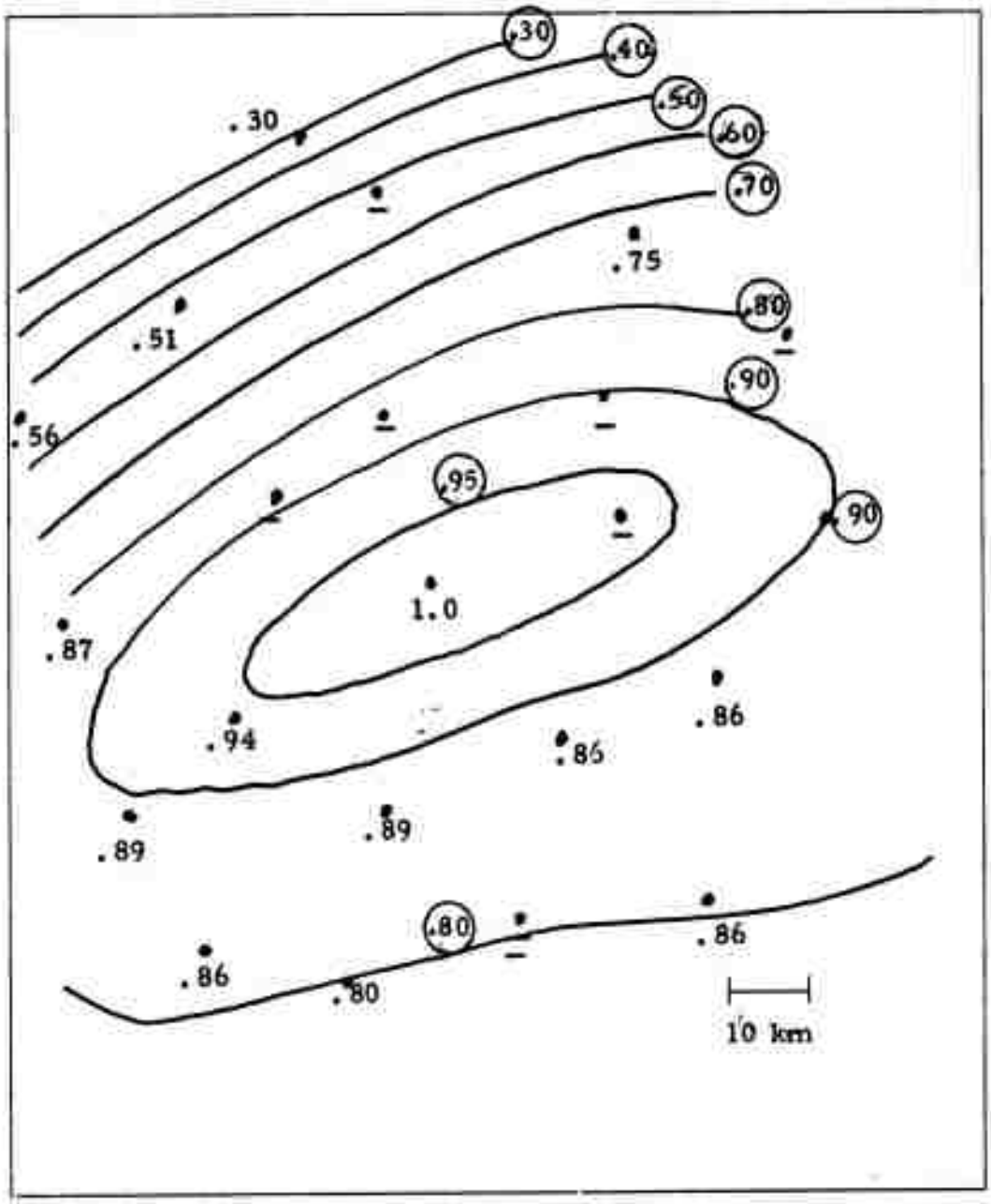

CHI/156/10NL Reference Site 1 LR-Vertical
Azimuth = 60°

FIGURE III-9

NORSAR SIGNAL SIMILARITY

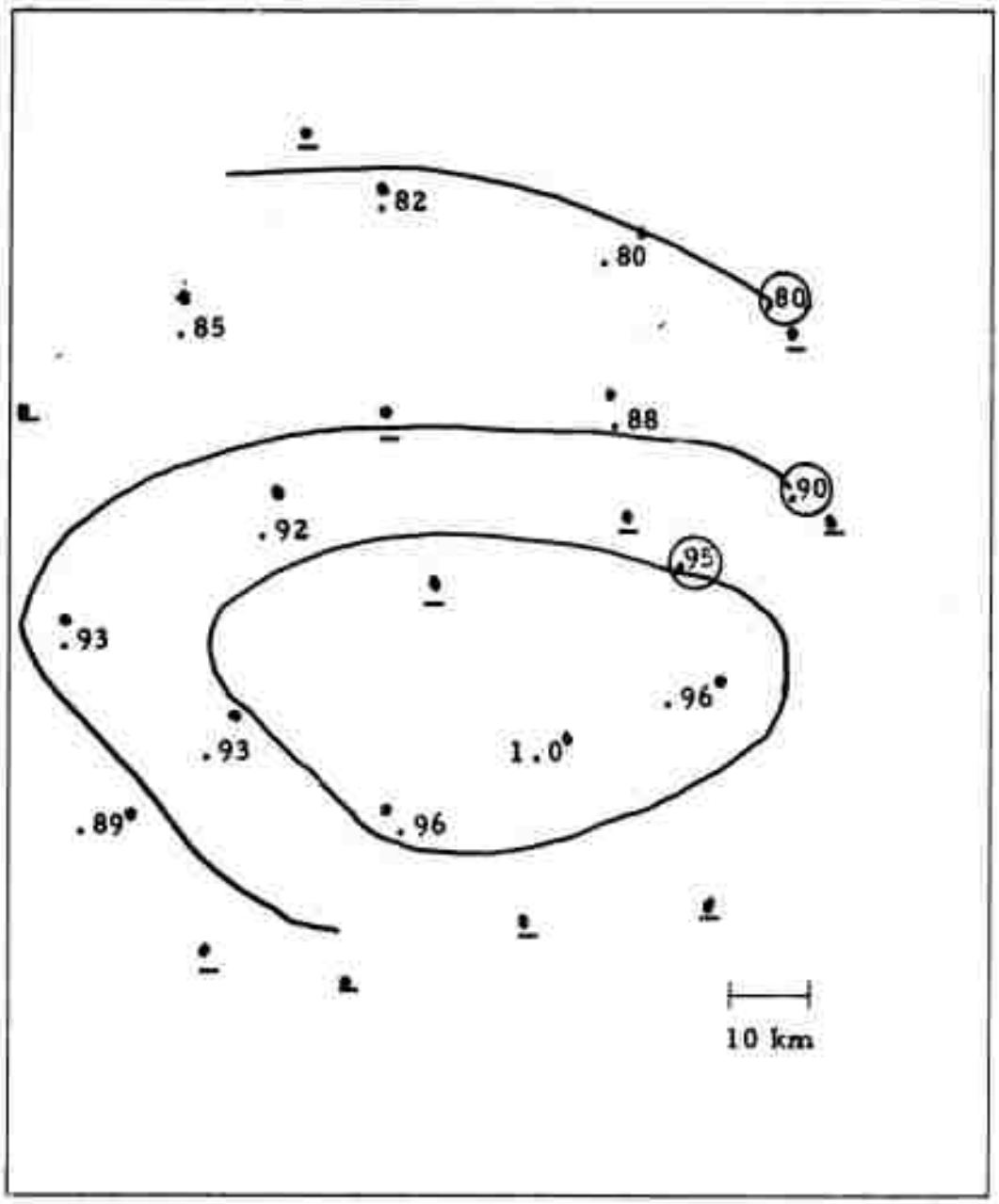

TIB/123/00NL Reference Site 5 LR-Vertical
Azimuth = 87°

FIGURE III-10

NORSAR SIGNAL SIMILARITY

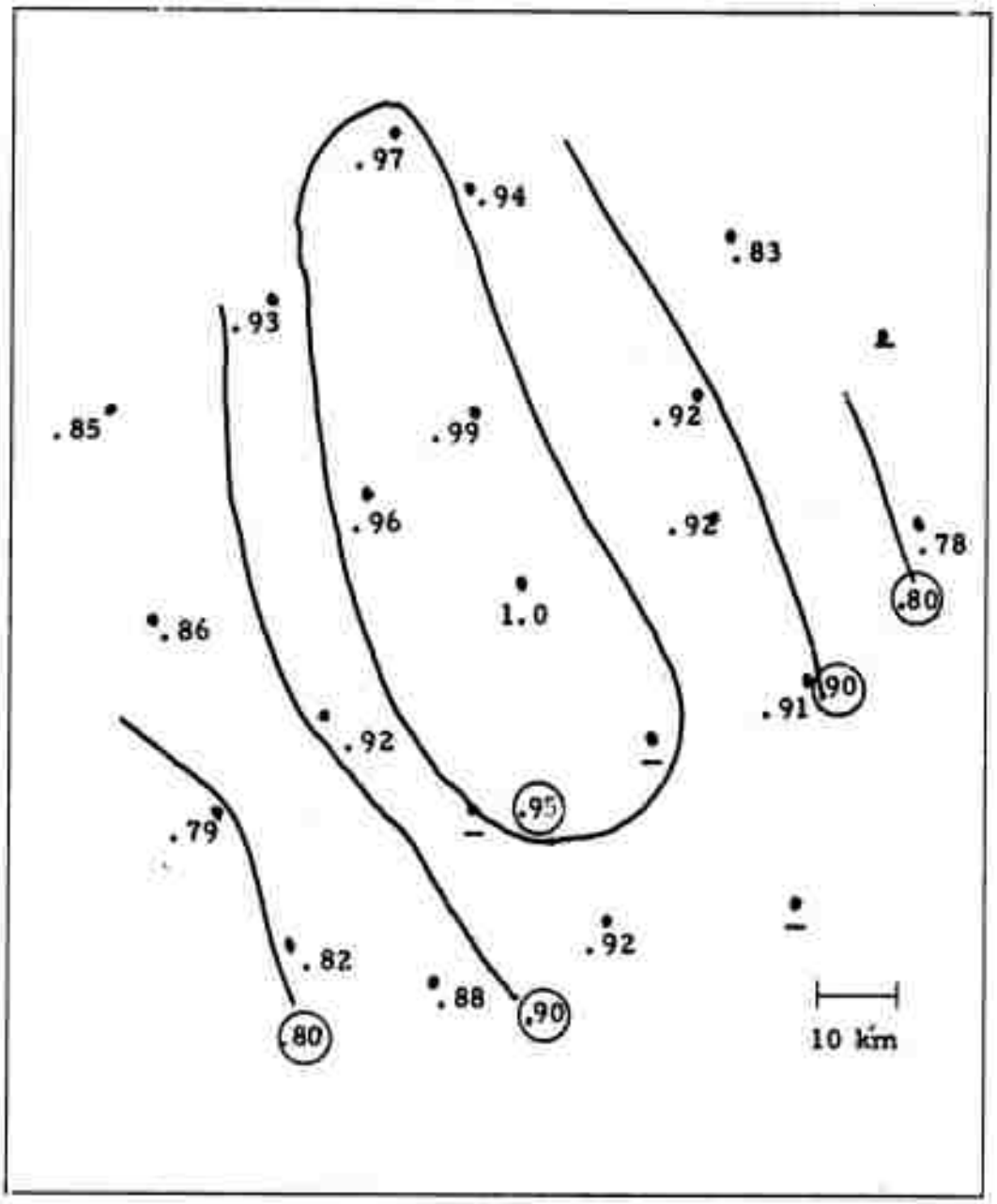

TUR/161/09N1 Reference Site 1 LR-Vertical
Azimuth = 142°

FIGURE III-11

NORSAR SIGNAL SIMILARITY

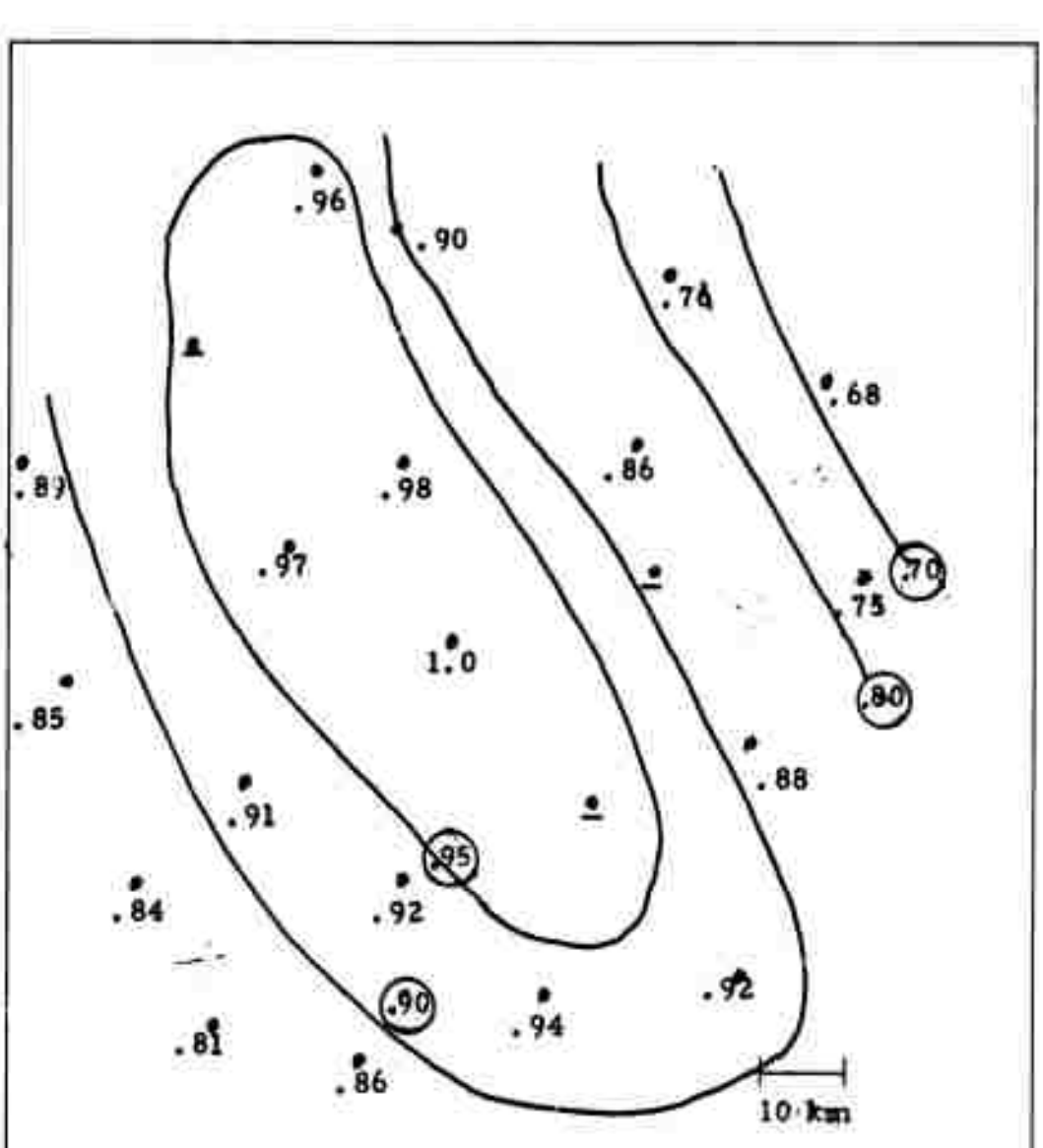

TUR/126/04NL Reference Site 1 LR-Vertical
Azimuth = 143°

FIGURE III-12

NORSAR SIGNAL SIMILARITY

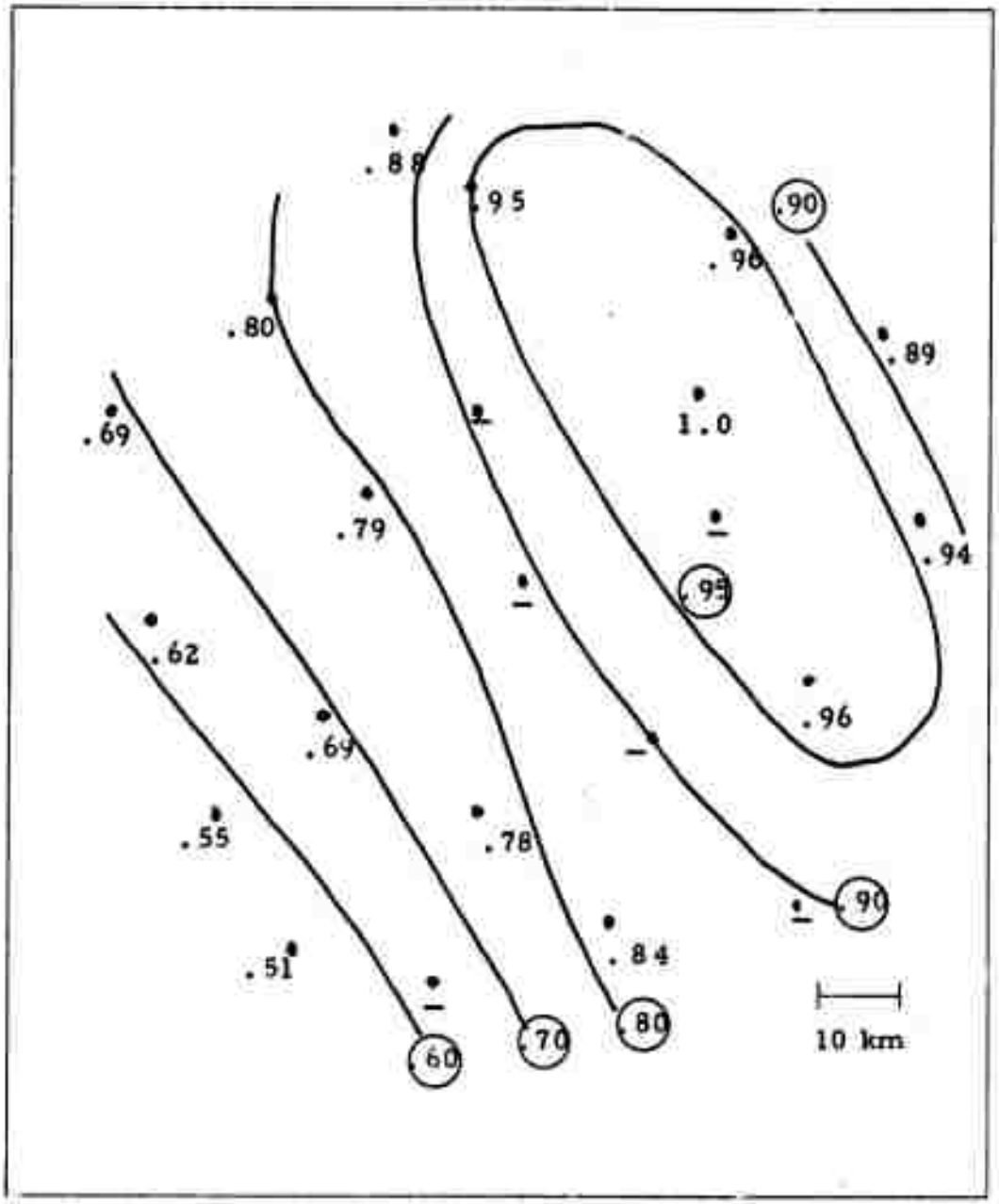

TUR/143/01NL Reference Site 3 LR-Vertical
Azimuth = 144°

FIGURE III-13

NORSAR SIGNAL SIMILARITY

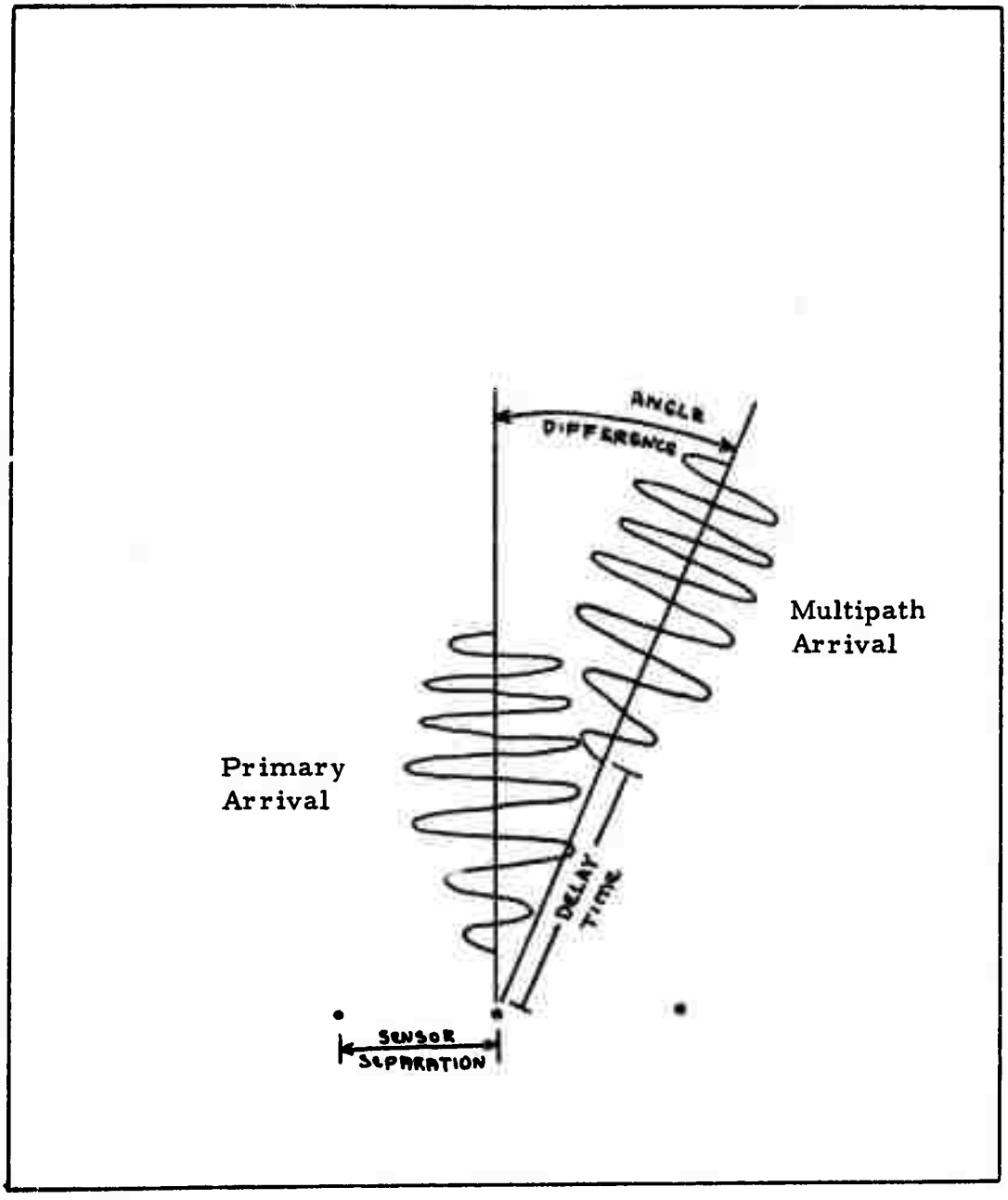

FIGURE III-14

MODEL STUDY TO INVESTIGATE SIGNAL SIMILARITY VARIATION

TABLE III-2

SEVERITY OF SIGNAL DISSIMILARITY

Event	$\delta\rho$	Azimuth	Delta	Number of Values Below 0.75
ALT/310/22NL	0.25	8.6°	66.7°	0
KOM/148/10NL	0.20	15.0°	61.8°	0
KAM/166/14NL	0.49	19.7°	66.8°	4
KUR/213/02NL	0.30	22.0°	65.1°	1
CHI/156/10NL	0.70	60.0°	63.7°	3
TIB/123/00NL	0.18	87.0°	55.6°	0
TUR/161/09NL	0.21	142.0°	24.7°	0
TUR/126/04NL	0.32	143.0°	24.7°	1

traces were aligned prior to crosscorrelation computation by assuming plane wave propagation along the great circle path and using a phase velocity of 3.6 km/sec for Rayleigh waves and 4.3 km/sec for Love waves; the lags represent deviations from plane wave propagation.

In Table III-3 the vertical Rayleigh wave lag values for the various events are tabulated by site. The values are in seconds and a plus value indicates the signal at that site arrived earlier than the reference and a minus indicates the signal arrived later than the reference.

Three events KAM/166/14NL, KOM/148/10NL, and ALT/310/22NL had a large number of non-zero values and were the only events with deviations greater than one sample ($\pm$ 2 seconds). The KOM/148/10NL event deviations are probably due to a 15^{o} azimuth deviation (see the next subsection), the explanation for the deviations of the other two events is not known. The fact that the observed deviations do not carry over from event to event indicates that they are event related rather than site related.

Two sites, 4 and 7, in the inner ring and with signal similarities consistently above 0.90 have consistent delay anomalies other than zero. Site 4 has 7 of 9 events with a +2 second time anomaly and site 9 has 10 of 14 events with a -2 second time anomaly. The consistency of these small anomalies for events reasonably well distributed in azimuth suggest that they are real and not simply data scatter; a possible explanation is that the phase responses of these instruments (which is presently unknown) are somewhat different from the other seismometers. A 30^{o} phase shift at a 20 second period relative to the other sites would produce a two-second time shift.

Excluding the three events previously mentioned, there are no consistent anomalies on outer ring sensors.

In conclusion, there do not appear to be significant intra-array surface wave travel time anomalies at NORSAR. Again, this result is similar to that observed at ALPA (Texas Instruments, 1971).

TABLE III-3

LR-VERTICAL DELAY ANOMALIES IN SECONDS
(SAMPLE PERIOD = 2 SECONDS)

Event	Site																					
	1	2	3	4	5	6	7	8	9	10	11	12	13	14	15	16	17	18	19	20	21	22
TUR/126/04NL	r	0	0	-	-	0	-2	0	0	2	0	-	2	2	0	2	0	0	0	-2	0	0
TUR/143/01NL	-	-	r	-	-	0	0	-2	0	0	0	-	0	0	-	0	-	-	-	-	-2	-2
TUR/161/09N1	r	0	0	0	-	-	-2	0	0	0	0	-	2	2	-	0	0	0	0	-2	-2	-2
TUR/229/04NL	r	0	0	2	0	0	0	0	-	-	-	-	-	-	0	-	0	0	0	0	0	0
KUR/190/16NL	r	-	2	2	0	-2	-2	0	2	0	0	-	-	-	-	-	-2	-2	-	-2	-2	0
KUR/213/02NL	r	-	0	2	-2	0	-2	0	2	2	0	0	-	-	-2	-	0	0	0	0	2	2
KAM/166/14NL	r	-	-	-2	-	-2	-	-	6	4	-	-	-	-4	-	-4	-	-	0	-	-	6
KOM/148/10NL	r	-	-	-	-	0	-2	0	0	0	-	-	-	0	2	0	-	-2	-2	-4	-2	0
KUR/235/21NL	r	-	2	-	0	-	-2	0	-	2	0	-	-	-	-	-	-2	-2	-	-	-	-
TIB/123/00NL	-	-	0	-	r	0	-2	0	-	0	2	-	-	0	-	-	-	-	-2	-2	-	-2
CHI/156/10NL	r	-	-	-	0	-2	0	-	-	-	-	-	0	0	0	-	-2	-2	0	0	-	-
CHI/228/04NL	r	0	0	2	0	0	-2	0	-	-	-	-	2	-	0	-2	-	0	-	-	0	2
IRA/221/02NL	r	0	0	2	0	0	0	-2	-	-	-	-	0	-	2	0	2	0	0	0	0	0
IRA/234/17NL	r	0	2	2	2	-	-2	0	-	0	-	-	2	0	0	2	-2	0	-	0	-2	0
ALT/310/22NL	r	0	-	2	0	0	-2	-2	0	0	2	2	2	2	0	-2	-2	-2	-2	-4	-2	-2

D. AZIMUTHAL VARIATION

Another factor that could affect the beamsteer and MCF processing results is that the signal could have arrived at the array along other than the great circle path. To investigate this possibility, the entire Rayleigh wave was Fourier transformed and the peak frequency was chosen to generate conventional and high resolution wavenumber spectra. The azimuth and velocity of the peak of the various events is tabulated in Table III-4. Table III-4 is grouped by events with similar azimuths and the number of sites used are tabulated to give a measure of the reliability of the results.

The events from Turkey show consistent arrivals 6° to 12° greater than the great circle path. On TUR/143/01NL an investigation of possible multipathing was made by generating wavenumber spectra at different frequencies and different portions of the wave train, but there was no significant change in arrival azimuth.

The Kurile area events tend to have azimuths smaller than the great circle azimuths; KOM/148/10NL has a -15.2° deviation, which probably explains the moveout anomalies observed for this event in the last subsection.

The effect of these azimuthal variations on the beamsteered output was measured by computing the array response of NORSAR for beamsteered output. In all cases the -1 dB level at 3.6 km/sec was $\pm 10^{\circ}$ wide; thus these small variations will have little effect on the beamsteered output.

E. GROUP VELOCITY CURVES

Preliminary NORSAR Rayleigh wave group velocity curves were estimated from the time traces of four large signals that were well dispersed and, for a significant length, free from multipathing. The four signals also cover the range of azimuths expected from the Asian continent.

Figure III-15 shows the estimated group velocity curves; a typical continental curve is included for reference (Linville, 1971). The curves obtained

TABLE III-4

AZIMUTHAL WANDER

Event	Peak Frequency	Great Circle Azimuth	Spectral Azimuth	Azimuth Difference	Velocity km/sec	No. of Sites
TUR/126/04NL	0.042	143.0°	152°	11.0	4.0	16
TUR/143/01NL	0.047	143.5°	155°	11.5	3.8	18
TUR/161/09N1	0.037	142.8°	148°	5.2	3.9	14
TUR/229/04NL	0.055	133.7°	141°	6.3	3.7	14
KUR/190/16NL	0.039	31.9°	30°	-1.9	3.8	18
KUR/213/02NL	0.035	22.1°	23°	0.9	3.9	16
KUR/235/21NL	0.035	28.8°	19°	-9.8	4.0	12
KAM/166/14NL	0.043	19.7°	17°	-2.7	3.6	12
KOM/148/10NL	0.037	15.2°	0°	-15.2	4.0	15
IRA/221/02NL	0.043	113.7°	117°	3.3	3.8	16
IRA/234/17NL	0.039	121.7°	122°	0.3	3.9	17
CHI/156/10NL	0.033	59.9°	65°	5.1	4.0	14
CHI/228/04NL	0.037	72.7°	75°	2.3	3.8	14
TIB/123/00NL	0.043	87.4°	95°	7.6	3.9	11

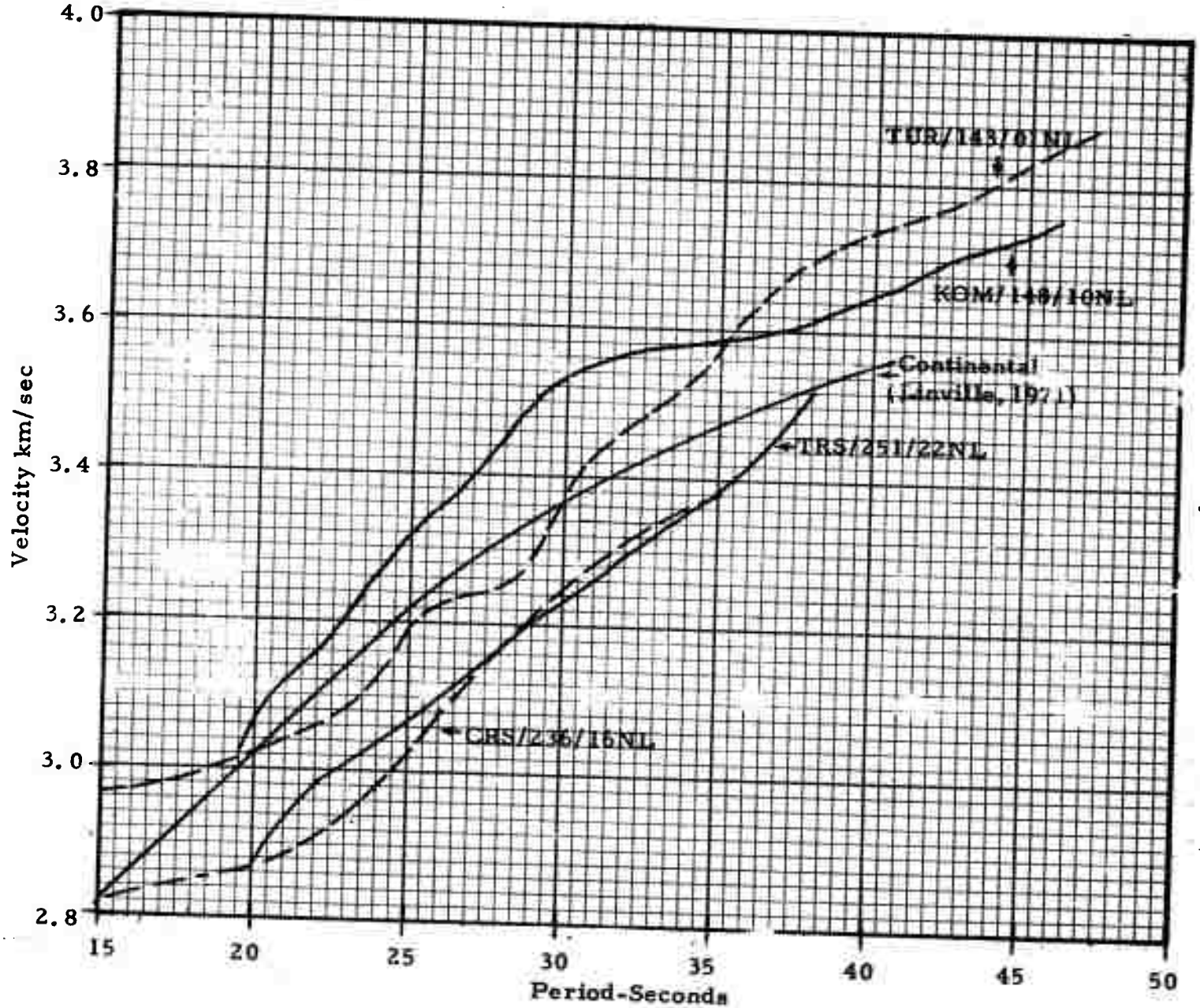

FIGURE III-15

ESTIMATED RAYLEIGH WAVE GROUP VELOCITY

from the TUR/143/01NL and KOM/148/10NL curves are close to Linville's curve. However, the two Central Asia events'curves (CRS/236/22NL and TRS/251/22NL) are significantly lower than the other two and are nearly identica even though their paths are quite different. As more group velocity estimates from large signals are made, the consistency of these two separate curves will be determined.

F. SPECTRAL CONTENT

In order to give an indication of the predominant signal band recorded at NORSAR, the -6 dB bandwidth (through the system response) of the average single site power spectrum was plotted for the Vertical, Transverse, and Radial (Figure III-16) for several large events.

Figure III-16 shows that a lower bandpass of 0.025 Hz would pass the -6 dB point for nearly all events; the exceptions are the Transverse components on KUR/235/21NL and IRA/221/02NL. A cutoff of 0.050 Hz is too low in most cases; a cutoff of 0.060 Hz would be more appropriate. Of interest in the 0.05 to 0.06 Hz band is the CHI/156/10NL event. About 400 seconds after the expected Rayleigh arrival a short (200 seconds) train with reverse dispersion appears; a cutoff frequency of 0.050 Hz on a bandpass filter would nearly eliminate this event.

Figure III-16 indicates that 0.025 to 0.060 Hz is the predominant signal band for events at NORSAR.

G. RATIOS OF RADIAL AMPLITUDES TO VERTICAL AMPLITUDES FOR THE RAYLEIGH WAVE

For two component processing of the Rayleigh mode energy the ratio of radial to vertical amplitude of the same cycle is of importance. Peak-to-peak amplitudes of corresponding cycles on the vertical and radial beamsteered traces of large magnitude events were made for 31 events. The average ratio of the radial amplitude to vertical amplitude was 0.68. This value is slightly less than the value of 0.8 observed at ALPA.

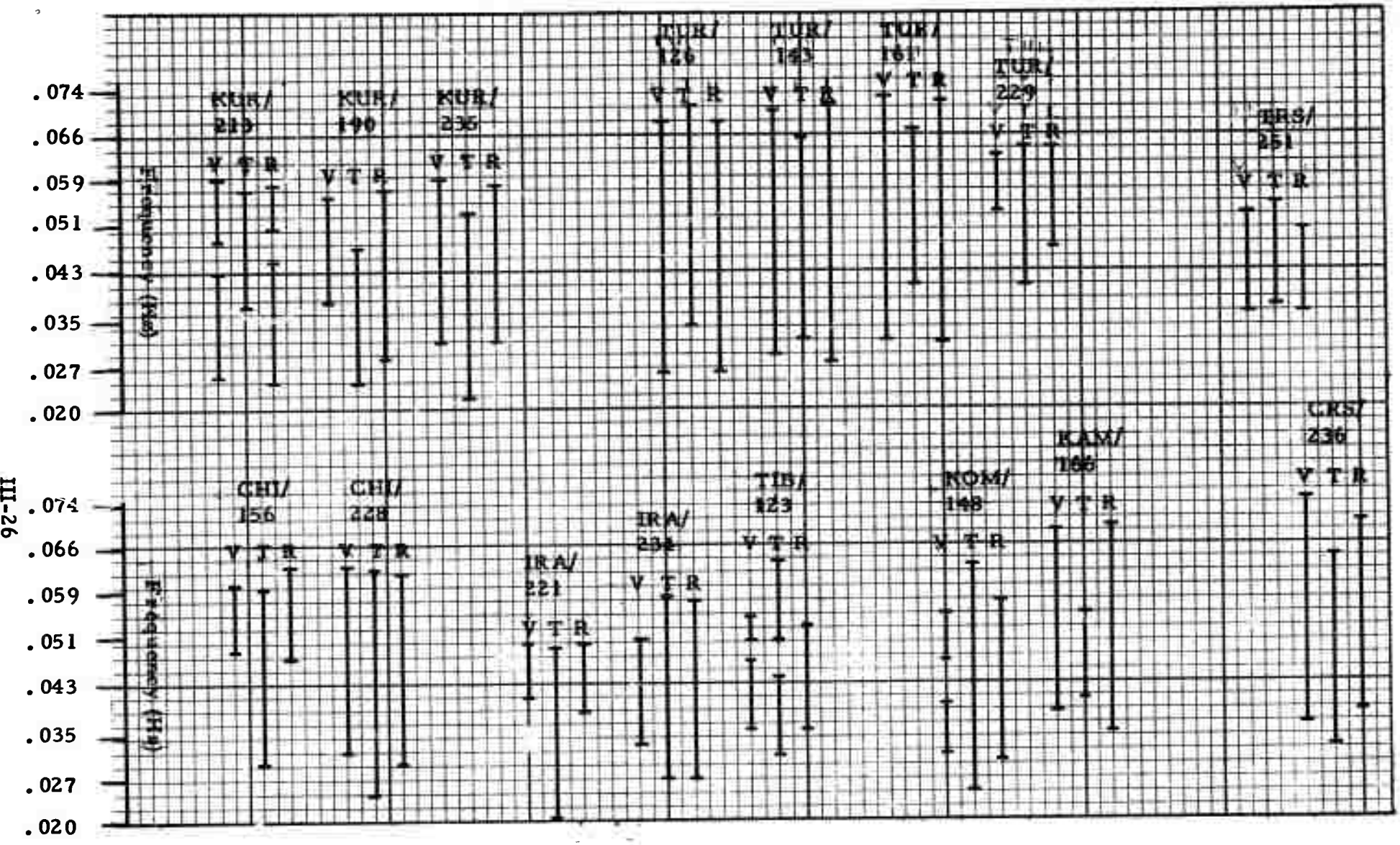

FIGURE III-16

SIGNAL SPECTRAL BANDWIDTH (-6 dB FROM PEAK POWER)

SECTION IV

ARRAY PROCESSING PERFORMANCE

A. INTRODUCTION

The principal objectives in evaluating the NORSAR array processing performance were to:

- Explore the feasibility of routinely designing and applying multichannel filters (MCF's)
- Compare noise rejection achieved by MCF over beamsteer array processors
- Estimate the signal degradation of a beamsteer processor
- Examine the stationarity of a long noise sample

Beamsteer and multichannel filter processors were evaluated for 13 noise samples in terms of noise rejection only. Difficulties in obtaining sufficient data to permit reliable MCF design precluded measurements of meaningful signal-to-noise ratio improvements by applying the MCF's to events of interest. Signal degradation from beamforming was measured for 22 events.

B. MCF AND BEAMSTEER NOISE REJECTION

Thirteen noise samples, listed in Table IV-1, were used for designing sets of multichannel filters to estimate array processing performance. These samples are a subset of the samples used in general noise analysis. The first sample (day 164) was used only for studying noise directionality. The shortest noise sample extended for approximately two hours and the longest for approximately seven hours. Prior to forming crosspower matrices, the time data were checked for quality and for surface waves from unreported events. The data from bad sites and the portions of the data including signals were not used to compute the matrices.

TABLE IV-1

NOISE SAMPLE DATA USED TO ESTIMATE

ARRAY PROCESSING PERFORMANCE

Noise Sample Designation	Date	Start Time	Duration of Edited Sample		MCF Design Parameters	
			Hr:Min:Sec	Segments†	No. of Sites	Duration of Gate
NOIS/164/1NL	06/13/71	10:00:00	7:06:40	100	13	3:33:20
NOIS/256/18A	09/13/71	18:00:00	6:02:40	85	16	2:20:48
NOIS/261/05A	09/18/71	05:20:00	3:03:28	43	8	1:46:40
NOIS/272/17A	09/29/71	17:00:00	4:03:12	57	8	1:50:56
NOIS/281/20A	10/08/71	20:30:00	6:41:04	94	15	4:11:44
NOIS/301/00A	10/28/71	00:06:18	5:02:56	71	8	1:38:08
NOIS/310/04A	11/06/71	04:00:00	3:12:00	45	13	2:08:00
NOIS/321/20B	11/17/71	20:15:00	4:16:00	60	18	2:33:36
NOIS/331/06A	11/28/71	06:00:00	4:03:12	57	19	2:42:08
NOIS/340/07A	12/06/71	07:45:00	2:16:16	32	6	1:08:16
NOIS/348/04N	12/14/71	04:00:00	2:03:44	29	6	0:55:28
NOIS/361/21N	12/27/71	20:00:00	3:03:28	43	10	1:46:40
NOIS/009/16*	01/09/72	16:30:00	6:24:00	90	13	3:54:40

† 1 segment is 256 seconds long.

Multichannel filters were designed for the vertical component of the Rayleigh mode only. The following parameters were used in the MCF design:

- Dispersive signal model oriented to a beam direction of 090° (except for the first noise sample)
- Signal-to-noise ratio equal to four at all frequencies
- Two percent white noise added to the data
- Frequency domain design by transforming, cross-multiplying and stacking 256-second segments at all frequencies 0.004 - 0.246 Hz. The data were not hanned.
- Typically, 14 good sites and a design gate of 3 hours duration were used

The frequency domain filters were then inverse-transformed to time domain operators and applied to the data to form beams. Passband filters then were applied and values obtained for the RMS output of the MCF and the BS beams. Passbands used were 0.02 to 0.059 Hz, 0.02 to 0.055 Hz, 0.02 to 0.051 Hz, 0.025 to 0.055 Hz and 0.025 to 0.051 Hz.

Improvements in noise reduction of the MCF and BS processors over a single site are presented in Table IV-2 which also shows the number of sites used and random noise $\sqrt{N}$ improvement. MCF improvements over the single sensor ranged from about 4 to 20 dB for both on-design and off-design noise, although off-design improvements were generally lower; beamsteer improvements ranged from 4 to 15 dB. Generally speaking, the MCF improvements exceed $\sqrt{N}$ improvement slightly, BS improvements fall slightly short.

Noise rejection improvements of MCF over BS processors were determined from values in Table IV-2 in each passband of on- and off-design noise by subtracting the BS noise rejection figure from the corresponding MCF noise rejection figure. The calculated noise rejection improvements are summarized in Table IV-3. The number of sites used for MCF design is also shown, and

TABLE IV-2

NOISE REJECTION (dB) OF MCF AND BS PROCESSORS FOR VARIOUS PASSBANDS
(PAGE 1 OF 2)

1971 Day	Number of Sites Used	Expected Random Noise Improvement dB	Processor	Noise Rejection (dB) of MCF and BS Processors for Various Passbands. Frequencies Shown in Hz											
				On-Design						Off-Design					
				.02-.059	.02-.055	.02-.051	.025-.055	.025-.051	.004-.246	.02-.059	.02-.055	.02-.051	.025-.055	.025-.051	.004-.246
256	16	12.0	MCF	11.4	11.6	11.3	11.8	11.5	--	10.0	9.9	9.6	10.1	9.7	--
			BS	9.4	9.8	10.6	9.8	10.7	--	9.1	9.6	10.2	9.6	10.3	--
261	8	9.0	MCF	13.6	12.9	12.1	13.2	12.4	13.1	12.7	12.0	10.6	12.1	10.6	11.8
			BS	10.9	10.3	9.5	10.6	9.8	9.1	10.6	10.7	10.4	11.1	10.9	8.7
272	8	9.0	MCF	5.9	5.9	8.5	5.7	8.3	9.8	4.2	4.2	6.5	6.8	6.3	6.8
			BS	4.3	4.3	7.2	4.1	7.1	6.5	3.8	7.7	7.5	7.9	7.7	6.3
281	15	11.8	MCF	11.3	10.8	10.5	11.2	10.8	--	10.5	10.1	9.8	10.4	10.1	--
			BS	10.2	10.0	9.6	10.2	9.8	--	11.0	10.7	10.7	10.9	10.9	--
301	8	9.0	MCF	11.5	11.4	11.8	11.6	12.0	12.0	9.0	9.1	9.4	8.4	8.7	10.1
			BS	5.4	5.2	5.2	5.8	6.0	6.2	5.2	5.2	5.2	5.7	5.8	5.7
310	13	11.1	MCF	13.4	13.5	13.7	13.5	13.8	14.9	9.6	9.6	9.8	9.4	9.8	10.8
			BS	10.5	10.5	10.8	10.5	10.8	11.0	10.0	10.0	10.0	9.8	9.9	10.9

TABLE IV-2

NOISE REJECTION (dB) OF MCF AND BS PROCESSORS FOR VARIOUS PASSBANDS
(PAGE 2 OF 2)

1971 Day	Number of Sites Used	Expected Random Noise Improvement dB	Processor	Noise Rejection (dB) of MCF and BS Processors for Various Passbands. Frequencies Shown in Hz											
				On-Design						Off-Design					
				.02-.059	.02-.055	.02-.051	.025-.055	.025-.051	.004-.246	.02-.059	.02-.055	.02-.051	.025-.055	.025-.051	.004-.246
321	18	12.6	MCF	18.4	17.4	16.4	17.7	16.7	19.0	14.5	12.8	12.1	12.9	11.8	16.6
			BS	14.9	13.5	12.9	13.6	13.0	11.8	12.9	12.7	11.8	12.9	12.1	12.2
332	19	12.8	MCF	20.8	18.5	17.1	19.2	17.7	19.7	20.2	18.1	16.4	19.1	17.4	18.8
			BS	13.4	14.0	13.6	14.1	13.7	13.2	14.5	13.2	14.2	13.4	14.8	13.0
340	6	7.8	MCF	20.7	20.4	18.9	20.7	19.3	15.9	19.6	18.9	18.4	19.7	19.0	13.7
			BS	13.7	13.4	12.8	13.5	12.9	10.3	14.0	13.8	12.9	14.3	13.1	10.3
348	6	7.8	MCF	17.5	16.3	14.9	16.7	15.6	14.7	17.3	19.1	16.9	19.4	17.5	11.1
			BS	10.4	11.4	9.9	11.5	10.1	9.7	7.7	11.2	11.7	11.2	11.9	8.5
361	10	10.0	MCF	13.7	13.2	13.0	13.4	13.1	14.5	11.9	11.3	10.0	11.5	10.3	12.8
			BS	10.1	9.7	9.5	9.9	9.6	9.9	10.4	11.1	10.6	11.2	10.9	9.9
1972 009	13	11.1	MCF	20.7	19.5	17.8	19.7	18.0	18.0	17.7	16.3	15.1	16.3	15.0	16.4
			BS	14.8	15.0	14.5	15.1	14.5	12.8	15.4	15.1	14.9	15.4	15.0	13.2

the duration of the design gate is expressed both as a number of segments and in hours, minutes, and seconds. Off-design portions sometimes preceded and sometimes followed corresponding on-design portions. Mean values of the noise rejection improvements for various passbands are listed in Table IV-4.

For the on-design region, MCF gain exceeds BS gain in all cases, typically by 3 to 4 dB, and there is a tendency toward larger gain at wider passbands. For example, on day 261 the noise rejection improvements are 4.0, 3.3, and 2.6 dB in passbands 0.004 to 0.246 Hz, 0.02 to 0.059 Hz and 0.025 to 0.051 Hz, respectively. In general, on-design results are about the same as those obtained at ALPA (Texas Instruments, 1971).

For the off-design region, MCF noise rejection improvement occasionally falls below BS noise rejection improvement. This occurs more often with narrower passbands. Results on day 361 illustrate this, since MCF off-design improvement is 0.6 dB less than BS off-design improvement over the two narrowest passbands, but MCF off-design improvement is 2.9 dB greater than BS off-design improvement over the widest passband. On the average, MCF processing gives 1 to 3 dB more rejection than beamsteering for off-design noise and occasionally improvements of 6 dB are achieved. The larger improvements are achieved only when the predominant noise source is well separated from the signal direction; but the converse is not true.

These improvements are better than those observed at ALPA and indicate that MCF processing at NORSAR can be useful on some occasions.

From the noise sample of 13 June 1971 (day 164), multichannel filters were designed having look directions of 0^{o}, 30^{o}, 60^{o}, 90^{o}, 120^{o}, 150^{o} and 180^{o}. These MCF's used 13 sites and a design gate duration of 3 hours, 33 minutes, 20 seconds. The MCF's and beamsteer filters having the same look directions were then applied to 68 minutes, 16 seconds of on-design and off-design noise. The noise rejection improvements for MCF's and BS filters

TABLE IV-3

IMPROVEMENTS (dB) IN NOISE REJECTION OF MCF OVER BS PROCESSORS FOR VARIOUS PASSBANDS
(PAGE 1 OF 2)

1971 Day	MCF Design Data: No. of Sites	MCF Design Data: Number of Segments / Duration of Gates	Numbers of the Segments Filtered by MCF and BS Processors	Improvements (dB) in Noise Rejection of MCF over BS Processors for Various Passbands. Frequencies Shown in Hz. 0.02-0.059	0.02-0.055	0.02-0.051	0.025-0.055	0.025-0.051	0.004-0.246
256	16	33	On-Design 6-21	2.0	1.8	0.7	2.0	0.8	-
		2:20:48	Off-Design 24-35	0.9	0.3	(-0.6)	0.5	(-0.5)	-
261	8	25	On-Design 14-24	3.3	2.6	2.6	2.6	2.6	4.0
		1:46:40	Off-Design 28-36	2.1	1.3	0.2	1.0	(-0.3)	3.1
272	8	26	On-Design 40-48	1.6	1.6	1.3	1.6	1.2	3.3
		1:50:56	Off-Design 22-32	0.4	(-3.5)	(-1.0)	(-1.1)	(-1.4)	0.5
281	15	59	On-Design 73-88	1.1	1.8	0.9	0.9	1.0	-
		4:11:44	Off-Design 41-56	(-0.5)	(-0.6)	(-0.8)	(-0.4)	(-0.8)	-
301	8	23	On-Design 49-64	6.1	6.2	6.6	5.8	6.0	5.8
		1:38:08	Off-Design 33-39	3.8	3.9	4.2	2.7	2.9	4.4
310	13	30	On-Design 15-30	2.9	3.0	2.9	3.0	3.0	3.9
		2:08:00	Off-Design 31-45	(-0.4)	(-0.4)	(-0.2)	(-0.4)	(-0.1)	(-0.1)

TABLE IV-3

IMPROVEMENTS (dB) IN NOISE REJECTION OF MCF OVER BS PROCESSORS FOR VARIOUS PASSBANDS
(PAGE 2 OF 2)

1971 Day	MCF Design Data: No. of Sites	MCF Design Data: Number of Segments / Duration of Gates	Numbers of the Segments Filtered by MCF and BS Processors	Improvements (dB) in Noise Rejection of MCF over BS Processors for Various Passbands. Frequencies Shown in Hz. 0.02-0.059	0.02-0.055	0.02-0.051	0.025-0.055	0.025-0.051	0.004-0.246
321	18	36	On-Design 21 - 36	3.5	3.9	3.5	4.1	3.7	7.2
		2:33:36	Off-Design 37 - 52	1.6	0.1	0.4	0.0	(-0.3)	4.4
332	19	38	On-Design 23 - 38	7.4	4.5	3.5	5.1	4.0	6.5
		2:42:08	Off-Design 39 - 54	5.7	4.9	2.2	5.7	2.6	5.8
340	6	16	On-Design 1 - 16	7.0	7.0	6.1	7.2	6.4	5.6
		1:08:16	Off-Design 17 - 32	5.6	5.1	5.5	5.4	5.9	3.4
348	6	13	On-Design 11 - 18	7.1	4.9	5.0	5.2	5.1	5.0
		0:55:28	Off-Design 22 - 29	9.6	7.9	5.2	8.2	5.6	2.6
361	10	25	On-Design 10 - 25	3.6	3.5	3.5	3.5	3.5	4.6
		1:46:40	Off-Design 31 - 43	1.5	0.2	(-0.6)	0.3	(-0.6)	2.9
1972 009	13	55	On-Design 56 - 71	5.9	4.5	3.3	4.6	3.5	5.2
		3:54:40	Off-Design 72 - 87	2.3	1.2	0.2	0.9	0.0	3.2

TABLE IV-4

MEAN IMPROVEMENTS (dB) OF MCF OVER BS PROCESSORS FOR VARIOUS PASSBANDS (12 SAMPLES)

	Mean Improvements (dB) of MCF over BS Processors for Various Passbands					
Passbands (Hz)	0.02-.059	.02-.055	.02-.051	.025-.055	.025-.051	.004-.246
On-design	4.3	3.6	3.0	3.7	3.1	5.1
Off-design	2.7	1.7	1.2	1.9	1.1	3.0

were calculated in five passbands. The results are plotted in Figures IV-1 through IV-10. Note that, at the microseismic peak (0.059 Hz), the predominant noise propagation azimuth for this sample was around 240°, and a secondary peak around 90°.

Important features of the results are:

- In the on-design portion, MCF's did better than BS filters for every azimuth and every passband
- In the off-design portion, MCF's generally did better, but some BS filters with azimuths of 060° and 120° did slightly better than the corresponding MCF
- Serious deterioration in improvement persisted at the 090° secondary peak azimuth in all passbands containing the 0.059 Hz microseismic peak
- The 090° deterioration disappeared when the high-cut side of the passband was reduced to 0.050 Hz, thus excluding the microseismic peak
- For off-design noise, the MCF outperformed the beamsteer by the largest amount (about 2 dB) at 090°
- The performance of both MCF and BS processors drops rapidly for the wide bands at 180°; presumably, the effects of the major 240° noise peak are beginning to be seen
- Maximum variation with azimuth is about 4dB; this number probably would be higher if we had included the 240° azimuth. Note also that we are refering to fairly broad frequency bands; at the microseismic peak, variations of 8 dB were observed.

These observations demonstrate that the array's detection threshold can vary by about a factor of 2 (0.3 M_s units) with azimuth at a given time, depending on the relation of signal azimuth to noise azimuths.

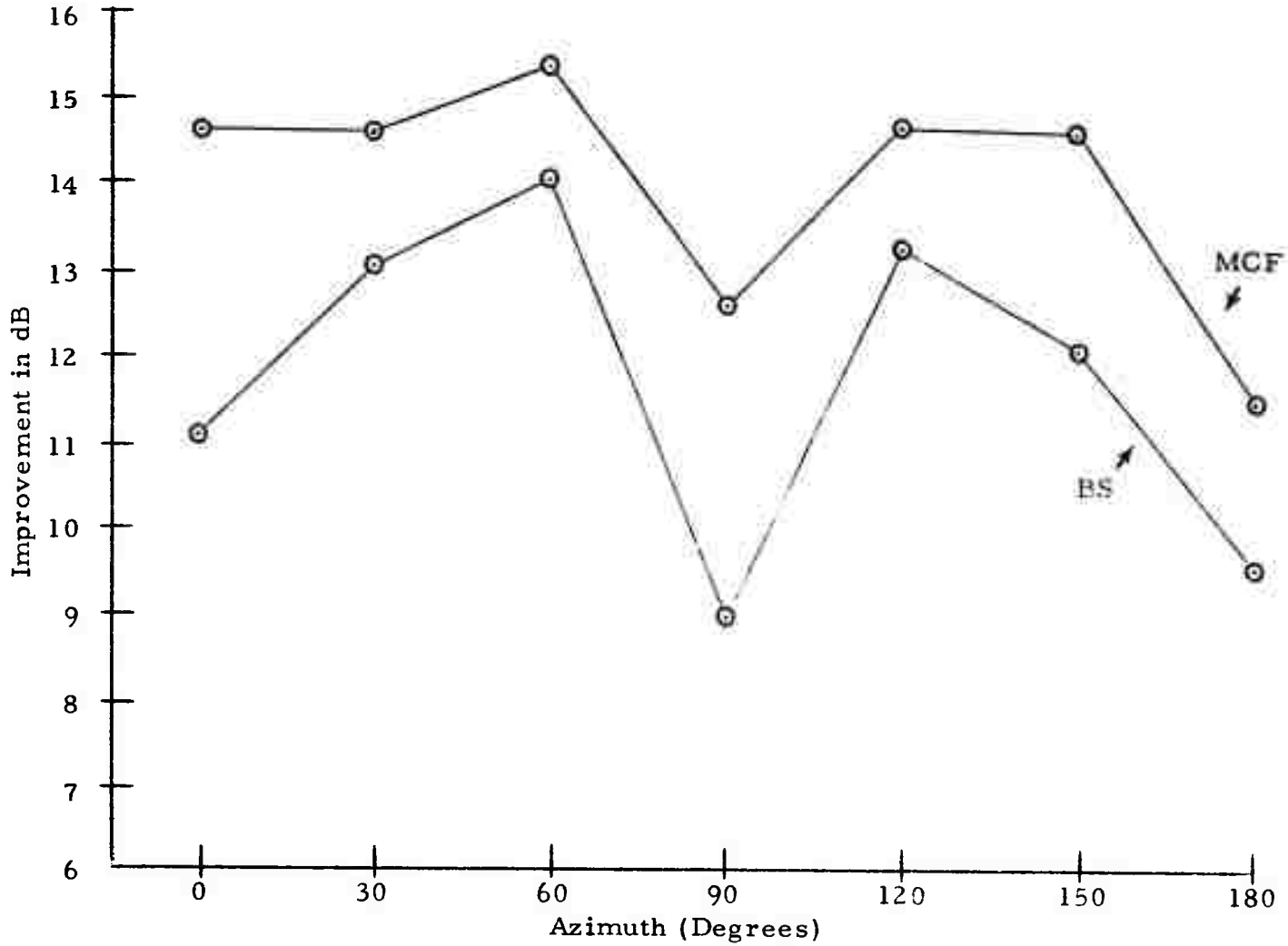

FIGURE IV-1

IMPROVEMENT vs. AZIMUTH FOR MCF AND BS PROCESSORS
0.02 TO 0.06 Hz
ON-DESIGN NOISE, 13 JUNE 1971

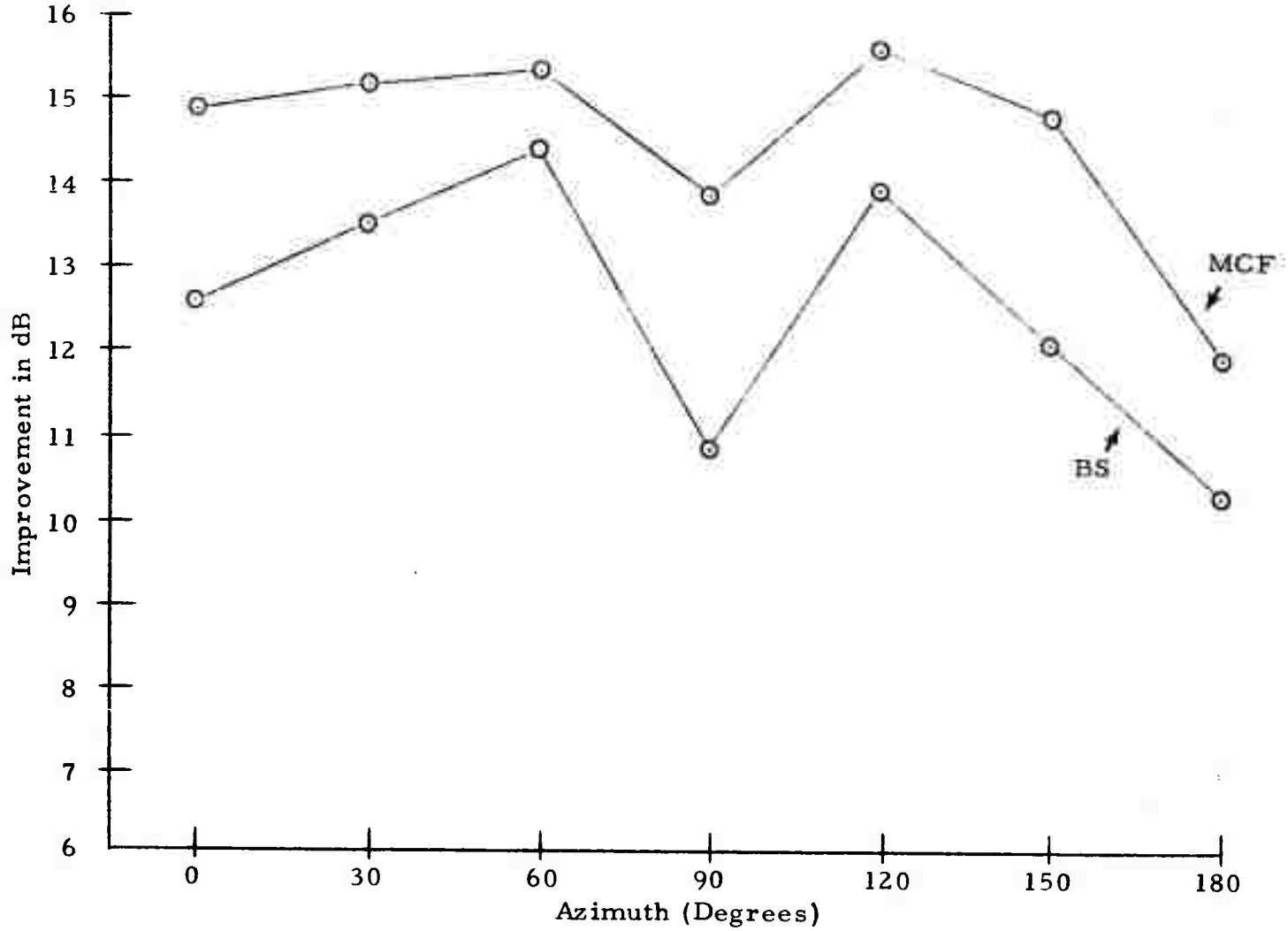

FIGURE IV-2

IMPROVEMENT vs. AZIMUTH FOR MCF AND BS PROCESSORS
0.02 TO 0.055 Hz
ON-DESIGN NOISE, 13 JUNE 1971

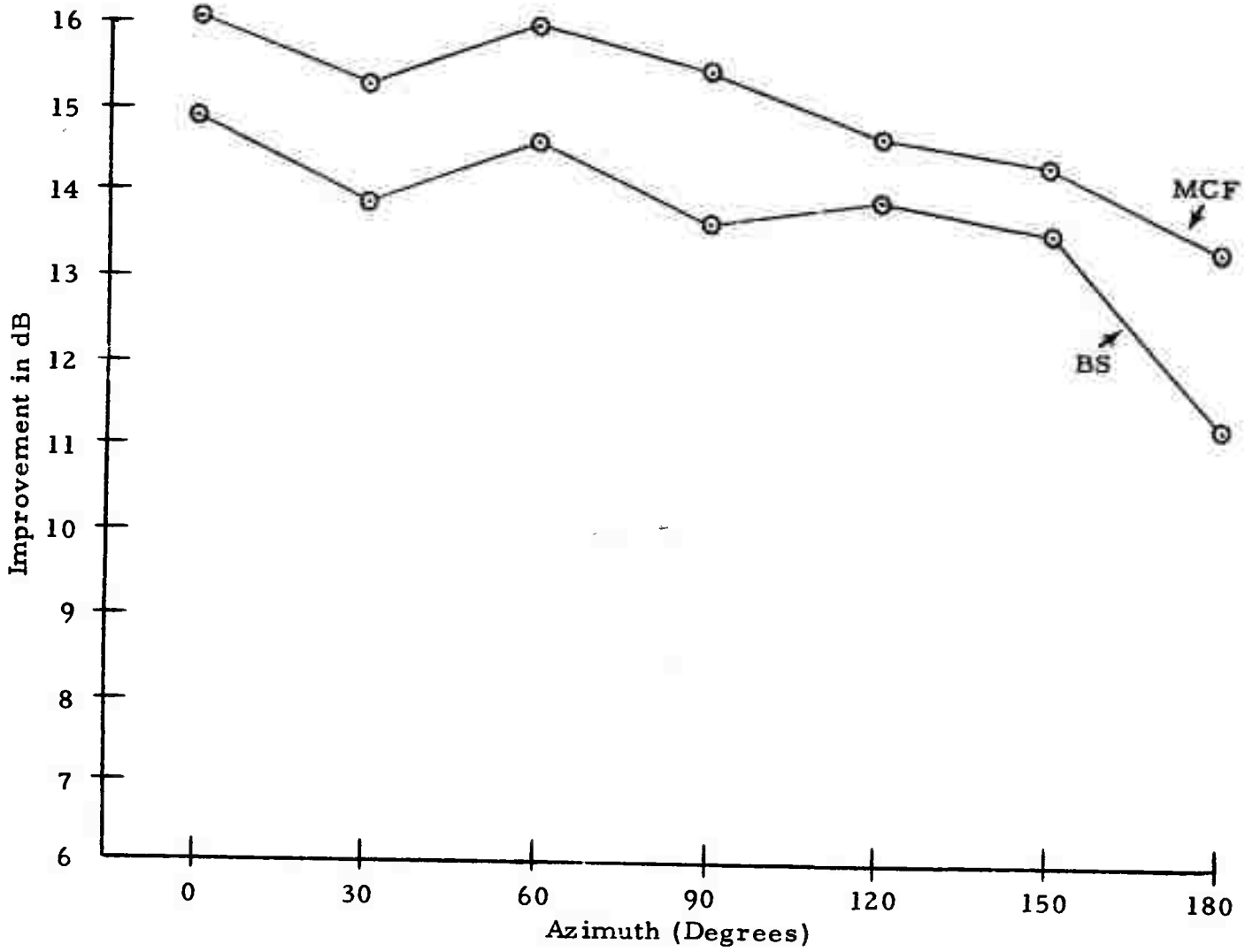

FIGURE IV-3

IMPROVEMENT vs. AZIMUTH FOR MCF AND BS PROCESSORS
0.02 TO 0.05 Hz
ON-DESIGN NOISE, 13 JUNE 1971

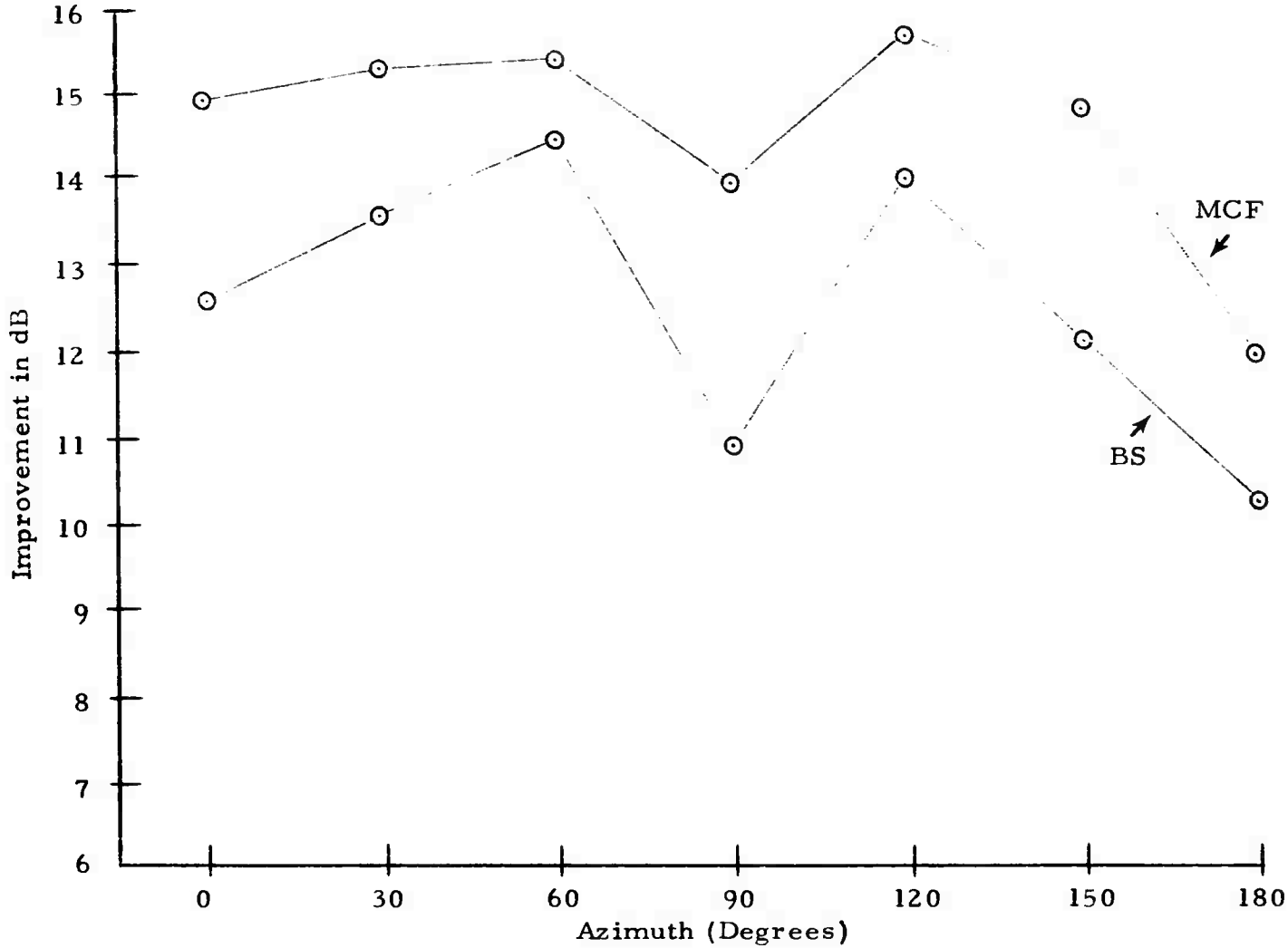

FIGURE IV-4

IMPROVEMENT vs. AZIMUTH FOR MCF AND BS PROCESSORS
0.025 TO 0.055 Hz
ON-DESIGN NOISE, 13 JUNE 1971

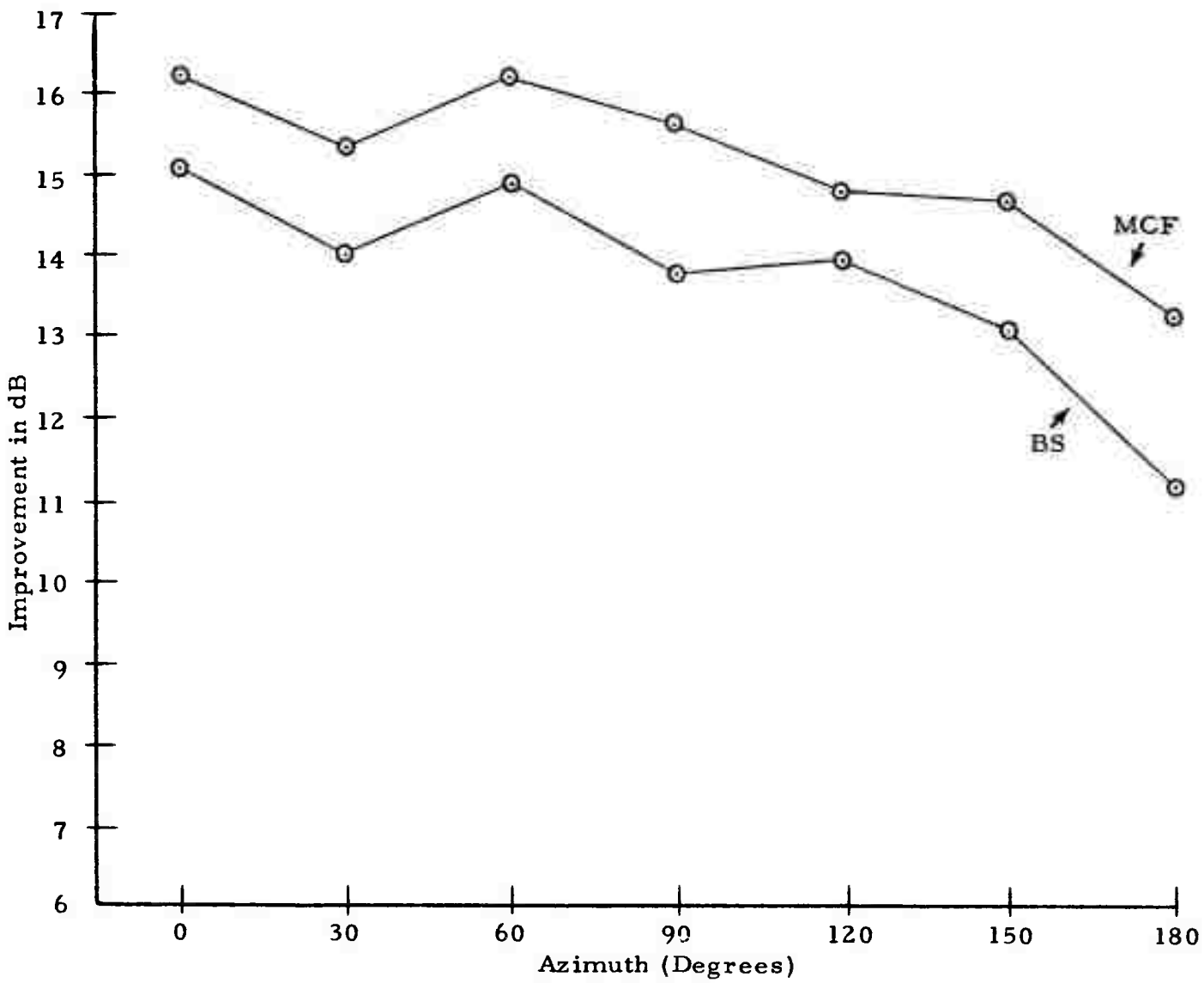

FIGURE IV-5

IMPROVEMENT vs. AZIMUTH FOR MCF AND BS PROCESSORS
0.025 TO 0.050 Hz
ON-DESIGN NOISE, 13 JUNE 1971

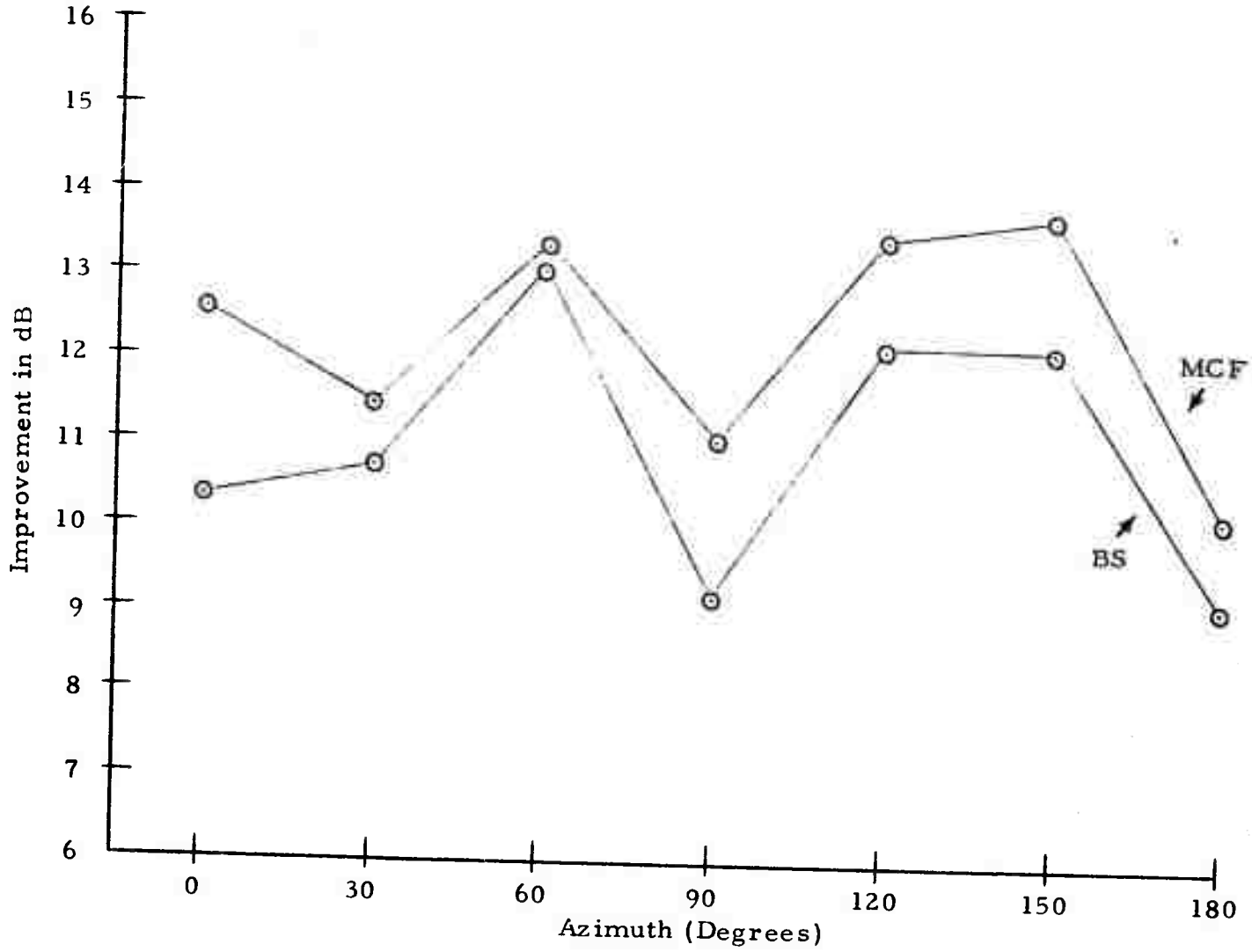

FIGURE IV-6

IMPROVEMENT vs. AZIMUTH FOR MCF AND BS PROCESSORS
0.02 TO 0.06 Hz
OFF-DESIGN NOISE, 13 JUNE 1971

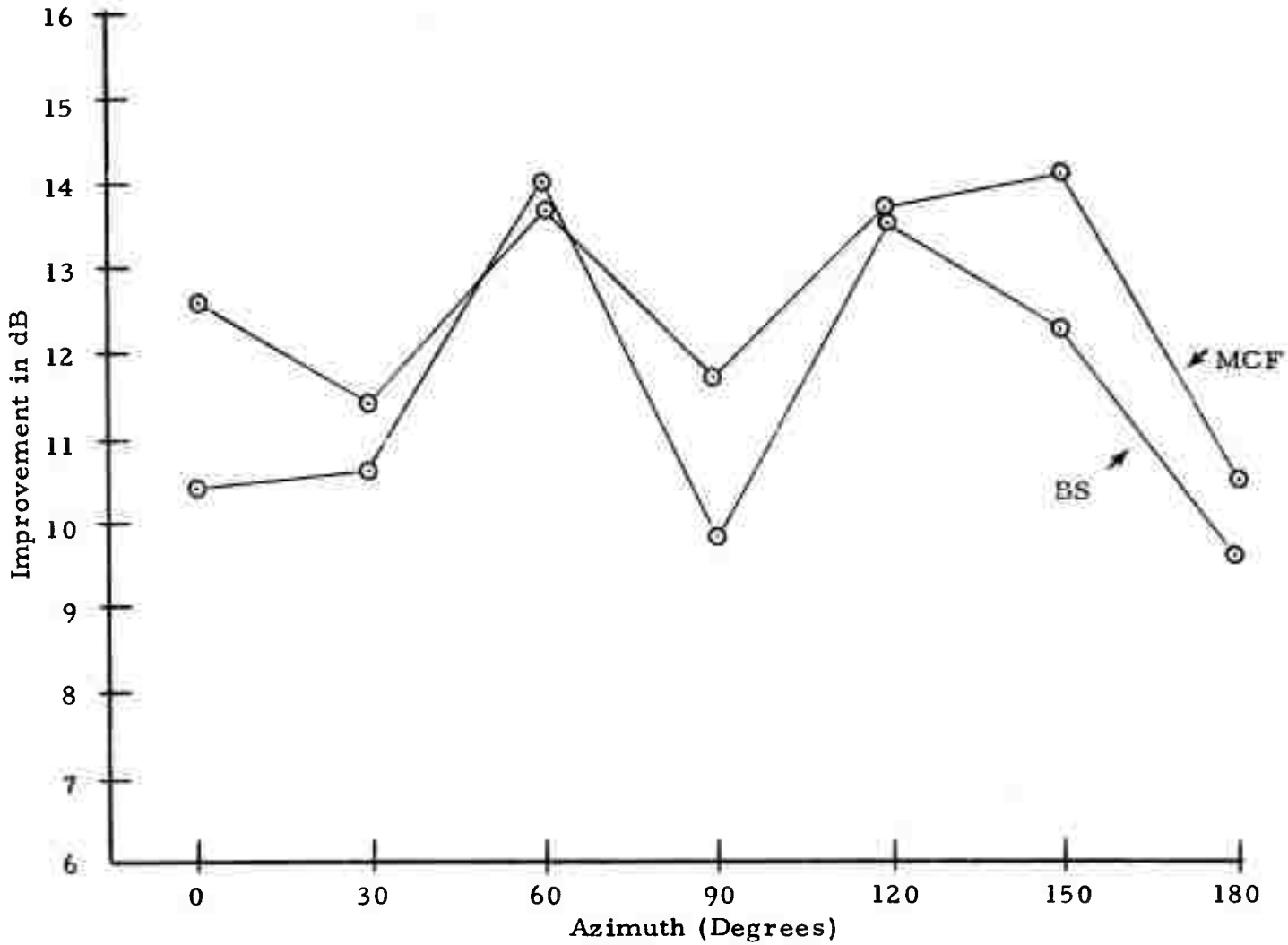

FIGURE IV-7

IMPROVEMENT vs. AZIMUTH FOR MCF AND BS PROCESSORS
0.02 TO 0.055 Hz
OFF-DESIGN NOISE, 13 JUNE 1971

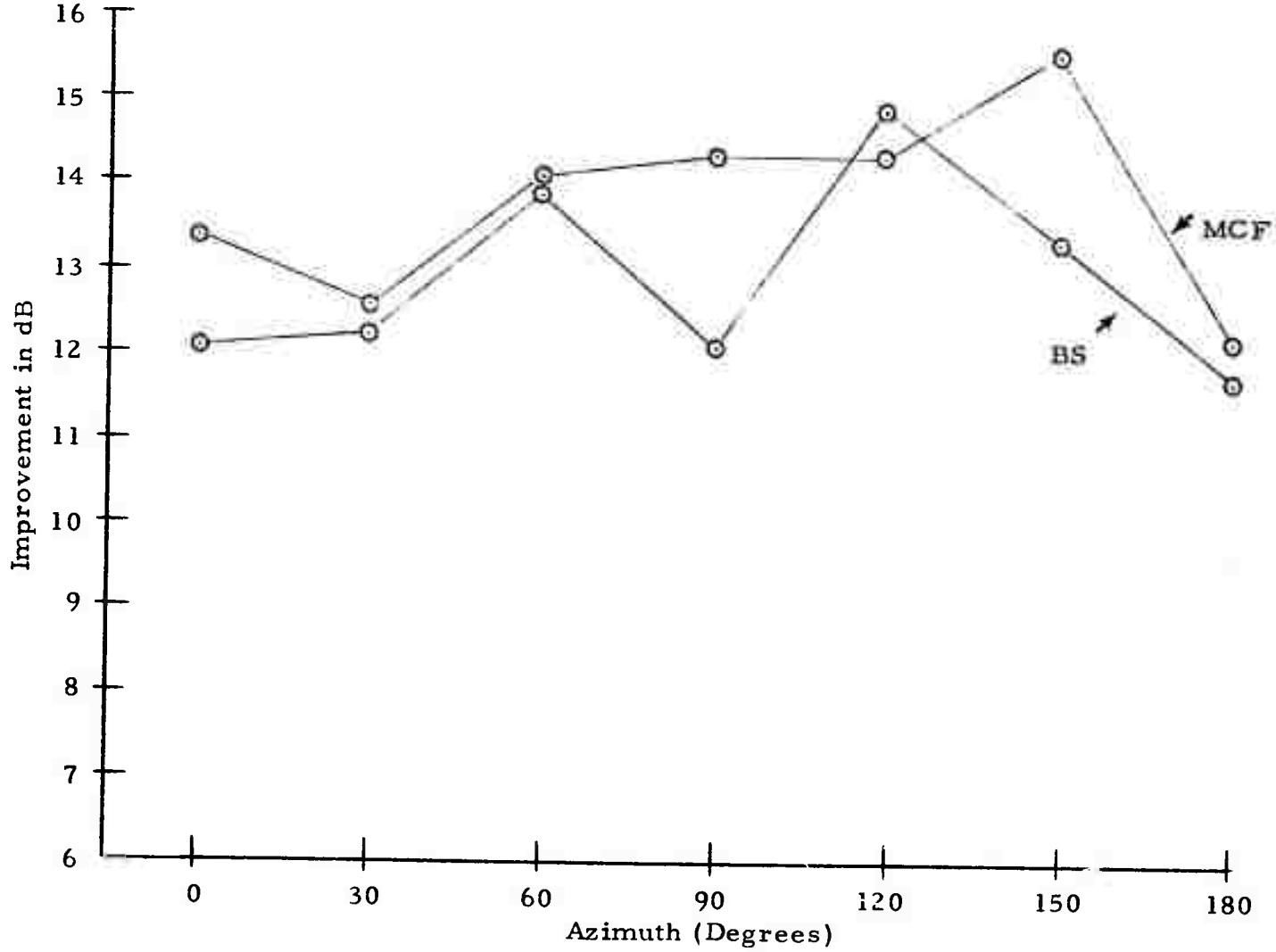

FIGURE IV-8

IMPROVEMENT vs. AZIMUTH FOR MCF AND BS PROCESSORS
0.02 TO 0.05 Hz
OFF-DESIGN NOISE, 13 JUNE 1971

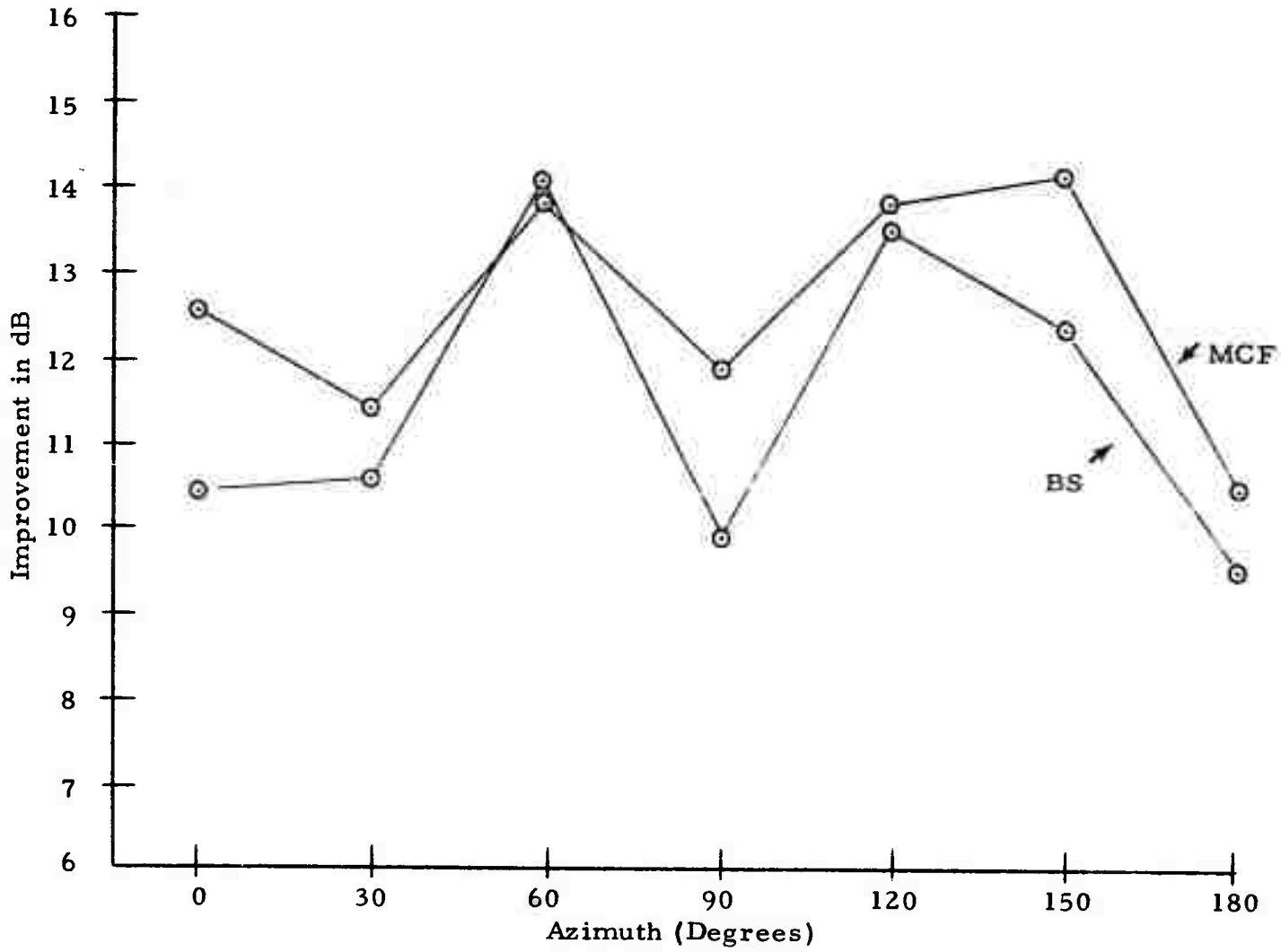

FIGURE IV-9

IMPROVEMENT vs. AZIMUTH FOR MCF AND BS PROCESSORS
0.025 TO 0.055 Hz
OFF-DESIGN NOISE, 13 JUNE 1971

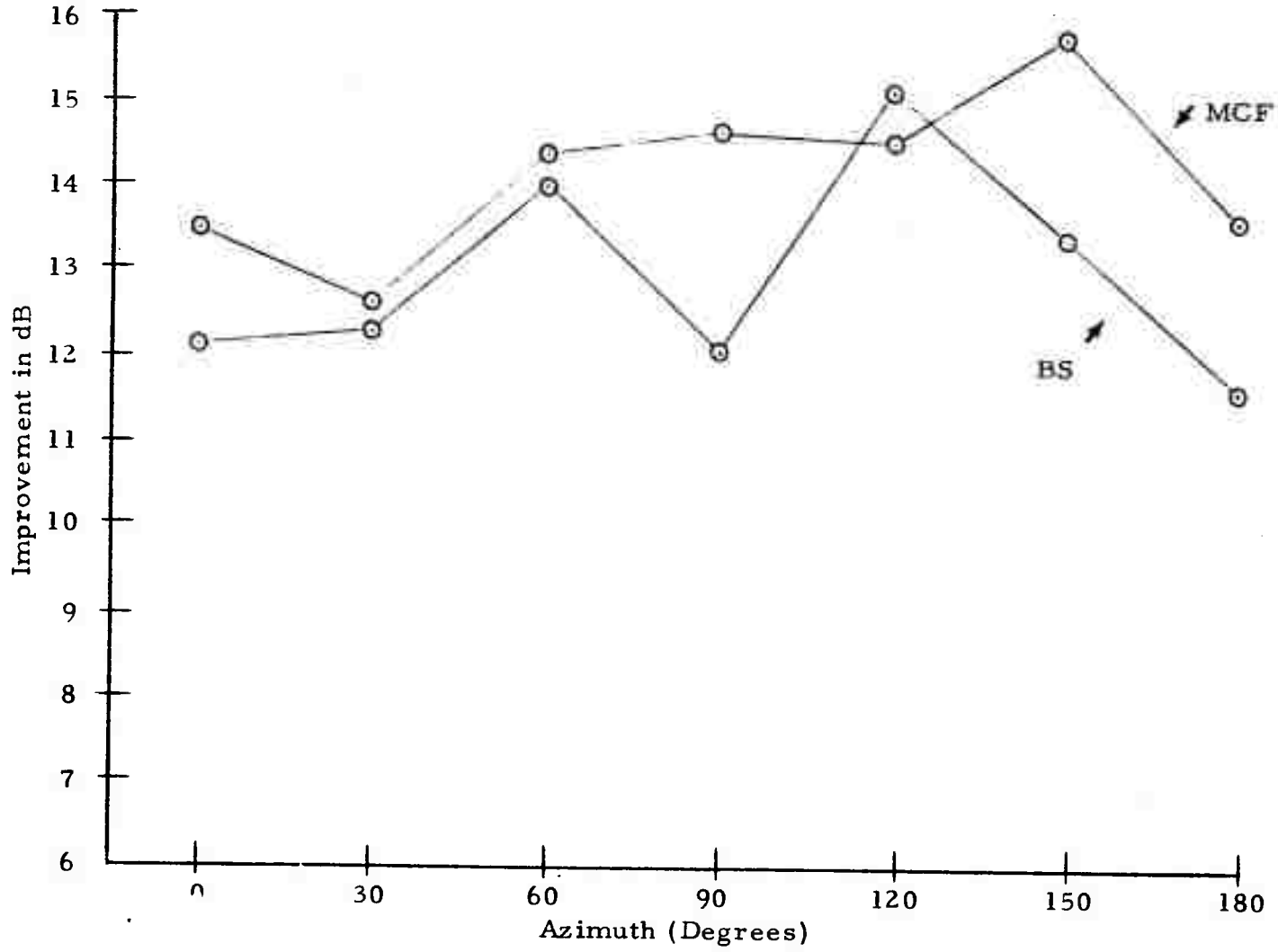

FIGURE IV-10

IMPROVEMENT vs. AZIMUTH FOR MCF AND BS PROCESSORS
0.025 TO 0.050 Hz
OFF-DESIGN NOISE, 13 JUNE 1971

In summary, it appears that multichannel filtering may be worthwhile in special cases, but probably not in a routine fashion. The signal analysis indicated that there is significant signal energy out to 0.06 Hz; the MCF performance (relative to beamsteer processing) is best when the passband includes the microseismic peak. Thus, for certain high-frequency, narrow-band signals, MCF processing might be desirable.

C. SIGNAL DEGRADATION OF THE BEAMSTEER PROCESSOR

Signals from 22 events were used to determine signal degradation from beamforming. All of the events originated on or near the Asian continent. The events covered a range of magnitudes but all had moderate to large signal-to-noise ratios.

Beam signal degradation is defined as the ratio of peak-to-peak signal amplitude on a reference sensor to that on a beamsteer beam, with the same cycle being considered for each corresponding component. Measurements were made on the raw traces of a reference site (usually site 1) and on the beamsteer output. All data were rotated to the event azimuths, but were not bandpass filtered.

Signal degradation values, expressed in dB, are given for the 22 events in Table IV-5. The negative values mean that beamsteer outputs actually exceeded reference site input data. Values ranged from -0.7 dB to 2.8 dB; note that no positive value exceeded 3 dB and only 6 out of 65 exceeded 2 dB. Mean signal degradation due to beamsteering was on the order of 1 dB for the complete data set. No correlation between signal azimuth and degradation could be discerned.

D. STATIONARITY OF THE NOISE OF 9 JANUARY 1972

The basic assumption in the theory of MCF design is that the ambient noise field is stationary. This means that the noise is stable in

TABLE IV-5

SIGNAL DEGRADATION OF BEAMSTEER PROCESSOR FOR VARIOUS EVENTS

Event Designation	m_b	Delta	Azimuth	Signal Degradation (dB)		
				Vertical	Transverse	Radial
TIB/123/00NL	5.4	56°	087°	0.3	0.7	0.5
TDZ/147/00N1	4.8	42°	095°	1.8	1.7	2.6
KOM/148/10NL	4.5	62°	015°	1.6	2.1	2.1
CHI/156/10NL	4.7	64°	060°	1.2	1.2	1.0
SIN/166/22N1	5.6	45°	083°	1.0	0.5	1.5
SIN/170/17NL	5.2	45°	083°	0.7	0.3	0.4
KUR/190/16BE	4.9	68°	032°	1.9	2.2	2.8
CHI/208/13NL	5.3	46°	087°	0.8	0.2	0.4
SIN/219/15NL	4.8	47°	089°	1.7	1.0	0.6
CHI/229/09NL	4.9	66°	073°	0.7	0.2	0.2
CRS/236/16N2	5.2	42°	064°	0.1	0.7	0.8
TRS/251/22NL	4.8	28°	120°	1.1	0.3	0.3
NRS/270/05N3	6.4	21°	035°	0.4	0.7	2.0
SIN/273/12NL	4.5	42°	068°	1.2	1.2	1.1
CHI/283/05NL	4.4	58°	077°	0.3	0.0	0.6
CAU/283/09NL	4.0	26°	117°	1.4	0.7	0.7
BUR/283/18NL	5.1	66°	082°	0.4	0.1	0.7
IRA/288/14N1	4.7	36°	111°	2.0	1.6	2.1
CAU/288/17NL	4.9	30°	113°	1.4	0.2	0.4
KRG/301/13N2	5.5	41°	089°	0.1	0.1	0.5
TIB/302/17NL	5.0	54°	084°	0.6	0.2	1.0
WKZ/356/06NL	6.0	25°	104°	1.5	--	0.3
Average Values of Signal Degradation				0.7	0.7	1.0

structure and in wavenumber space. The 6 hour, 24 minute noise sample of 9 January 1972, which was the longest available edited noise sample not interrupted by discernible seismic events , was used to study this noise stationarity.

The vertical components of five typical sites were chosen for analysis. These were sites 1, 3, 13, 17, and 20, located at the array center, in the northeast, the east, the south and the west, respectively. The noise samples were divided into 10 gates, each being 38 minutes, 24 seconds in duration. Power density spectra and RMS noise power were computed for these sites in each gate. The mean power in each gate taken over 13 good sites was also determined and conventional wavenumber spectra were computed using the good sites.

Table IV-6 shows the RMS noise in the passband 0.004 to 0.246 Hz in each gate for the five typical sites together with the gate mean over 13 good sites. The means and the standard deviations over all 10 time gates are listed for each typical site and for the 13 good sites.

Table IV-7 shows that the RMS noise in the passband 0.025 to 0.051 Hz in each gate for the five typical sites together with the gate mean over 13 good sites. The means and the standard deviations over all 10 time gates are listed for each typical site and for the 13 good sites. Within each passband, the deviations between the mean power of each site are not statistically significant.

Power density spectra were determined for the vertical noise component, averaged over the 13 good sites, in each gate. These spectra are shown in Figure IV-11. There is a good degree of similarity between these ten curves. The spectral levels at each frequency were not tested for significant variations; however, there seems to be no persistent difference among the spectra from each gate.

TABLE IV-6

RMS NOISE LEVEL OF VERTICAL COMPONENT
IN PASSBAND 0.004 TO 0.246 Hz FOR 10 TIME
GATES OF CONTINUOUS NOISE ON 9 JANUARY 1972

Time Gate	Segment Numbers	RMS Noise Level in Millimicrons					
		Gate Mean of 13 Sites	Site #1	Site #3	Site #13	Site #17	Site #20
1	1-9	93.8	98.3	90.8	91.9	98.4	90.0
2	10-18	99.5	94.0	95.7	100.8	93.4	92.7
3	19-27	88.9	85.3	90.0	89.3	92.4	90.5
4	28-36	93.5	95.9	96.1	97.7	89.7	91.5
5	37-45	92.0	90.3	95.8	92.2	85.6	89.7
6	46-54	90.9	95.1	90.9	91.3	95.6	90.9
7	55-63	89.9	97.8	88.4	86.3	95.5	84.7
8	64-72	88.4	86.2	86.4	88.7	96.7	89.5
9	73-81	91.3	92.4	87.5	90.6	88.0	99.1
10	82-90	90.9	99.5	88.4	89.8	89.6	91.7
Site Mean of 10 Gates		92.0	93.6	91.0	92.0	92.6	91.1
Standard Deviation		3.2	4.9	3.6	4.3	3.9	3.6

TABLE IV-7

RMS NOISE LEVEL OF VERTICAL COMPONENT
IN PASSBAND 0.025 TO 0.051 Hz FOR 10 TIME
GATES OF CONTINUOUS NOISE ON 9 JANUARY 1972

Time Gate	Segment Numbers	RMS Noise Level in Millimicrons					
		Gate Mean of 13 Sites	Site #1	Site #3	Site #13	Site #17	Site #20
1	1-9	37.7	42.8	33.0	36.1	43.0	37.1
2	10-18	35.3	35.0	39.6	39.9	27.5	34.5
3	19-27	34.5	31.8	34.0	38.0	34.5	34.4
4	28-36	33.6	37.0	38.0	31.1	28.6	29.9
5	37-45	33.4	35.3	31.4	28.2	26.1	30.3
6	46-54	32.9	33.2	30.5	39.2	30.5	27.2
7	55-63	29.7	29.7	28.2	28.2	26.1	28.8
8	64-72	31.1	29.5	31.3	31.1	28.8	33.9
9	73-81	29.3	32.7	23.6	30.8	29.9	28.9
10	82-90	33.0	39.4	28.3	34.3	26.6	25.5
Site Mean of 10 Gates		33.1	34.6	31.8	33.7	30.2	31.1
Standard Deviation		2.5	4.2	5.4	4.6	5.2	3.7

Results of the frequency - wavenumber analysis performed at the lower and upper microseismic peaks are summarized in Table IV-8. For the lower microseismic peak, the major propagation azimuth remains essentially fixed at north, except during gates 2 and 3 when it appears to change to west. Even in these gates, however, a secondary peak exists in the north, so it is possible that the westerly energy is due to an event that is not reported in source bulletins and not visible in time domain plots. These spectra generally are sharp, well-defined structures, so that picking the peaks is easy. An indication of a westerly noise source also is seen in gates 6, 8 and 10.

For the upper microseismic peak, the major propagation azimuth stays within the southwest quadrant for the entire ten gates, although the time gate 7 peak looks different. These spectra are usually medium-sharp structures; two gates indicate a possible secondary noise source to the northwest.

It was seen above in Table IV-3 that in the 0.02 to 0.059 Hz passband, MCF's outperformed BS processors by 5.9 dB in the on-design portion and by 2.3 dB in the off-design portion for this noise sample. Note that the on-design portion approximately coincided with time gates 1, 2, 3, 4, 7 and 8 and included the time period when propagating noise in the lower microseismic peak apparently came from the west. Note also that the off-design portion approximately coincided with time gates 9 and 10 and included only time periods when the propagating noise in the lower microseismic peak came from the north. Therefore, the drop in improvement between on- and off-design portions may be due to different wavenumber spectra between the off-design noise and some segments of the on-design noise.

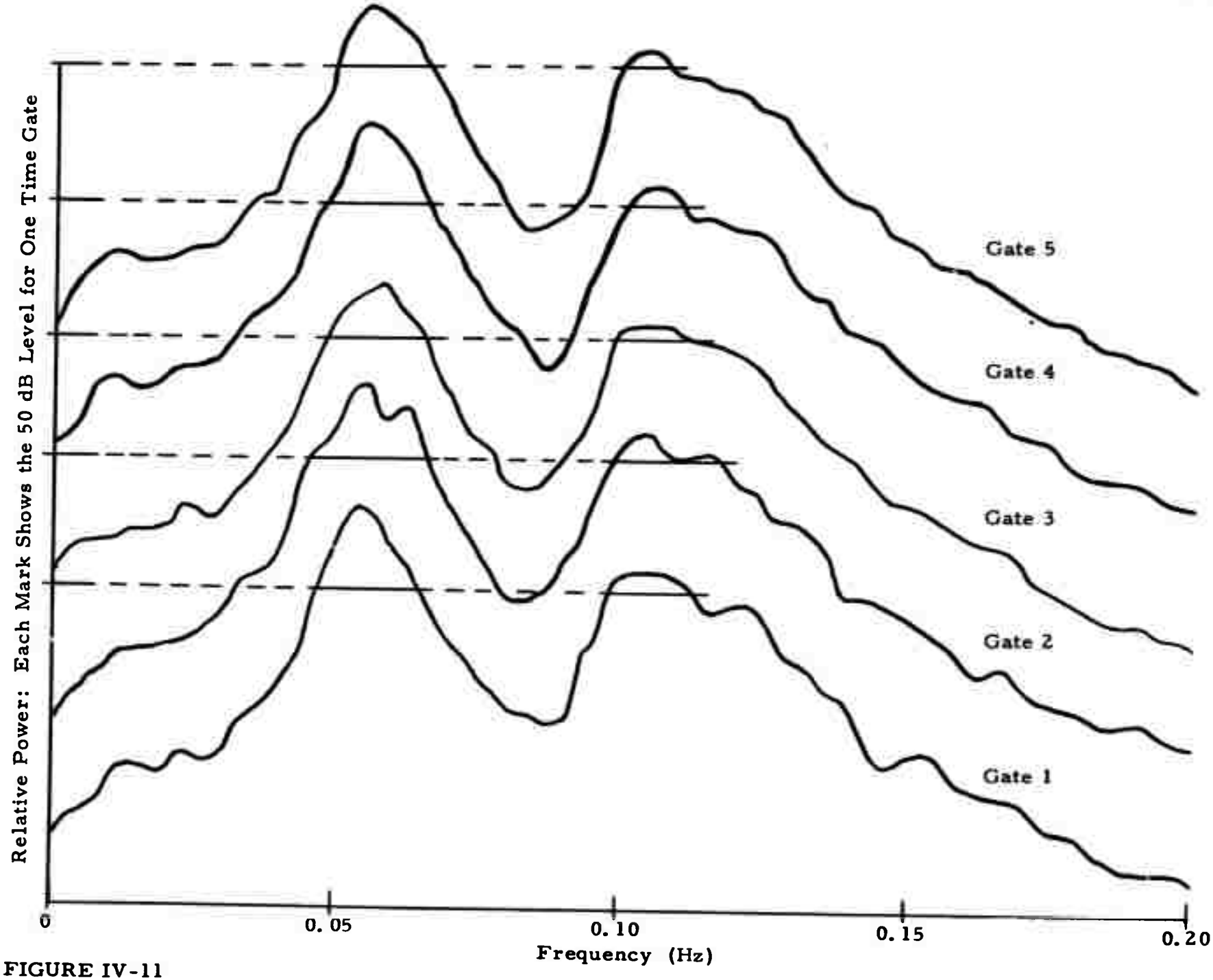

FIGURE IV-11

(PAGE 1 OF 2) POWER DENSITY SPECTRA. VERTICAL COMPONENTS OF NOISE ON 9 JANUARY 1972 AVERAGED OVER 13 GOOD SITES. TIME GATES 1 THROUGH 5

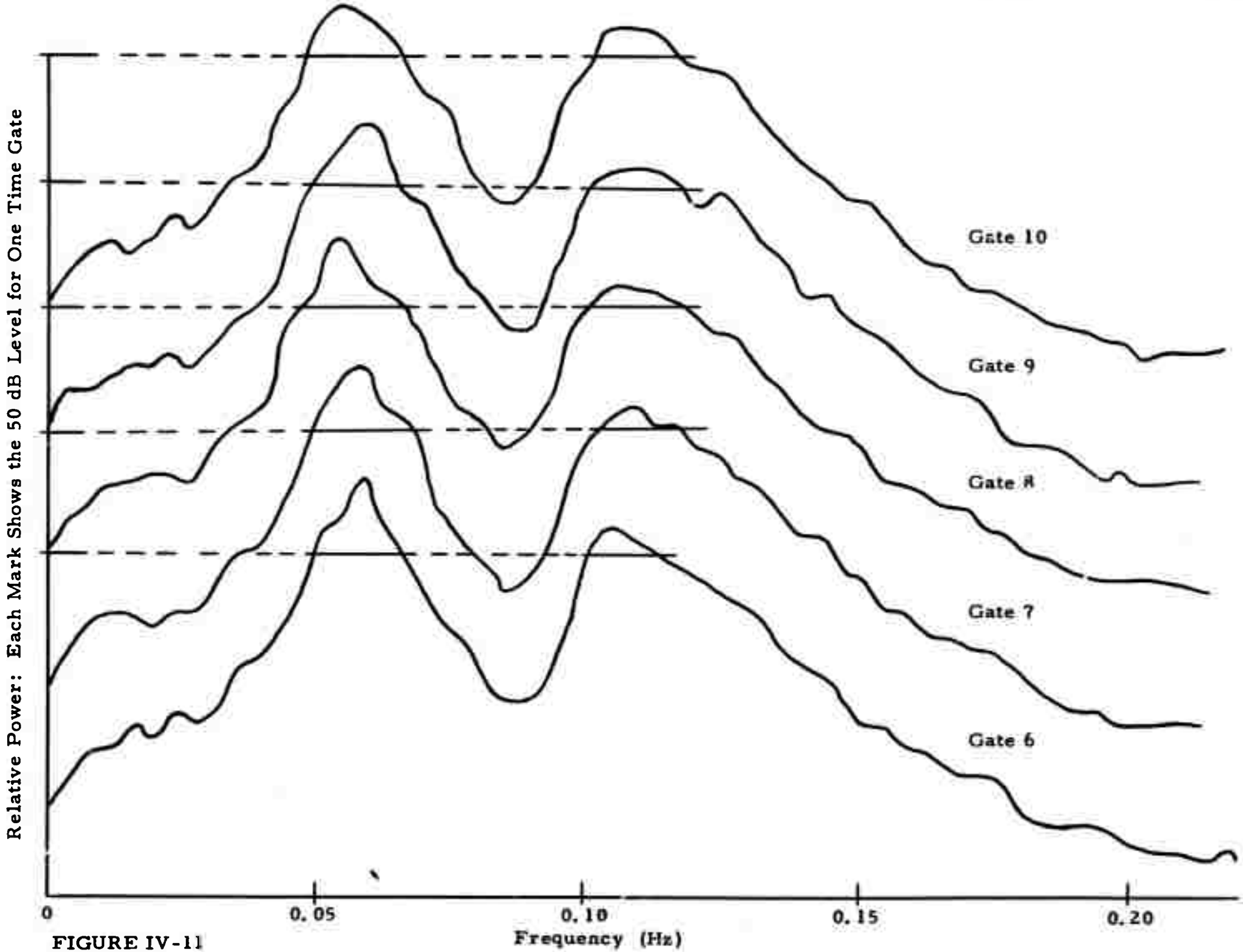

FIGURE IV-11

(PAGE 2 OF 2)

POWER DENSITY SPECTRA. VERTICAL COMPONENTS OF NOISE ON 9 JANUARY 1972
AVERAGED OVER 13 GOOD SITES. TIME GATES 6 THROUGH 10

TABLE IV-8

CHARACTERISTICS OF VERTICAL COMPONENT IN 10 TIME GATES
OF CONTINUOUS NOISE ON 9 JANUARY 1972
EACH TIME GATE IS 38 MINUTES 24 SECONDS LONG

Day 009 1972 Time Gate	Azimuth and Velocity			
	Lower Microseismic Peak		Upper Microseismic Peak	
	0.055 Hz	0.059 Hz	0.105 Hz	0.109 Hz
1	347° 3.7 km/s		216° 3.3 km/s	
2	273° 3.6 km/s		253° 3.5 km/s	
3		293° 3.9 km/s	230° 3.2 km/s	
4	356° 3.8 km/s		233° 3.4 km/s	
5	356° 3.5 km/s		218° 3.6 km/s	
6		360° 3.5 km/s	250° 3.4 km/s	
7		352° 3.8 km/s		187° 3.2 km/s
8	357° 3.6 km/s			244° 3.2 km/s
9		356° 3.8 km/s		218° 3.5 km/s
10	360° 3.5 km/s			247° 3.4 km/s
Velocity Mean	3.7 km/s		3.4 km/s	

SECTION V

MATCHED FILTERING PERFORMANCE

A. INTRODUCTION

Matched filters were applied to NORSAR long period beams to evaluate their effectiveness in increasing the signal-to-noise ratio of dispersed seismic signals. The filters, both master event waveforms and chirps, were applied to the vertical and radial Rayleigh waves and the transverse Love waves. The goals of this analysis were:

- To determine potential signal-to-noise ratio gains of master event and chirp filters.
- To investigate regional effects on matched filter effectiveness.
- To determine if seismic regions in the Eurasian landmass can be categorized by matched filter parameters.
- To compare relative effectiveness of master event and chirp filters.

Master events from twelve areas on the Asian continent were selected as master event filters. These events are listed in Table V-1. The location of the epicenters of these events as well as the great circle paths to NORSAR and circles of 5° distance from each epicenter are shown in Figure V-1.

Linear chirp filters were designed in the frequency domain by specifying upper and lower frequencies of the passband and the duration of the filter. The chirp filters were linear in the sense that their time domain waveforms were dispersive with linear group delay. Three passbands were used for all events, while the duration was selected on the basis of the best signal-to-noise ratio increase. These passbands (which were also used for the master event filter) were:

TABLE V-1

MASTER WAVEFORM EVENT LIST

Area Code	Designation
A	TUR/143/01
B	KUR/190/16
C	SIN/166/22
D	CHI/229/09
E	TIB/302/17
F	TDZ/147/00
G	CRS/236/16
H	KUR/213/02
I	CAU/288/17
J	ERS/165/13
M	EKZ/364/06
N	BLS/263/06

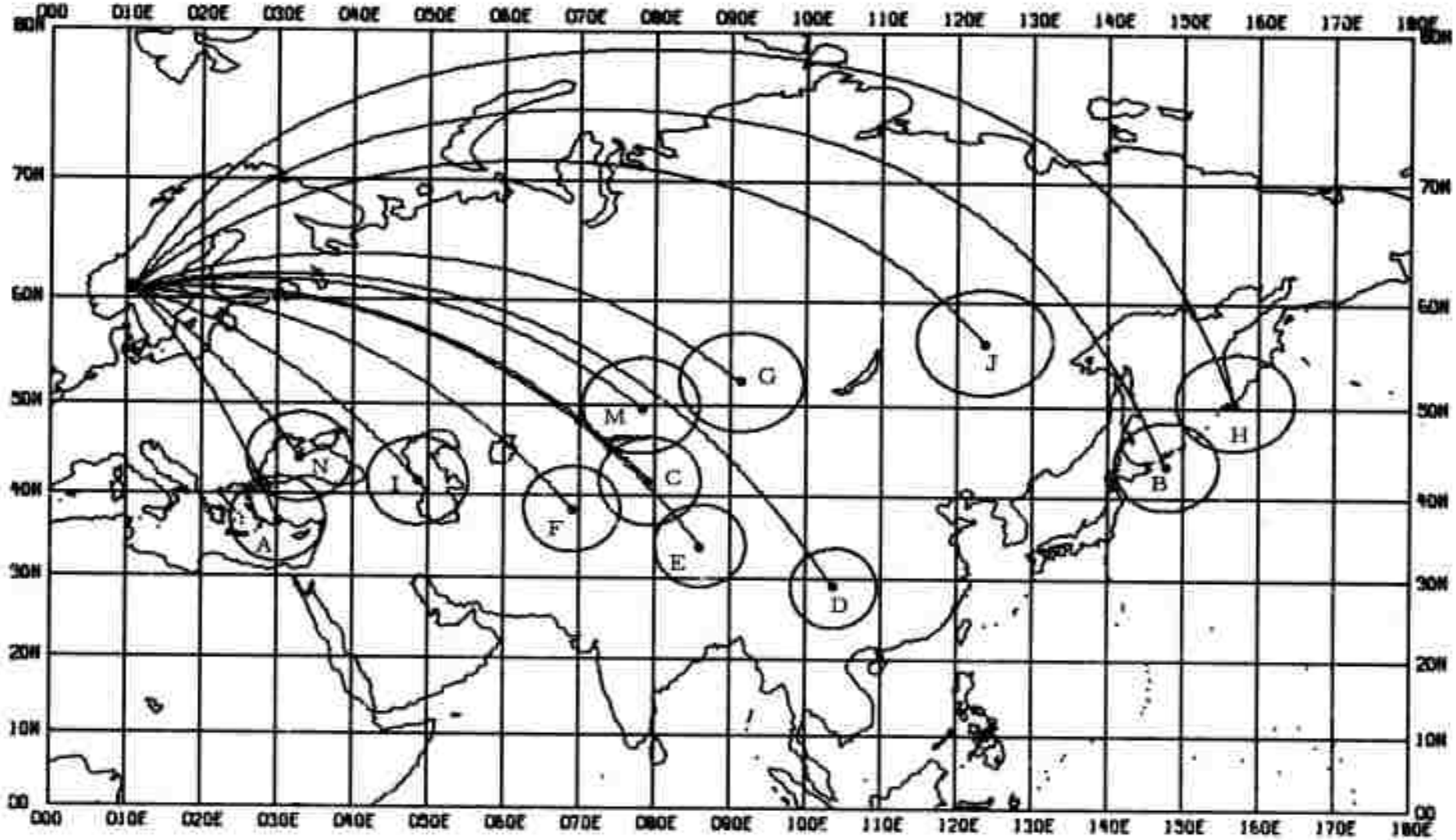

MILLER MODIFIED MERCATOR PROJECTION
MAP SCALE: 0.500 IN./ 10 DEG. LONGITUDE

FIGURE V-1

MASTER EVENT AREAS AND GREAT CIRCLE PATHS

(1) 0.020 - 0.059 Hz

(2) 0.025 - 0.055 Hz

(3) 0.025 - 0.051 Hz

Fifty-nine events were selected for analysis. Master waveform filters were applied to 49 of these events and chirp filters were applied to all 59 events. The events selected are given in Table V-2. For complete epicenter information, refer to Table I-1.

After the data had been examined for quality, it was rotated and summed to form a beam in the direction of the great circle path to the event. Beams were formed using a phase velocity of 3.5 km/sec for the vertical and radial components and 4.0 km/sec for the transverse components.

Signal plus noise-to-noise ratio (SNNR) improvement was computed as 20 log of the ratio of the SNNR of the matched filter output to the SNNR of the equivalent bandpass filter output. That is:

$$\text{Improvement (dB)} = 20 \log_{10} R$$

where

R = SNNR matched/SNNR bandpass

and

SNNR = signal peak amplitude + noise / RMS noise

B. MASTER WAVEFORM FILTER PERFORMANCE

The master events were chosen with three considerations:

- Location in an area of interest.
- Adequate signal-to-noise ratio.
- Surface or near-surface focus.

TABLE V-2

MATCHED FILTER TEST EVENTS
(PAGE 1 OF 3)

Area Code	Event Designation	Filters C= Chirp, M= Master	Master-Test Separation (Km)
A	TUR/143/01	C, M	Master
	TUR/126/04	C, M	236
	TUR/161/09	C, M	248
B	KUR/190/16	C, M	Master
	KUR/135/21	C, M	34
	KUR/146/01	C, M	80
	KUR/147/16	C, M	110
	KUR/152/21	C, M	202
	KUR/191/03	C, M	11
	KUR/191/09	C, M	278
C	SIN/166/22	C, M	Master
	SIN/166/23	C, M	14
	SIN/170/17	C, M	0
	SIN/219/15	C, M	616
	SIN/221/01	C, M	346
	SIN/241/15	C, M	560
	CHI/208/13	C	306
D	CHI/229/09	C, M	Master
	CHI/229/17	C, M	0
	CHI/258/07	C, M	523
	CHI/258/11	C, M	621

TABLE V-2

MATCHED FILTER TEST EVENTS
(PAGE 2 OF 3)

Area Code	Event Designation	Filters C= Chirp, M= Master	Master-Test Separation (Km)
E	TIB/302/17	C	Master
	TIB/123/00	C	382
	TIB/155/20	C	602
F	TDZ/147/00	C, M	Master
	TDZ/274/16	C, M	77
	TDZ/259/10	C, M	208
	KRG/301/13	C, M	493
G	CRS/236/16	C, M	Master
	SIN/273/12	C, M	340
H	KUR/213/02	C, M	Master
	KOM/148/10	C, M	874
	KAM/166/14	C, M	384
I	CAU/288/17	C, M	Master
	CAS/135/04	C, M	369
	CAU/262/06	C, M	216
	CAU/283/09	C, M	438
	WKZ/356/06	C, M	723
	TRS/251/22	C, M	402
J	ERS/165/13	C, M	Master
	ERS/165/14	C, M	6
	ERS/266/21	C, M	376

TABLE V-2

MATCHED FILTER TEST EVENTS
(PAGE 3 OF 3)

Area Code	Event Designation	Filters C= Chirp, M= Master	Master-Test Separation (Km)
M	EKZ/364/06	C, M	Master
	EKZ/145/04	C, M	13
	EKZ/157/04	C, M	40
	EKZ/170/04	C, M	86
	EKZ/282/06	C, M	44
	EKZ/294/06	C, M	49
	EKZ/333/06	C, M	11
	EKZ/349/07	C, M	36
N	BLS/263/06	C, M	Master
	BLS/263/08	C, M	14
	BLS/263/10	C, M	96
	BSA/210/19	C	111
Other	WRS/191/17	C	
	SRS/200/20	C	
	SIB/212/01	C	
	CHI/249/21	C	
	CHI/156/10	C	

Generally, the signals used as test events were acquired through routine data edit runs throughout the year. Occasionally, because an event suitable as a master for some area would not yet be included in the ensemble, processing of events from that area would be deferred. In other instances, a poor master would be replaced by a better one requiring reprocessing of some events. This was done to obtain the best results whenever possible.

The lengths of the master waveforms were chosen to include the majority of primary signal energy. The beginning of the filter was usually chosen to be the predicted mode arrival time, even if little or no long period energy was observed. This was frequently the case for events from Eastern Kazakh and Sinkiang Province. The end of the signal usually was obvious; however, some signals were terminated at the beginning of what appeared to be predominantly scattered energy.

As discussed previously (Texas Instruments, 1971), the master event filter spectrum was scaled so that the largest component was set to 2.0. This resulted in a filtered output of approximately the same amplitude as the chirp output. This method of scaling does not produce filters with uniform energy for different master events. To reduce the effect of gain differences, the filters were applied to the signal and to the noise preceding it (whenever possible) to measure the true signal-to-noise ratio.

The results of performing master waveform filtering on 39 test events are given in Table V-3. The events are grouped by area with the master event listed first. Average improvements are given, even though for some areas such averages may not be useful. Improvement of the master applied to itself is not included in the average.

Some general observations about these results are presented below and will be followed by a discussion of master event filter results for each area. The general observations are:

TABLE V-3

MASTER WAVEFORM FILTER IMPROVEMENTS
(PAGE 1 OF 5)

Event Designation	Master-Test Separation (km)	dB Improvement Over the Equivalent Bandpass Filter								
		0.020-0.059 Hz.			0.025-0.055 Hz.			0.025-0.051 Hz.		
		LQT	LRV	LRR	LQT	LRV	LRR	LQT	LRV	LRR
AREA A:										
TUR/143/01	M	6.3	8.8	8.7	4.6	8.9	8.7	4.0	7.7	7.6
TUR/126/04	236	2.5	6.0	4.6	0.7	5.3	6.8	0.7	5.5	6.0
TUR/161/09	248	4.0	6.5	5.7	0.2	7.3	7.3	-0.1	6.0	5.4
Average Improvement:		3.2	6.2	5.2	0.4	6.3	7.0	0.3	5.8	5.7
AREA B:										
KUR/190/16	M	11.0	8.0	9.6	10.5	7.4	9.8	8.3	6.0	8.8
KUR/135/21	34	0.0	5.8	2.8	-1.2	3.8	1.8	-1.4	2.9	1.4
KUR/146/01	80	0.0	8.5	6.7	-0.5	7.5	6.8	-0.1	7.6	5.0
KUR/147/16	110	8.5	7.9	8.6	7.1	8.6	8.8	7.0	7.2	7.8
KUR/152/21	202	5.0	2.4	2.4	4.4	2.3	2.1	2.7	2.0	1.6
KUR/191/03	11	8.9	6.9	11.5	8.9	7.0	10.4	8.4	7.5	10.7
KUR/191/09	278	1.1	0.7	0.7	0.0	0.6	0.5	-0.1	0.3	0.9
Average Improvement:		3.9	5.4	5.4	3.1	5.0	5.1	2.8	4.6	4.6

TABLE V-3

MASTER WAVEFORM FILTER IMPROVEMENTS
(PAGE 2 OF 5)

Event Designation	Master-Test Separation (km)	dB Improvement Over the Equivalent Bandpass Filter								
		0.020-0.059 Hz.			0.025-0.055 Hz.			0.025-0.051 Hz.		
		LQT	LRV	LRR	LQT	LRV	LRR	LQT	LRV	LRR
AREA C:										
SIN/166/22	M	4.9	7.6	8.1	3.7	6.4	7.7	3.3	6.2	6.8
SIN/166/23	14	4.6	0.3	3.6	3.4	-0.8	2.0	3.4	-0.4	-0.4
SIN/170/17	0	3.7	0.6	3.3	2.4	-1.2	1.6	2.4	-2.7	-0.4
SIN/219/15	616	1.3	-1.9	-2.0	2.0	-3.0	-2.3	2.6	-3.6	-1.3
SIN/221/01	346	1.8	-2.7	1.0	0.6	-2.6	1.4	0.2	-2.6	0.7
SIN/241/15	560	ND	ND	ND	ND	ND	ND	ND	ND	ND
Average Improvement:		2.8	-0.9	1.5	2.1	-1.9	0.7	2.2	-2.3	-0.4
AREA D:										
CHI/229/09	M	5.9	6.8	9.3	4.3	6.6	7.9	4.3	5.4	7.2
CHI/229/17	0	5.4	5.8	5.5	4.1	4.1	4.9	4.4	4.7	5.1
CHI/258/07	523	0.5	2.0	1.8	1.8	3.2	2.4	0.6	ND	1.2
CHI/258/11	621	2.9	ND	ND	ND	ND	ND	ND	ND	ND
Average Improvement:		3.0	3.9	3.6	3.0	3.6	3.6	2.5	--	3.2

TABLE V-3

MASTER WAVEFORM FILTER IMPROVEMENTS
(PAGE 3 OF 5)

Event Designation	Master-Test Separation (km)	dB Improvement Over the Equivalent Bandpass Filter								
		0.020-0.059 Hz.			0.025-0.055 Hz.			0.025-0.051 Hz.		
		LQT	LRV	LRR	LQT	LRV	LRR	LQT	LRV	LRR
AREA F:										
TDZ/147/00	M	9.7	6.7	--	14.5	9.6	--	10.3	8.4	--
TDZ/274/16	77	0.5	-2.3	-0.6	-1.0	-1.5	-1.5	4.1	-1.8	-3.3
KRG/301/13	493	-1.9	-0.2	-1.0	-3.3	0.8	0.6	-2.3	1.5	1.9
TDZ/259/10	208	ND	ND	ND	ND	ND	ND	ND	ND	ND
Average Improvement:		-0.7	-1.2	-0.8	-2.2	-0.4	-0.4	0.9	-0.1	-0.7
AREA G:										
CRS/236/16	M	3.7	3.3	--	2.8	2.8	--	2.8	2.4	--
SIN/273/12	340	-0.2	3.0	2.4	0.2	3.4	3.2	0.4	4.6	4.3
AREA H:										
KUR/213/02	M	9.2	11.5	9.8	8.1	9.7	7.8	6.9	8.4	6.4
KOM/148/10	874	-5.4	4.6	4.2	-6.6	5.8	3.0	-4.5	5.3	3.1
KAM/166/14	384	-7.8	-6.6	-2.0	-8.9	-6.2	-4.5	-10.0	-5.6	-3.4

TABLE V-3

MASTER WAVEFORM FILTER IMPROVEMENTS
(PAGE 4 OF 5)

Event Designation	Master-Test Separation (km)	dB Improvement Over the Equivalent Bandpass Filter								
		0.020-0.059 Hz.			0.025-0.055 Hz.			0.025-0.051 Hz		
		LQT	LRV	LRR	LQT	LRV	LRR	LQT	LRV	LRR
AREA I:										
CAU/288/17	M	5.1	6.9	7.2	3.1	5.2	5.8	3.3	5.1	4.9
CAS/135/04	369	-0.2	-0.8	-0.7	-2.6	-1.8	-1.6	-2.6	-2.4	-1.6
CAU/262/06	216	ND	0.5	ND	ND	-1.1	ND	ND	-2.8	ND
CAU/283/09	438	-1.4	0.6	-0.6	-1.9	0.9	0.1	-0.9	2.9	1.9
WKZ/356/06	723	3.8	5.4	3.0	3.1	5.6	3.1	0.8	5.5	2.8
TRS/251/22	402	-0.1	1.4	3.2	-0.5	0.8	3.0	0.0	0.6	3.2
Average Improvement:		0.5	1.6	1.2	-0.5	1.4	1.2	-0.7	1.6	1.6
AREA J:										
ERS/165/13	M	6.7	3.9	5.9	5.1	2.8	5.2	2.8	4.7	6.9
ERS/165/14	6	ND	ND	ND	ND	ND	ND	ND	ND	ND
ERS/266/21	376	2.9	-0.6	-0.1	2.6	-1.4	2.9	1.6	-0.9	2.3

TABLE V-3

MASTER WAVEFORM FILTER IMPROVEMENTS
(PAGE 5 OF 5)

Event Designation	Master-Test Separation (km)	dB Improvement Over the Equivalent Bandpass Filter								
		0.020-0.059 Hz.			0.025-0.055 Hz.			0.025-0.051 Hz.		
		LQT	LRV	LRR	LQT	LRV	LRR	LQT	LRV	LRR
AREA M:										
EKZ/364/06	M	2.0	2.8	3.2	1.6	2.8	2.5	1.5	2.9	3.2
EKZ/145/04	13	ND	4.1	ND	ND	3.5	ND	ND	2.7	ND
EKZ/157/04	40	0.2	2.2	-0.6	0.7	2.5	0.2	-0.8	2.5	0.0
EKZ/170/04	86	1.3	2.0	4.6	-0.5	0.8	3.4	-0.2	0.8	2.2
EKZ/282/04	44	ND	4.3	ND	ND	2.8	ND	ND	1.8	ND
EKZ/294/06	49	0.1	3.5	0.9	-0.7	4.2	-0.1	-0.6	4.5	-0.2
EKZ/333/06	11	0.4	2.9	1.8	-1.0	2.5	1.8	-0.6	2.7	2.0
EKZ/349/07	36	ND	ND	ND	ND	ND	ND	ND	ND	ND
Average Improvement:		0.5	2.6	1.7	-0.4	2.5	1.3	-0.6	2.6	1.0
AREA N:										
BLS/263/06	M	4.1	3.8	3.6	5.0	4.3	4.0	5.8	5.8	5.9
BLS/263/08	14	ND	4.7	ND	ND	ND	ND	ND	ND	ND
BLS/263/10	96	6.8	6.5	4.6	5.1	5.1	3.2	4.7	4.3	2.8
Average Improvement:		None								

- Master event matched filter performance is both highly regional and event dependent. As may be seen from Table V-3 performance averages can be very misleading.

- There is only a weak correlation between performance and test-master separation (Figure V-2). In any given region, similarities in source mechanism and relative fault orientation are probably much more important than separation in predicting performance.

- The ensemble of events from Eastern Kazakh provides a measure of expected scatter in master event filter improvement. These events are confined to a small area and presumably have identical source mechnisms.

- Results of the LRV and LRR modes are similar although LRR tends to be 1 to 2 dB smaller.

- Average (all events) improvements for both LRV and LRR show only slight degradation for narrower bandwidths; about 0.5 dB from 0.020-0.059 Hz to 0.025-0.051 Hz. LQT improvements were more sensitive with about 1.0 dB between these bands.

- Improvements for individual areas may go either up or down with bandwidth. This implies that a specific bandwidth should be chosen for each area.

The two Turkey (Area A) test events showed better improvements than most other areas. Rayleigh wave improvements were stable with bandwidth while Love improvements degraded sharply with narrower bandwidth. Both test and master events had generally similar Rayleigh waves; however, the two test events had similar Love waves which were distinctly different from that of the Master.

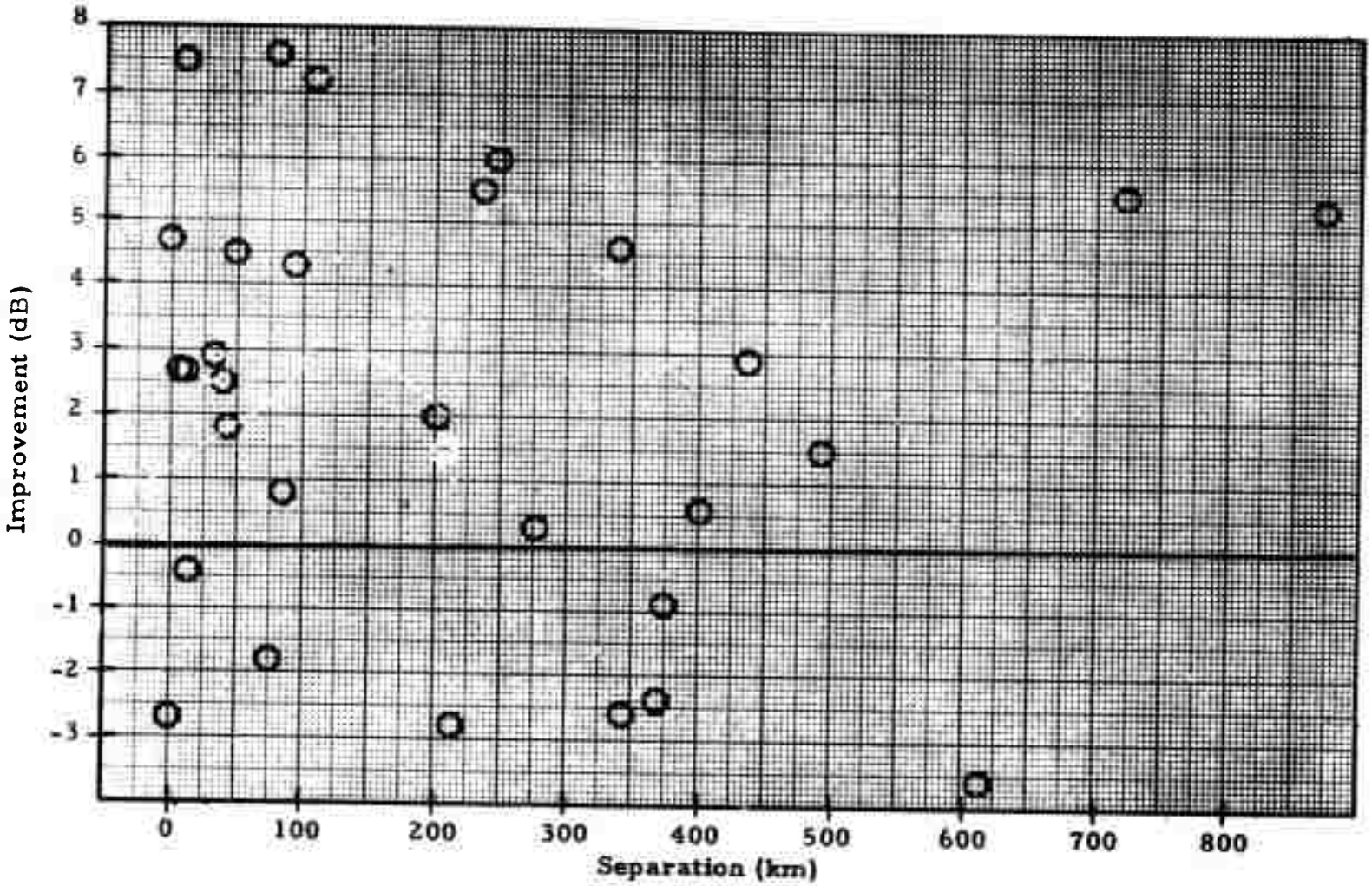

FIGURE V-2

MASTER EVENT IMPROVEMENT (dB) 0.025 - 0.051 Hz vs. MASTER TEST SEPARATION (km)

The lower Kurile Islands region (area B) had 6 test events processed. This area yielded the highest average and highest individual improvements of any area. At the same time, however, variations between events were large. Some events matched strongly with the Love wave filter and not with the Rayleigh filter while other events behaved oppositely. The large LRR improvements (relative to LRV) for KUR/190/16 (Master) and KUR/191/03 (which was almost identical in wavetrain) were due to Love wave energy leakage onto the radial component. This is unusual because this phenomenon was not observed for other nearby events. Improvements showed a distinct decline with narrower bandwidths.

The upper Kurile-Kamchatka region (area H) group had only two test events and these were widely separated from the master and each other. KOM/148/10 had relatively simply dispersed Rayleigh waves and almost non-existent Love waves. Matching on the Rayleigh modes was surprisingly good considering its 874 km separation. KAM/166/14 had badly multipathed waves which were also very narrowband even though well-dispersed. The master event is not suitable for these test events.

For the Black Sea group (area N) two test events were processed. One of these was detected only on the vertical component of the widest bandwidth. These events (and the master) are probably from the same fault zone, yet the master and the larger test event behaved oppositely with regard to variation of improvement with bandwidth. Improvements were comparable to the Turkey events.

Five test events from the Caucasus-Caspian Sea region (area I) were processed. These events were scattered throughout this area and the range of separations from the master was from 216 km to 723 km. The largest improvement was for the furthest event, which was the only one that gave any significant improvement at all. It appears that the master duration was somewhat longer than most of the other events. A better master should cause an increase in the improvements. Improvement did not change significantly with bandwidth.

For the Sinkiang region (area C), five events were processed. Events from this area are characterized by well-developed Love waves and unusual Rayleigh waves. The latter mostly have little or no long period energy and appear as very short high frequency pulses with a reversed frequency-time relationship (i.e., reversely dispersed). The waveforms for the Kazakh events (area M) are very similar except that they have smaller Love waves. An example of these waveforms is shown in Figure V-3 for SIN/170/17 and EKZ/364/06. LQT improvements were 3 to 4 dB better than Rayleigh wave improvements. Poor improvements would be expected for the Rayleigh waves. The events occurred in two smaller widely separated subareas of area C and those from each subarea behaved differently. At least two different masters would be needed. Improvements generally decreased with narrowing bandwidths.

The Eastern Kazakh group (area M) had eight test events whose epicenters were relatively close together. These events had very small surface waves but those that were visible had waves very similar to the Sinkiang events (Figure V-3). Rayleigh waves were stronger for this group and showed greater improvement. Since the source functions for these events presumably are similar, the scatter in observed improvements probably reflects the effect of ambient noise on the improvements. There was no change in improvement with change in bandwidth.

For the Tadzhik area (area F) three events were processed; one of these events was not detected. Improvements were mostly negative although there was a slight indication that improvement increased with a narrower bandwidth. The master apparently is poor although it appeared fairly similar to the others, and gave very large improvements when matched with itself.

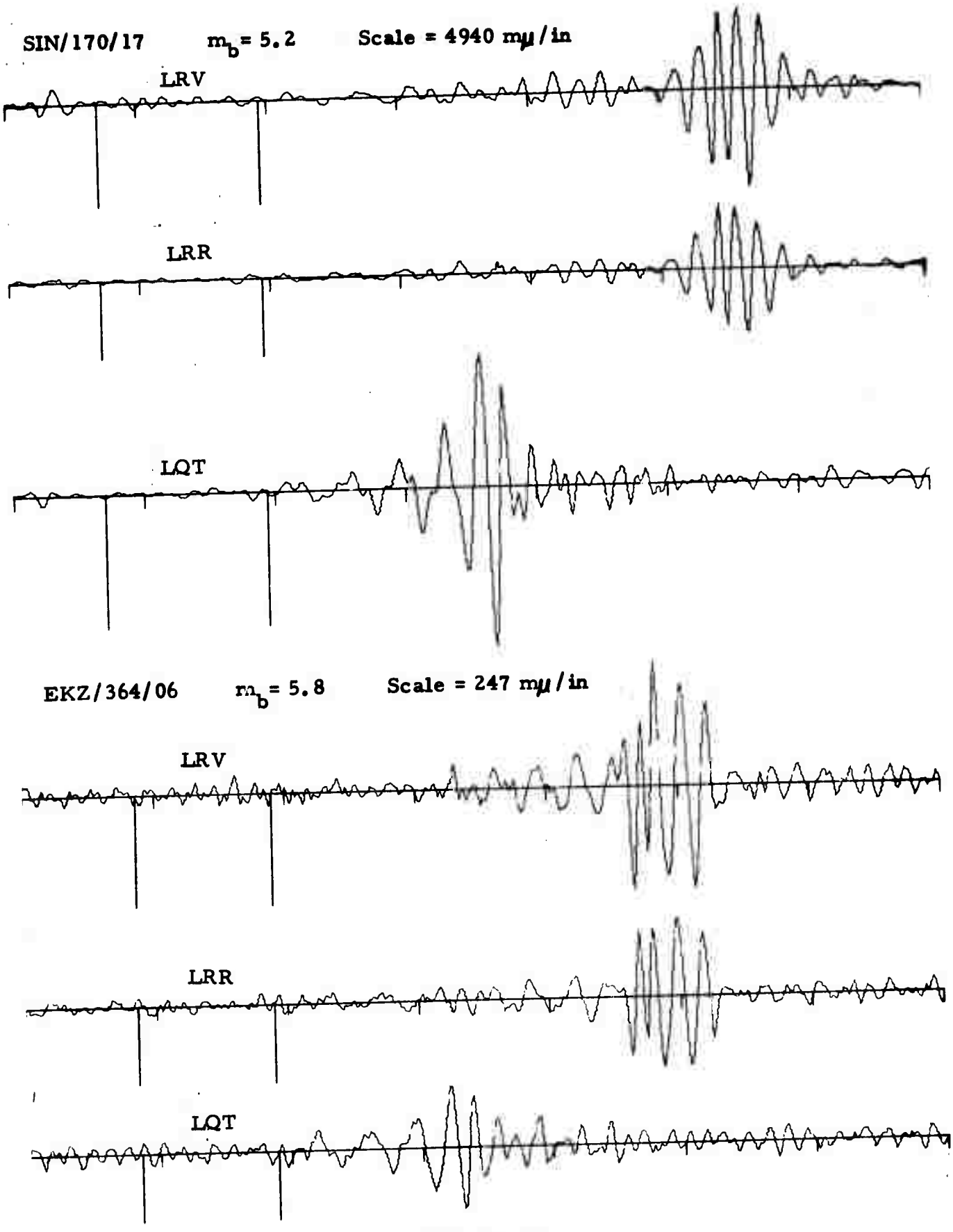

FIGURE V-3

UNBANDPASSED BEAM OUTPUTS FOR A SINKIANG EARTHQUAKE AND A KAZAKH PRESUMED EXPLOSION

The central China group (area D) consisted of three test events. One event, an aftershock of the master event, gave approximately a 5 dB improvement. The other two events were in excess of 500 km away and the one that was detected gave about 2 dB improvement.

Areas G and J had so few results that they cannot be discussed in a meaningful manner.

C. CHIRP FILTER PERFORMANCE

Linear chirp filters were applied to the same event ensemble as the master event filtered ensembles of Table V-2. Ten extra events which had not been master event filtered were chirp filtered. This group, excluding master events, is listed as "other" at the end of the table.

The chirp filters differ from the master event filters in both spectral amplitude, which is a constant value (1.0) for the chirp, and group delay which is linear for the chirps used here. Since the linear chirp filters differ from the bandpass filters only in phase response, the RMS value of noise output from each filter should be the same. This was found to be essentially true for this ensemble. Average deviation of the noise RMS values before and after chirp filtering was less than 4 percent.

The general procedure for selecting chirp lengths was to apply chirps to the master event for that area to find the length giving the best improvement. For each test event from that area, five chirps with lengths centered about the "optimum" length were applied. The improvement was measured from the chirp giving the best improvement. The range of lengths was chosen subjectively depending on the event delta and the "optimum" length. For those cases where master and test events had obviously different signal waveforms (either duration, frequency content, or both), chirp lengths were chosen to fit the test event.

Table V-4 presents the results of the chirp filter application for the fifty-nine test events. The events are grouped into the same areas as the master waveform groups; several additional events are included at the end of the table.

The results of the chirp filtering improvement studies are summarized below:

- Average LRV performance was about 2.7 dB with no change with bandwidth. This is 0.5 to 1.0 dB less than master event performance, depending on bandwidth. LQT performance was about the same as for master event filters with slightly smaller improvement at narrower bandwidths. LRR average performance was the same as that of the LRV.
- Chirp improvements are more regular than master event improvements. Results are still strongly region dependent.
- Largest average improvements were obtained from Turkey and the Kurile-Kamchatka areas. Smallest improvements were from Sinkiang, Tibet, and the Caucasus.
- Performance for several areas can probably be substantially improved with more complex chirp operators. These would be either non-linear group delay or N-part chirps.
- Results from Sinkiang and Tibet events which had almost the same travel paths showed only generally similar behavior. LQT differences were the most pronounced. This is probably due to differences in source mechanism.
- The effect of bandwidth on improvements was variable for different areas. For decreasing bandwidths, performance

TABLE V-4

CHIRP FILTER IMPROVEMENTS
(PAGE 1 OF 6)

Event Designation	Master-Test Separation (km)	dB Improvement Over the Equivalent Bandpass Filter								
		0.020-0.059 Hz.			0.025-0.055 Hz.			0.025-0.051 Hz.		
		LOT	LRV	LRR	LOT	LRV	LRR	LOT	LRV	LRR
AREA A:										
TUR/143/01	M	2.5	6.5	6.4	1.9	6.2	5.8	1.4	4.7	4.7
TUR/126/04	236	3.2	5.3	4.2	2.6	4.0	5.8	2.3	3.3	4.1
TUR/161/09	238	4.8	5.6	4.9	3.0	5.3	5.8	1.7	3.6	3.3
Average Improvement:		3.5	5.8	5.2	2.5	5.2	5.8	1.8	3.9	4.0
AREA B:										
KUR/190/16	M	6.9	4.4	4.6	6.8	4.4	5.4	6.4	5.0	5.2
KUR/135/21	34	-0.6	4.8	4.1	0.1	3.6	4.4	0.4	4.7	4.6
KUR/146/01	80	5.7	6.8	6.2	3.7	6.1	6.7	3.0	5.1	5.2
KUR/147/16	110	6.3	4.8	7.1	5.8	6.2	7.6	5.5	5.0	6.9
KUR/152/21	202	2.7	5.9	4.9	2.2	5.5	5.2	1.3	5.3	4.7
KUR/191/03	11	6.2	4.0	7.2	6.9	4.5	4.9	7.9	4.4	7.7
KUR/191/09	278	0.5	0.8	0.5	0.4	0.7	1.2	2.2	2.8	1.4
Average Improvement:		4.0	4.5	4.9	3.7	4.4	5.1	3.8	4.6	5.1

TABLE V-4

CHIRP FILTER IMPROVEMENTS
(PAGE 2 OF 6)

Event Designation	Master-Test Separation (km)	dB Improvement Over the Equivalent Bandpass Filter: 0.020-0.059 Hz. LQT	LRV	LRR	0.025-0.055 Hz. LQT	LRV	LRR	0.025-0.051 Hz. LQT	LRV	LRR
AREA C:										
SIN/166/22	M	1.6	1.2	0.0	1.2	1.2	1.0	1.2	2.2	1.5
SIN/166/23	14	1.4	-0.6	-0.2	0.8	-0.1	1.6	1.6	0.8	1.2
SIN/170/17	0	0.7	1.3	1.9	0.7	2.4	2.6	0.9	1.7	1.4
SIN/219/15	616	3.1	3.0	0.3	5.3	3.8	3.1	5.2	2.4	1.2
SIN/221/01	346	1.9	0.6	0.3	1.0	1.2	1.5	1.2	1.2	2.8
SIN/241/15	560	ND	0.7	ND	ND	ND	ND	ND	2.9	ND
CHI/208/13	306	--	--	--	0.4	1.3	1.2	--	--	--
Average Improvement:		1.7	1.1	0.5	1.8	1.7	2.0	2.0	1.7	1.6
AREA D:										
CHI/229/09	M	2.3	4.0	4.3	2.8	4.0	4.3	2.4	2.7	3.0
CHI/229/17	0	1.6	1.9	1.4	2.1	2.7	2.0	2.4	2.6	1.7
CHI/258/07	523	2.5	3.2	3.1	1.2	ND	ND	0.4	ND	ND
CHI/258/11	621	ND	ND	ND	ND	ND	ND	ND	ND	ND
Average Improvement:		2.1	3.0	2.9	2.0	3.4	3.2	1.7	2.6	2.4

TABLE V-4

CHIRP FILTER IMPROVEMENTS
(PAGE 3 OF 6)

Event Designation	Master-Test Separation (km)	dB Improvement Over the Equivalent Bandpass Filter								
		0.020-0.059 Hz.			0.025-0.055 Hz.			0.025-0.051 Hz.		
		LQT	LRV	LRR	LQT	LRV	LRR	LQT	LRV	LRR
AREA E:										
TIB/302/17	M	2.3	1.0	1.2	2.2	0.4	0.2	2.0	0.6	0.4
TIB/123/00	382	4.5	1.2	3.5	3.4	1.9	2.2	3.7	-1.2	0.4
TIB/155/20	602	3.2	1.0	1.6	0.7	1.3	1.4	1.0	1.1	0.8
Average Improvement:		3.3	1.1	2.1	2.1	1.2	1.3	2.2	0.2	0.5
AREA F:										
TDZ/147/00	M	2.1	3.6	--	2.2	3.0	--	3.2	6.6	--
TDZ/274/16	77	-3.2	3.7	3.8	-3.5	3.4	3.1	-1.9	2.8	2.6
KRG/301/13	493	1.5	2.9	1.8	1.1	3.2	3.2	1.2	3.8	3.4
TDZ/259/10	208	ND	ND	ND	ND	ND	ND	ND	ND	ND
Average Improvement:		0.1	3.4	2.8	-0.1	3.2	3.2	0.8	4.4	3.0
AREA G:										
CRS/236/16	M	2.6	2.5	--	2.5	3.0	--	1.6	3.1	--
SIN/273/12	340	1.7	1.5	0.4	1.7	2.9	2.7	1.7	5.0	4.1

TABLE V-4

CHIRP FILTER IMPROVEMENTS
(PAGE 4 OF 6)

Event Designation	Master-Test Separation (km)	dB Improvement Over the Equivalent Bandpass Filter								
		0.020-0.059 Hz.			0.025-0.055 Hz.			0.025-0.051 Hz.		
		LQT	LRV	LRR	LQT	LRV	LRR	LQT	LRV	LRR
AREA H:										
KUR/213/02	M	4.7	8.7	7.9	3.6	8.2	7.3	2.9	6.9	6.2
KOM/148/10	874	0.0	4.6	6.3	-2.0	5.3	5.3	-1.2	5.2	5.2
KAM/166/14	384	-0.1	1.3	0.8	-2.0	3.2	-1.0	-0.1	-1.2	0.1
Average Improvement:		2.3	4.9	5.0	-0.1	5.6	3.9	0.5	3.6	3.8
AREA I:										
CAU/288/17	M	2.5	2.3	3.4	1.4	1.2	1.5	1.9	1.7	2.8
CAS/135/04	369	3.4	1.2	1.0	1.6	0.6	1.2	2.2	0.3	0.4
CAU/262/06	216	ND	0.5	ND	ND	-0.5	ND	ND	-0.3	ND
CAU/283/09	438	1.0	0.9	0.3	0.5	0.4	0.3	0.5	0.9	0.9
WKZ/356/06	723	1.9	1.4	1.2	1.7	1.7	1.4	0.9	1.6	1.5
TRS/251/22	402	2.6	2.6	2.6	1.6	2.2	2.7	1.3	2.7	3.2
Average Improvement:		1.8	1.7	2.8	1.4	1.2	1.4	1.4	1.4	1.8

TABLE V-4

CHIRP FILTER IMPROVEMENTS
(PAGE 5 OF 6)

Event Designation	Master-Test Separation (km)	dB Improvement Over the Equivalent Bandpass Filter								
		0.020-0.059 Hz.			0.025-0.055 Hz.			0.025-0.051 Hz.		
		LQT	LRV	LRR	LQT	LRV	LRR	LQT	LRV	LRR
AREA J:										
ERS/165/13	M	4.7	1.0	1.1	3.9	-0.1	1.5	2.2	0.5	1.7
ERS/165/14	6	ND	ND	ND	ND	ND	ND	ND	ND	ND
ERS/266/21	376	2.8	-0.6	0.6	3.4	-1.5	3.4	2.3	-0.8	3.7
Average Improvement:		3.8	0.2	0.8	3.6	-0.8	2.4	2.2	-0.2	2.7
AREA M:										
EKZ/364/06	M	1.3	1.1	1.2	0.6	1.2	1.3	0.8	2.2	2.4
EKZ/145/04	13	ND	4.0	ND	ND	3.8	ND	ND	2.6	ND
EKZ/157/04	40	1.3	1.8	0.2	2.6	3.1	1.5	1.2	3.4	1.7
EKZ/170/04	86	0.5	0.3	1.8	0.6	0.0	0.6	0.8	0.6	1.6
EKZ/282/06	44	ND	2.7	ND	ND	2.5	ND	ND	2.0	ND
EKZ/294/06	49	0.9	0.8	-1.6	0.4	1.3	-1.2	0.4	1.9	0.2
EKZ/333/06	11	1.4	0.5	1.1	0.2	0.4	0.8	0.6	1.6	0.9
EKZ/349/07	36	ND	ND	ND	ND	ND	ND	ND	ND	ND
Average Improvement:		1.1	0.9	0.5	0.9	1.2	0.6	0.8	1.9	1.4

TABLE V-4

CHIRP FILTER IMPROVEMENTS
(PAGE 5 OF 6)

Event Designation	Master-Test Separation (km)	dB Improvement Over the Equivalent Bandpass Filter								
		0.020-0.059 Hz.			0.025-0.055 Hz.			0.025-0.051 Hz.		
		LQT	LRV	LRR	LQT	LRV	LRR	LQT	LRV	LRR
AREA N:										
BLS/263/06	M	1.3	3.8	3.3	0.5	1.8	1.7	0.6	1.9	1.8
BLS/263/08	14	ND	ND	ND	ND	ND	ND	ND	ND	ND
BLS/263/10	96	3.2	3.0	1.9	2.2	2.1	1.5	1.3	0.8	0.1
BSA/210/19	111	--	--	--	--	0.3	--	--	--	--
Average Improvement:		2.2	3.4	2.6	1.4	2.0	1.6	1.0	1.4	1.0
OTHER CHIRPS:										
SIB/212/01		--	--	--	ND	2.5	0.7	--	--	--
SRS/200/20		--	--	--	-1.6	2.1	3.3	--	--	--
URS/191/17		--	--	--	ND	ND	ND	--	--	--
CHI/249/21		2.1	2.7	2.5	2.3	3.0	2.2	4.0	4.2	3.2
CHI/156/10		3.4	2.2	2.0	2.7	3.7	3.4	2.8	5.6	6.1

degraded in Turkey, the Black Sea, and the Kamchatka areas; performance increased in Eastern Kazakh, Central Russia, and for two China events (CHI/156/10 and CHI/249/21).

D. COMPARISON OF MASTER EVENT AND CHIRP FILTER PERFORMANCES

Comparisons of Tables V-3 and V-4 indicate that master event filters are better than the chirp filters for LQT, for the areas of Sinkiang (area C), China (area D), and the Black Sea (area N). The chirp filters do better in Turkey (area A), the Kuriles (area B), the Caucasus (area I), and Eastern Kazakh (area M).

For LRV waves, chirp improvements are generally as good or better than master event filters for all areas except China, Eastern Kazakh, and the Black Sea.

While the master waveform matched filter offers potentially larger gains than chirp filters, the relative gains achieved for the small ensemble of events reported here are not significantly different. In addition, the chirp filters appear to produce more stable and uniform results and are relatively less sensitive to bandwidth than the master event filters.

Considering the greatly increased cost in computation and bookkeeping required by master event filters, their marginally superior performance does not seem generally worthwhile. A fruitful approach to matched filtering of beams would be to investigate more sophisticated chirp filters incorporating better approximations to the actual group velocity curves encountered in each region. Such filters would be specified by a few parameters rather than the entire response as required by the master event filters.

SECTION VI

NORSAR EARTHQUAKE SURFACE WAVE DETECTION CAPABILITY

The detection capability of the NORSAR array was estimated by two methods: a direct method based on the detection history of a suite of earthquake signals, and an indirect method based on necessary signal levels over measured noise values. The indirect measurement obtained an unusually low threshold estimate compared to the directly measured value. This will be discussed at the end of this section. The detection threshold measured is applicable to NORSAR assuming an average of 15 to 16 sites being used.

The 48 events used in the direct method are the same as those used for the matched filtering study but with presumed explosions excluded. The distribution of m_b values* for this group is shown in Figure VI-1. Detections were determined from the vertical component of the bandpassed (beamsteered) beam output. When necessary, matched filters were used to obtain additional detections. The three passbands used in the matched filter performance study, namely 0.020-0.059 Hz, 0.025-0.055 Hz, and 0.025-0.051 Hz, were used here also. However, there was no difference in number of detections with each passband.

The following criteria were used to obtain a detection:

- A peak occurs in the matched filter of 3 dB above any other peak occuring within 15 minutes
- A peak occurs within 100 seconds of the predicted time of the peak

---

* Source of m_b values is given in Table I-2

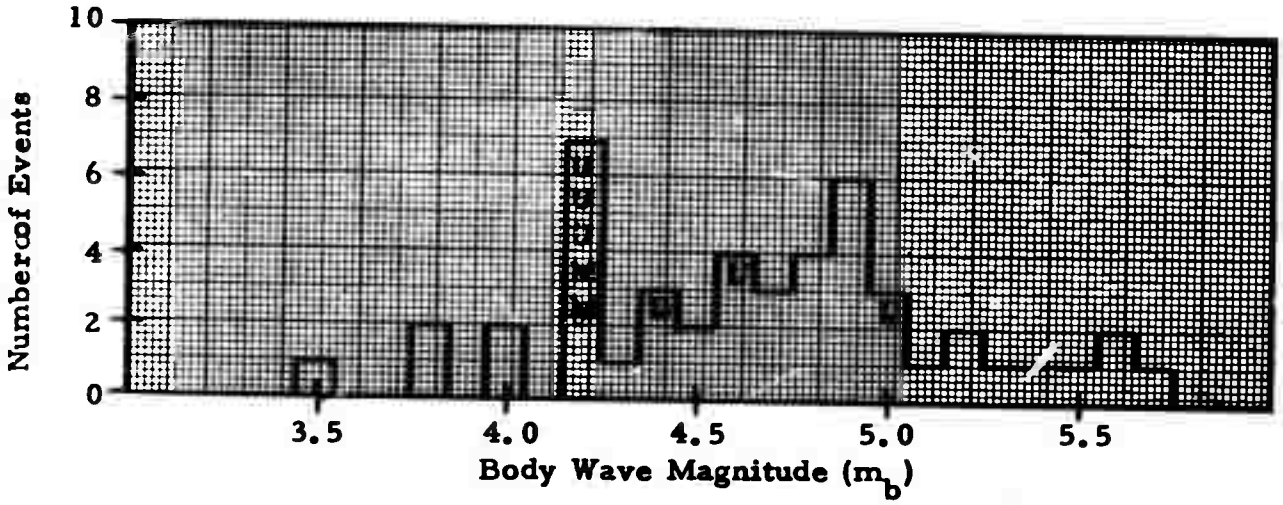

FIGURE VI-1

SURFACE WAVE DETECTION DATA FOR EURASIAN EARTHQUAKES

- Peaks occur on the vertical and radial matched filter outputs

It is difficult in practice to follow these criteria exactly. For example, for some events the LRR component detection was uncertain. If the LRV component was detected, and especially if the detection was clear, then the tendency was to rule in favor of a detection on the LRR.

Out of 48 events, six events were not detected; these are denoted by "U" in Figure VI-1. Two events were detected only after matched filters were applied; these are denoted by "M" in Figure VI-1

The histogram of Figure VI-1 was used to compute the percentage of detections within each magnitude bin. Since both the number of non-detections and the number of events in each magnitude bin were small, the data in successive pairs of bins of even and odd tenths of magnitude were grouped to reduce the scatter in the calculated percentages. These percentages are plotted in Figure VI-2. Thirty-two of the 48 events fall within the five bins representing the magnitude range of 4.0-5.0. Only three events smaller than magnitude 4.0 were included, so the detection capability estimate for these is essentially meaningless.

One large event, SIN/241/15 ($m_b = 5.0$), was not detected.* The depth of this event was listed by NOAA as normal. The only explanation for not detecting it is that NORSAR was on a null in the radiation pattern. Below magnitude 5.0, the detection percentage shows a reasonably smooth drop to 62 percent at about $m_b \cong 4.2$. If these points were extrapolated, the 50 percent detection level would be reached at about magnitude 4.1. This is about the same as obtained for ALPA.

*The event was barely detected on LRV but not LRR and only in the 0.020-0.059 passband.

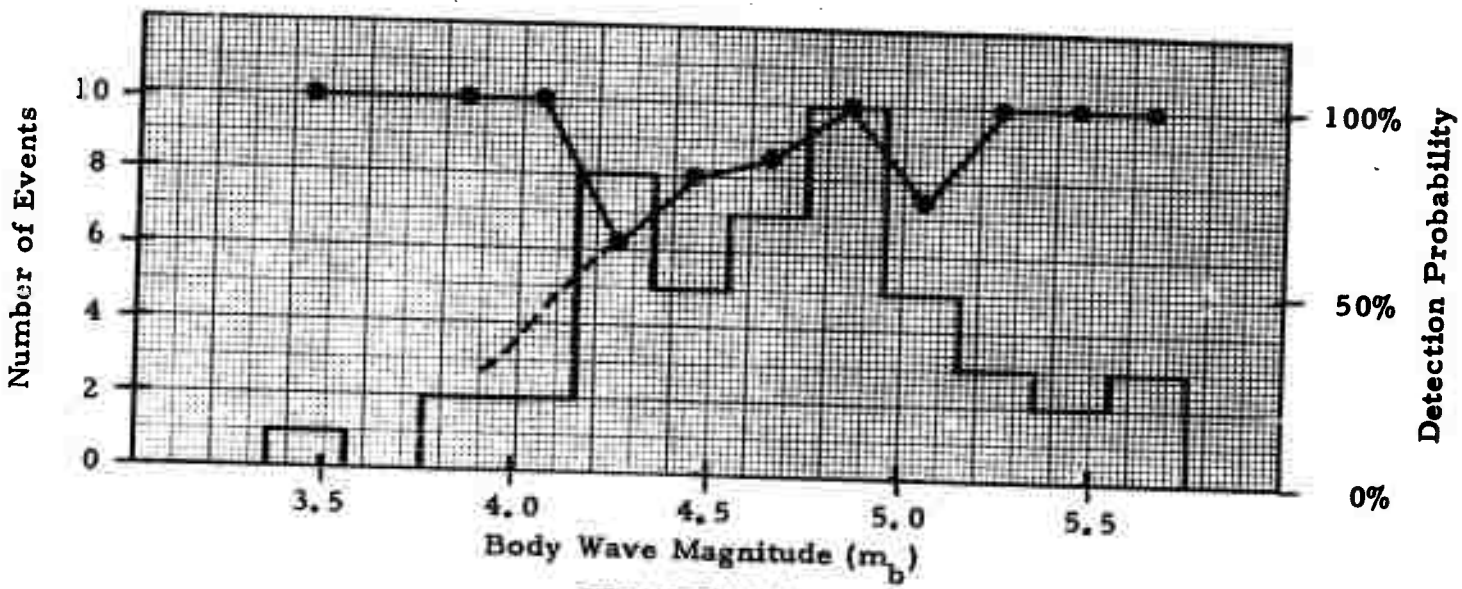

FIGURE VI-2

DIRECT ESTIMATE OF DETECTION PROBABILITY FROM GROUPED DATA

The attempt to measure the detection threshold indirectly gave a very low estimates of the NORSAR capability. The procedure for obtaining the threshold has been previously discussed (Lacoss, 1969; Texas Instruments, 1971). Central to this method is the functional relationship between M_s and m_b used to obtain an m_b for a given M_s. Many such functions exist, the most well known being the Gutenburg-Richter (GR) ($M_s = 1.59\ m_n - 3.97$). Both the GR and the experimental NORSAR curves ($M_s = 1.15\ m_b - 1.16$)* were used. Reasonably good agreement between the direct measurement and the indirect measurement was obtained using the GR curve. However, the results for the NORSAR curve, which probably has a more reasonable slope (for low magnitude events) of 1.15, gave estimates about 0.5 to 0.8 magnitude units smaller than indicated by the direct method. The probable cause for this discrepency is that the indirect method does not account for signal variance and hence is biased low. That is, a signal variance of 0.5 m_b units (which is typical) would shift the detection threshold curve obtained by the indirect estimate to significantly higher magnitudes. We plan to develop a method for including signal variance in the indirect estimate in the coming year.

---

* See Section VII

SECTION VII
BEHAVIOR OF STANDARD DISCRIMINANTS

A. INTRODUCTION

The purpose of this study was to calculate and plot three standard discriminants for the NORSAR array: $M_s - m_b$, $AR - m_b$, $AL - m_b$.

A list of Sino-Soviet events is given in Table VII-1 with m_b, M_s, AR and AL. The m_b values were taken from the NOAA-PDE lists whenever possible. The magnitudes of events with $m_b < 4.0$ are generally the LASA values. Table I-1 should be consulted for particular events.

Events from known test areas are indicated by an asterisk.

B. M_s/m_b MEASUREMENTS

The surface wave magnitude (M_s) was determined for each event listed in Table VII-1 by the equation

$$M_s = \log\left(\frac{A}{T}\right) + 1.66 \log \Delta$$

where

A = maximum peak-to-peak vertical Rayleigh wave amplitude in millimicrons

T = period in seconds of the cycle corresponding to A

Δ = epicentral distance to the event in degrees.

Measurements of M_s were made on unfiltered single site traces for all events with a clear vertical Rayleigh wave signal. For those events of poorer signal-to-noise ratio, measurements were taken from beamsteer output traces. For those events which still had poor SNR, amplitudes were taken from the chirp filtered output using a passband of 0.020-0.059 Hz. The amplitudes of these latter events were corrected using average chirp improvement for that area.

TABLE VII-1

SINO-SOVIET EVENTS
(PAGE 1 OF 3)

EVENT	m_b	M_s	AR	AL
TIB/123/00NL	5.4	5.2	109624	106885
TUR/126/04NL	4.4	4.4		
CAS/135/04BE	4.6	3.3	2935	3558
KUR/135/21NL	4.7	4.1	12339	7011
SIN/136/17NL	4.6	3.5		
CHI/141/02NL	4.9	3.5		
TUR/143/01NL	4.4	4.0		
EKZ/145/04NL *	5.0	2.6	671	-
KUR/146/01NL	4.7	4.0	6897	3989
TDZ/147/00NL	4.8	4.1	10827	9759
KUR/147/16NL	5.2	4.4	12226	13522
KOM/148/10NL	4.5	4.1	20192	10397
KUR/152/21NL	4.6	3.5	3416	1563
TIB/155/20NL	5.0	4.1	4013	9255
CHI/156/10NL	4.7	5.0	29756	50580
EKZ/157/04NL *	5.5	3.5	1546	1358
TUR/161/09N1	4.6	4.3		
ERS/165/13NL	5.6	5.6	226863	269969
ERS/165/14NL	4.6	4.1		
KAM/166/14NL	5.1	4.7	27884	29024
SIN/166/22N1	5.6	4.8	263982	482228
SIN/166/23NL	4.9	4.1	4640	5698
EKZ/170/04NL *	5.5	3.3	856	934
SIN/170/17NL	5.2	5.3	84921	127130
KUR/190/16BE	4.9	4.9	59584	61421
KUR/191/03NL	4.8	4.4	20703	15791

SINO-SOVIET EVENTS
(PAGE 2 OF 3)

EVENT	m_b	M_s	AR	AL
KUR/191/09NL	4.6	3.4		
SRS/200/20NL	3.8	3.1		
CHI/208/13NL	5.3	4.6		
BSA/210/19N1	4.5	2.5		
SIB/212/01NL	3.5	3.4		
KUR/213/02NL	5.3	5.4		
KUR/213/18NL	4.5	3.8		
SIN/219/15NL	4.8	4.3	21512	45359
TUR/219/17NL	4.5	3.9		
SIN/221/01NL	4.2	3.4	2031	2399
TUR/221/04NL	4.8	3.7		
KUR/224/20NL	4.5	4.5		
CHI/229/09NL	4.9	4.5	15166	19261
CHI/229/17NL	4.9	4.0	7805	7980
KUR/230/19NL	4.7	3.5		
KUR/236/09NL	4.7	3.6		
CRS/236/16NL	5.2	5.7	364336	336188
SRS/240/16NL	4.8	5.2		
SIN/241/15NL	5.0	3.6		
CHI/249/21NL	3.8	3.5	1563	2593
TRS/251/22NL	4.8	4.4	33590	51528
CHI/258/07NL	4.2	3.1		
CHI/258/11NL	4.2	< 2.8		
TDZ/259/10NL	4.2	3.1		
CAU/262/06NL	4.4	< 2.9		
BLS/263/06NL	4.0	3.7	14234	11175
BLS/263/08NL	4.2	3.4	5218	–
BLS/263/10NL	4.2	3.5	4458	4740
ERS/266/21N1	4.2	3.2		

TABLE VII-1
SINO-SOVIET EVENTS
(PAGE 3 OF 3)

EVENT	m_b	M_s	AR	AL
NRS /270/05N3 *	6.4	5.5		
SIN/273/12NL	4.5	4.2	6330	5185
TDZ/274/16NL	4.9	4.3	19742	7267
SIN/281/09NL	4.4	3.9		
EKZ/282/06NL *	5.4	2.8	1514	1201
CHI/283/05NL	4.4	4.2		
CAU/283/09NL	4.0	3.3	2252	3768
CAU/288/17NL	4.9	3.6	7678	7177
EKZ/294/06NL *	5.6	3.1	2608	2125
KRG/301/13N2	5.5	5.2	178494	234123
TIB/302/17NL	5.0	4.7	14429	21773
EKZ/333/06NL *	5.5	3.4	2225	2198
EKZ/349/07NL *	4.9	<3.3		
WKZ/356/06NL *	6.0	4.5	23158	5986
EKZ/364/06NL *	5.8	3.9	5995	3387

The M_s-m_b plot of the events in Table VII-1 are shown in Figure VII-1. Presumed nuclear explosions are signified by triangles, earthquakes by dots, and undetected events by a vertical bar underneath the appropriate symbol. M_s values for undetected events represent maximum possible values. For these cases, M_s was obtained from the largest noise peak having a period between 17 and 24 seconds within the expected signal gate.

The data show good separation between earthquakes and presumed explosions. There is good agreement with similar results from ALPA (Texas Instruments 1971). One event, BSA/210/19, had unusually small surface waves. Although it was not reported by NOAA-PDE, it was a clear signal on the output beams.

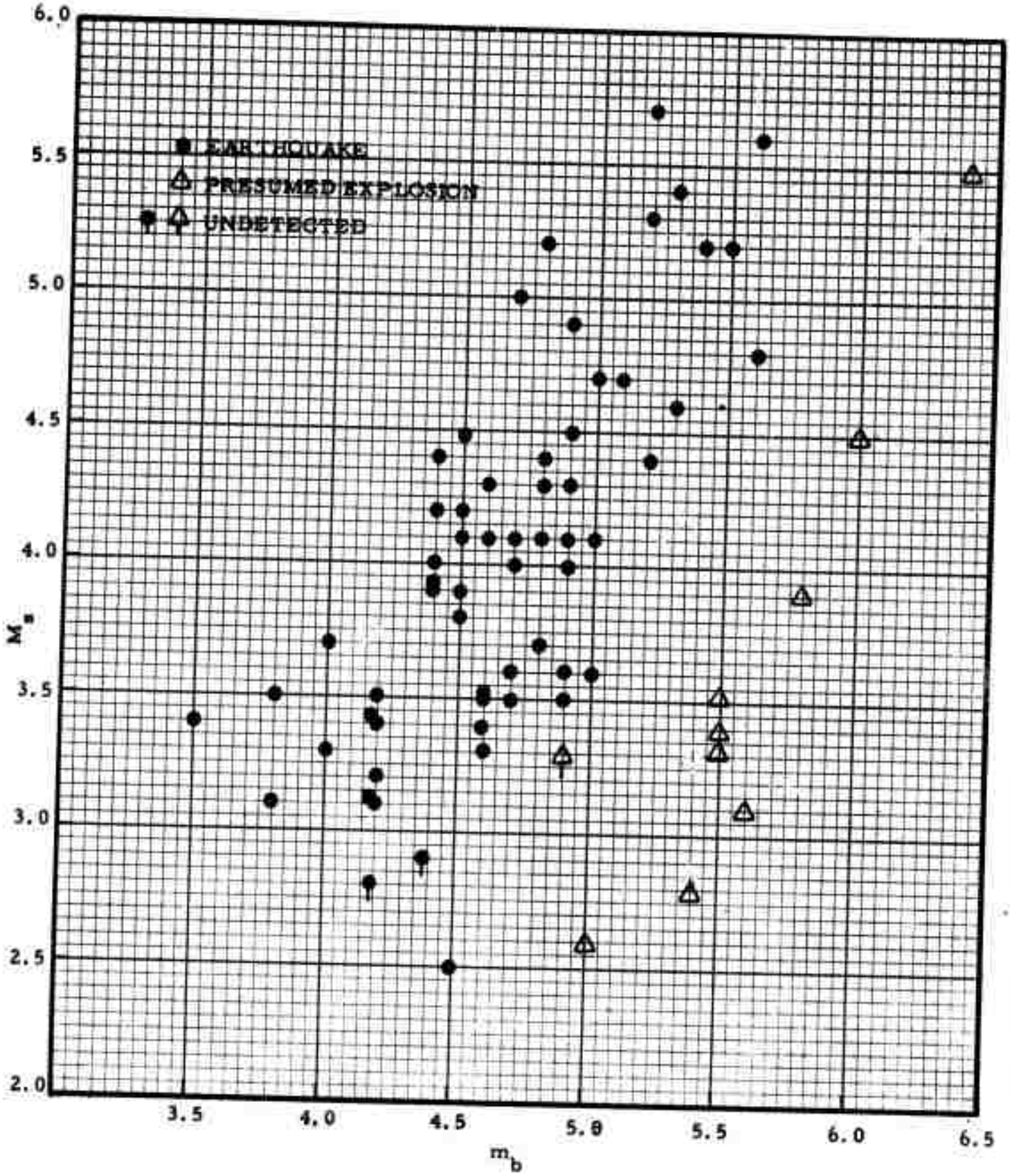

FIGURE VII-1

M_s/m_b FOR SINO-SOVIET EVENTS

C. AR/m_b MEASUREMENTS

The AR measurement was introduced by Brune, Espinosa, and Oliver (1963) and used by Evernden (1969). The procedure for scaling our data so as to make it comparable to Evernden's results has been described previously (Texas Instruments 1971) and results in a correction scale factor equal to $2\pi \times 10^{-3}$.

Our AR measurements were made from the vertical component of the beamsteer output after bandpassing with a 0.020 to 0.059 Hz filter. The AR gate duration was chosen on the basis of expected duration and enclosed the majority of the Rayleigh wave energy. The corrected AR values were then normalized to a body-wave magnitude of 5.0 by the multiplicative factor $10^{(5.0 - m_b)}$ and to a distance of 20° using the empirical curve given by Brune et al.

A plot of AR versus m_b is given by Figure VII-2. This discriminant shows very good separation between classes of events. Minimum separation between classes is about a factor of 3.0. General performance is similar to or slightly better than results reported for ALPA.

The group of presumed explosions appear to be slightly skewed which may indicate an incorrect magnitude scaling factor. No skew is apparent in the earthquakes, however, and none can be seen in the AL measurements discussed below. To determine whether the skew is real or not will require more data.

D. AL/m_b MEASUREMENTS

The AL values were computed by the same method described for AR except that in this case, measurements were taken on the Love wave energy for the transverse component of the beams.

The AL values for this suite of events are shown in Figure VII-3. This discriminant shows somewhat better separation between earthquakes and presumed explosions than does the AR. Minimum separation is by a factor of 8.1.

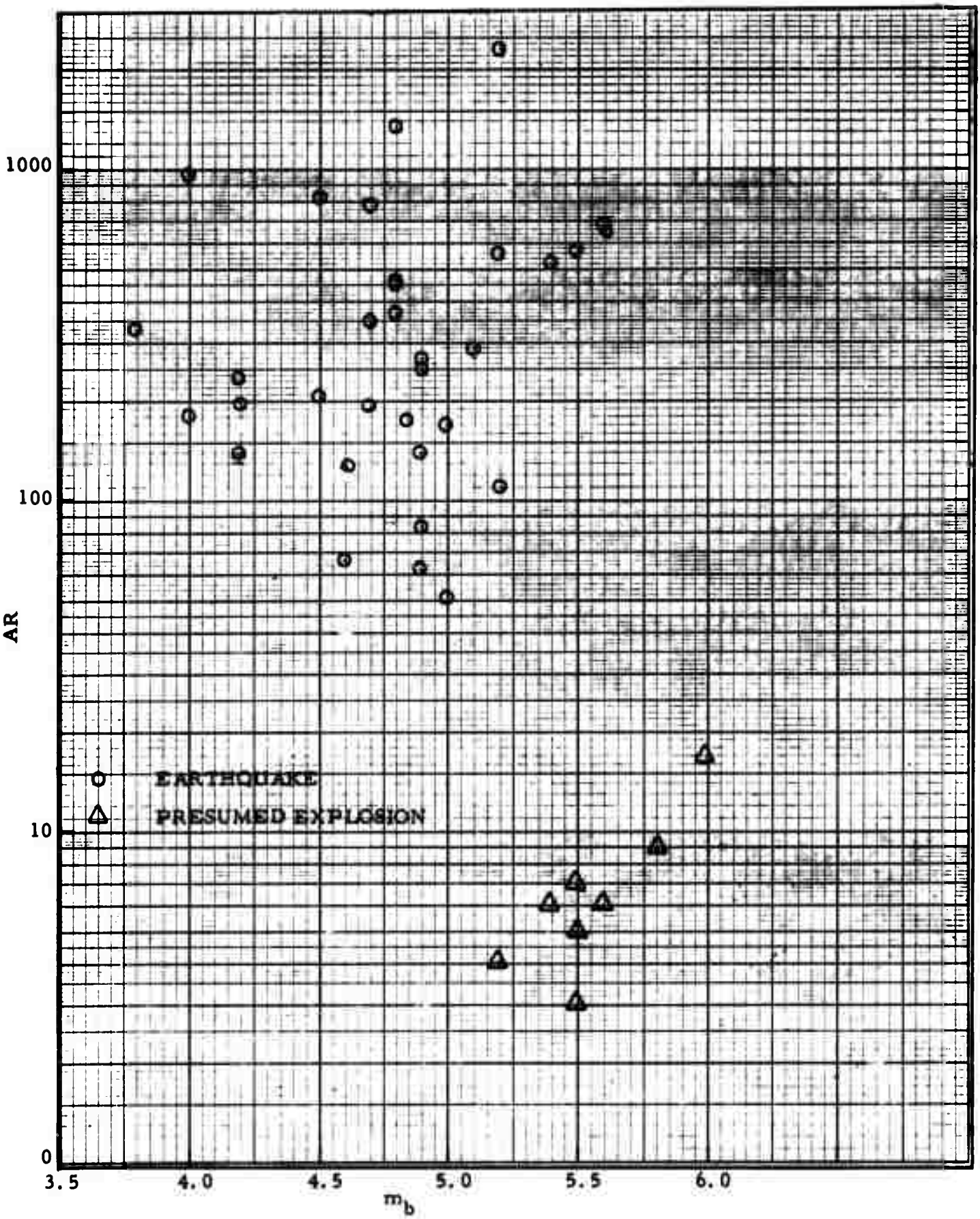

FIGURE VII-2

AR/m_b PLOT

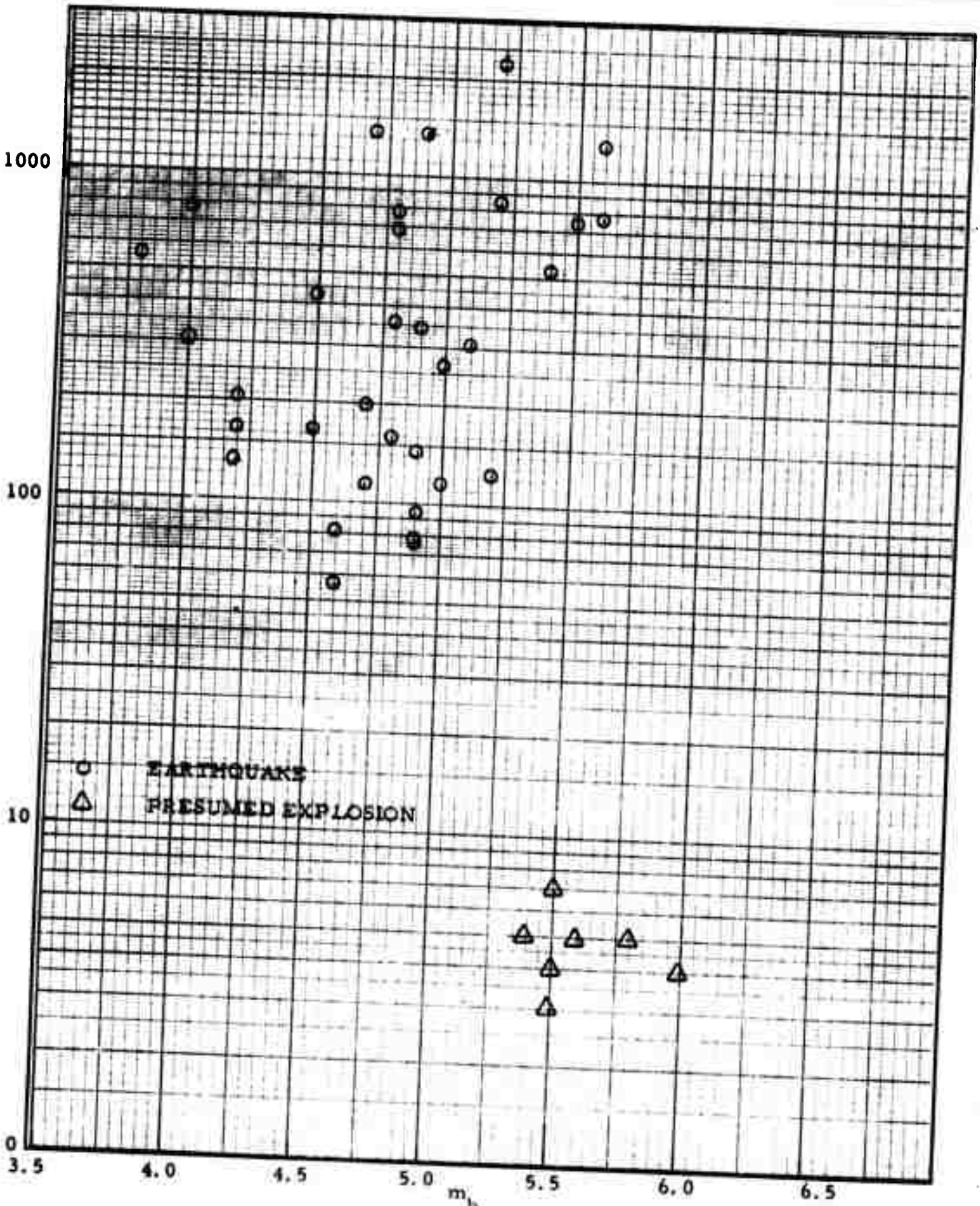

FIGURE VII-3

AL/m_b PLOT

The Western Kazakh event, which had a rather high AR value, does not show an unusual AL value. These results are considerably better than those obtained for ALPA.

SECTION VIII
CONCLUSIONS AND FUTURE PLANS

A. CONCLUSIONS

This section summarizes the results of the long-period NORSAR evaluation obtained to date. The results are based on data which were obtained from the interval of 1 May 1971 to 9 January 1972 and using an average of 15 to 16 sites out of the 22 total sites. Events were restricted almost exclusively to those occurring in or near the Sino-Soviet area.

The data for NORSAR as received at SAAC have generally been excellent since September 1971. Previous to that time, particularly during early summer, there was considerable difficulty in obtaining good data consistently. At any given time, usually 20 to 21 sites are operating. The difference between this number and the average number of 16 sites processed arises from the sites dropped because of particular problems such as spikes and transients.

Although much free-period and mass-position test information was received, no full frequency and phase response data were obtained. This prevented the drawing of conclusions in some areas such as the travel-time anomalies of signal waveforms mentioned below. However, results from noise analysis and array processing did imply good equalization.

A large amount of noise data was processed and several results can be given with confidence:

- There are definite seasonal changes in the spectral shape, average power level, and directionality of the ambient noise field at NORSAR. Summer noise is generally easterly with microseismic energy at 16-18 seconds, and 8-10 seconds. Winter noise arrives primarily from the northwest quadrant with average power levels increasing by a

factor of 2 or 3. In the winter, the 8-10 second energy increases and some 4-5 second energy appears.

- There was one clear-cut correlation of high noise level with weather (day 348). It is probable that with more detailed analysis, the increased winter noise levels could be correlated with weather in the north Atlantic.
- All sites seem to be well equalized based on average noise levels at each site.
- Multichannel squared coherence is generally greater than 0.7 between 0.03 Hz to 0.15 Hz. This suggests that MCF processing has some potential for additional array gain.

The number of events processed to ascertain signal characteristics was relatively small. However, the results show definite patterns. Major results are:

- Waveform similarity between sites shows only small changes across the array along the path of propagation. Much larger changes are observed along the wavefronts normal to the propagation path.
- Small but consistent travel-time anomalies have been observed at a few sites. These seem to be independent of event azimuth hence are probably caused by instrumental effects. Their cause could not be investigated because of lack of phase response calibrations.
- Wavefront arrival azimuth is generally the great circle path. Events from Turkey, however, show a more southerly shift in arrival angle by about five to eight degrees.
- All signal spectrum measurements were on the raw spectrum uncorrected for instrument response. On the uncorrected spectra, the -6 dB power points were generally between 40 sec. to 17 sec. Turkey events and very large Central Russian events may extend the upper -6 dB level to 13 seconds.

- The ratio of radial to vertical Rayleigh wave amplitudes was about 0.68. This is smaller than the ratio of 0.8 at ALPA.

The array processing performance results are based on relatively few (12) noise samples. This is because the intent was to obtain MCF's as reliable as possible which in turn required long-duration noise samples. The results for these samples are:

- Signal degradation due to beamsteer processing was about 0.7 dB for LRV and LQT modes and 1.0 dB for the LRR mode.
- Out of the MCF design gate both BS and MCF processors achieved about $\sqrt{N}$ array gain most of the time. Within the design interval MCF's always were better than $\sqrt{N}$. Array gains were larger when using wider bandwidths both inside and outside of the design gate.
- The extra array gain achieved by the MCF over the BS processor in the design gate averaged 5.1 dB wideband and 3.7 dB in the passband of 18-40 seconds. Outside of this gate, these extra gains were to 3.0 dB and 1.9 dB respectively. The enhanced performance of the MCF was particularly sensitive to the upper frequency limit of the passband. With a lower limit of 0.02 Hz, the MCF improvement for upper limits of 0.059Hz, 0.055 Hz, and 0.051 Hz were 4.3 dB, 3.6 dB, and 3.0 dB respectively in the design gate. For the same bands outside of the design gate, the improvements were respectively 2.7 dB, 1.7 dB, and 1.2 dB. The lower band limit had little effect on gain.
- Because of the amount of data required for reliable MCF design, it is probably not practicable to design MCF's routinely to optimize array gain for any particular event. However, the seasonal trends in noise level and directionality indicate that an MCF processing occasionally will be useful, particularly in the winter (when up to 9 dB additional noise rejection was achieved in the 17 to 50 second band on day 348 and 6 dB on day 332).

Matched filtering performance of master event and chirp filters were measured for a large number of events. Major results are:

- Master event and chirp filter improvements are highly variable from event-to-event and region-to-region. The chirp filters tended to give more stable, but slightly lower gains than the master event filters.
- Master event filters averaged 0.5 to 1.0 dB more gain than chirp filters. Signal plus noise-to-noise ratio improvements decreased with decreasing bandwidth. The improvements for 0.020-0.059 Hz and 0.025 - 0.051 Hz respectively were:

  LRV: 3.7 and 3.2 dB

  LRR: 3.8 and 3.2 dB

  LQT: 2.9 and 1.9 dB
- Chirp filter performance was not particularly bandwidth sensitive. The corresponding numbers for the chirp filters for the passbands above were:

  LRV: 2.7 and 2.7 dB

  LRR: 2.7 and 2.8 dB

  LQT: 2.4 and 1.9 dB
- There was no obvious correlation between improvement and master-test event separation. Source mechanism and relative fault orientation should be more important in predicting signal-to-noise ratio improvement.
- Some regions tend to larger improvements with wider bandwidths while for other regions, narrow bandwidths give better results.
- Master events for a few regions gave poor results even though their waveforms appeared to differ relatively little from the test events.
- More sophisticated chirp filters may provide enhanced performance without significantly increased algorithm complexity.

The incremental detection threshold of NORSAR, using 15 to 16 sites, was measured directly from event detection histories and indirectly using implied magnitudes based on ambient noise levels. The results show that:

- The direct estimate indicates the 90% detection level at an $m_b = 4.6$ and the 50% level at $m_b = 4.2$. These estimates are not reliable since they are based on only a few non-detections in an event ensemble whose mean m_b is around 4.8.
- The indirect measurement of detection threshold gave unrealistically low detection thresholds (90% at $m_b = 3.8$, 50% at $m_b = 3.3$). It is felt that failure to account for the signal variance causes this low bias.
- The best estimates of detection threshold will have to come from a larger event ensemble.
- There is no significant variation in detection behavior between the three different passbands used.

The behavior of three standard discriminants, M_s-m_b, AR-m_b, and AL-m_b was observed for a number of Sino-Soviet events. All three discriminants showed good separation between earthquakes and presumed explosions. Both AL-m_b and AR-m_b gave better separation than M_s-m_b with AL-m_b giving the best results.

B. FUTURE PLANS

General plans for future tasks in the NORSAR evaluation are directed to answering questions which arose during this preliminary evaluation, enlarging the event ensemble, particularly at smaller magnitudes, and obtaining data covering a full calendar year so that seasonal effects can be examined.

In particular, noise analysis will be continued, and weather maps will be obtained for additional work correlating surface weather with the ambient noise field.

Future signal analysis will investigate the amount and effect of multipath energy at NORSAR. Some work should be done to explain or categorize the signal characteristics on a regional basis. This would be useful, in conjunction with matched filtering studies, in constructing models for "best" master events and chirps for given areas.

Future array processing analysis will investigate MCF performance using long or combined noise samples on an extended basis. If investigation of the noise field reveals stable directional noise on a seasonal interval, the performance of modeled wavenumber filters will be tested.

Matched filter studies will be used in an effort to obtain a better estimate of SNR gains for different regions. Possibly, given sufficient data, models of optimum filters can be constructed.

The detection threshold estimate of NORSAR will be refined by obtaining considerably more event data at smaller magnitudes. This effort will comprise the majority of the work on the extended NORSAR evaluation program.

SECTION IX
REFERENCES

Brune, J., A. Espinosa, and J. Oliver, 1963, Relative Excitation of Surface Waves by Earthquakes and Underground Explosions in the California Nevada Region; Journal of Geophysical Research, Vol. 68, pp 3501-3513, 1 June.

Evernden, J. F., 1969, Identification of Earthquakes and Explosions by use of Teleseismic Data; Journal of Geophysical Research, Vol. 74, pp 3828-3856, July.

Harley, T. W., 1967, Long Period Signal Waveform Similarity at LASA, ARPA Special Report No. 9, Texas Instruments Incorporated, Dallas, Texas.

Lacoss, R. T., 1969, A Large Population LASA Discrimination Experiment; Lincoln Laboratory, Technical Note 1969-24, April.

Linville, A. F., 1971, Rayleigh-Wave Multipath Analysis Using a Complex Cepstrum Technique; Special Report No. 2, Texas Instruments Incorporated, Dallas, Texas.

Texas Instruments Incorporated, 1971, Long Period Array Processing Development; Final Report, AFTAC Project No. VT/9707, Contract No. F33657-69-C-1063, Dallas, Texas, May.